[redacted]

NASA TECHNICAL MEMORANDUM

NASA TM X-1005

NASA TM X-1005

FACILITY FORM 602

X64 16260
(ACCESSION NUMBER)

(THRU)

91
(PAGES)

2
(CODE)

(NASA CR OR TMX OR AD NUMBER)

02
(CATEGORY)

(NASA-TM-X-1005) SUPERSONIC AERODYNAMIC CHARACTERISTICS OF A RECOVERABLE BOOSTER WITH VARIATIONS IN WING PLANFORM D.L. Wassum, et al (NASA) Sep. 1964 94 p

N72-73270

Unclas
00/99 31993

UNCLASSIFIED

TO

By Authority of [redacted] Date [redacted]

SUPERSONIC AERODYNAMIC CHARACTERISTICS OF A RECOVERABLE BOOSTER WITH VARIATIONS IN WING PLANFORM

by Donald L. Wassum, Bernard Spencer, Jr., and Nickolai Charczenko

Langley Research Center
Langley Station, Hampton, Va.

NATIONAL AERONAUTICS AND SPACE ADMINISTRATION • WASHINGTON, D. C. • SEPTEMBER 1964

Reproduced by
NATIONAL TECHNICAL
INFORMATION SERVICE
U S Department of Commerce
Springfield VA 22151

SUPERSONIC AERODYNAMIC CHARACTERISTICS OF A RECOVERABLE BOOSTER WITH VARIATIONS IN WING PLANFORM

By Donald L. Wassum, Bernard Spencer, Jr.,
and Nickolai Charczenko

Langley Research Center
Langley Station, Hampton, Va.

[redacted]

NATIONAL AERONAUTICS AND SPACE ADMINISTRATION

SUPERSONIC AERODYNAMIC CHARACTERISTICS OF A RECOVERABLE BOOSTER WITH VARIATIONS IN WING PLANFORM*

By Donald L. Wassum, Bernard Spencer, Jr.,
and Nickolai Charczenko

SUMMARY

16260

An investigation has been made in the Langley Unitary Plan wind tunnel at Mach numbers from 1.60 to 4.65 to determine the aerodynamic characteristics of a manned, recoverable booster configuration incorporating external nacelles for an air-breathing propulsion system.

The results indicated that the 75° modified arrow wing configuration was longitudinally stable throughout the Mach number range and had a maximum untrimmed lift-drag ratio of about 4.4 at a Mach number of 1.60 and about 3.9 at a Mach number of 4.65. Deflection of the horizontal stabilizer having a 30° anhedral angle provided an effective means of control, although a substantial decrease in lift-drag ratio resulted. An increase in control effectiveness occurred with increasing lift at the higher Mach numbers as a result of an increase in dynamic pressure induced on the tail by the wing flow field. Increasing the anhedral of the horizontal tail provided an increase in directional stability, but, even with an anhedral angle of 90°, the configuration became directionally unstable throughout the angle-of-attack range at the higher test Mach numbers.

Author

INTRODUCTION

The National Aeronautics and Space Administration is presently concerned with studies to determine the aerodynamic characteristics of manned, recoverable booster configurations utilizing air-breathing propulsion systems. Primary mission requirements for vehicles of this type include both horizontal landing and horizontal take-off capability with sufficient thrust to accelerate to hypersonic speeds.

Aerodynamic characteristics for one such recoverable booster configuration at speeds up to Mach 1.13 are presented in reference 1. This configuration consisted of a high-finess-ratio body, engine nacelles, and a highly swept fixed wing.

As a continuation of the tests presented in reference 1, an investigation has been conducted in the Langley Unitary Plan wind tunnel to determine

[redacted]

aerodynamic characteristics of this configuration at Mach numbers from 1.60 to 4.65 and through an angle-of-attack range from -6° to 20° at sideslip angles from -4° to 6°. The tests were made at a Reynolds number per foot of 3.0×10^{6}. The results, presented herein, include the effects of horizontal-stabilizer anhedral and incidence, wing planform, and auxiliary outboard vertical tails on the performance and stability characteristics of the configuration.

SYMBOLS

The forces and moments are nondimensionalized with respect to the geometric characteristics of the corresponding wing. The lift, drag, and pitching-moment data are referred to the stability-axis system, and the yawing-moment, rolling-moment, and side-force data are referred to the body-axis system. The moment reference is located at 66 percent of the body length (including engines) behind the theoretical body apex and at 1.44 percent of the body length below the nacelle center line.

A	aspect ratio, b^2/S
b	wing span, ft
c	control-surface root chord, in.
c_r	wing root chord, in.
S	wing planform area, sq ft
t	control-surface thickness, in.
M	free-stream Mach number
p_t	free-stream stagnation pressure, lb/sq in. abs
q	dynamic pressure, lb/sq ft
T_t	free-stream stagnation temperature, $^{\circ}F$
α	angle of attack of fuselage center line, deg
β	angle of sideslip of fuselage center line, deg
i_t	horizontal-stabilizer incidence angle (positive with trailing edge down, measured in vertical plane), deg
Γ_t	horizontal-stabilizer anhedral angle (positive with tip down), deg
C_L	lift coefficient, Lift/qS

C_D	drag coefficient, Drag/qS
C_m	pitching-moment coefficient, Pitching moment/qSc_r
C_l	rolling-moment coefficient, Rolling moment/qSb
C_n	yawing-moment coefficient, Yawing moment/qSb
C_Y	side-force coefficient, Side force/qS
C_{L_α}	lift-curve slope at $\alpha = 0^\circ$, per deg
L/D	lift-drag ratio
$\partial C_m/\partial C_L$	longitudinal-stability parameter
$C_{m_{i_t}}$	horizontal-stabilizer effectiveness parameter at $\alpha = 0^\circ$, per deg
C_{l_β}	effective-dihedral parameter, $\Delta C_l/\Delta\beta$, per deg
C_{n_β}	directional-stability parameter, $\Delta C_n/\Delta\beta$, per deg
C_{Y_β}	side-force parameter, $\Delta C_Y/\Delta\beta$, per deg

Subscripts:

max	maximum
min	minimum

Model components:

W_1	75° delta wing
W_2	75° modified arrow wing
W_3	70°-80° cranked wing
B	body
H	horizontal stabilizer
V	center-line vertical tail
V_o	outboard vertical tail

MODEL AND APPARATUS

Model

Details of the model and components are presented in figures 1 and 2. Photographs of the 75° delta wing configuration are presented in figure 3. The model was constructed of wood and fiber glass with a steel insert in the fuselage to accommodate a strain-gage balance. The body had a modified 2/3-power series forebody, having a height-width ratio of approximately 2.0 with flat sides (fig. 1). Three wings - a 75° delta wing (W_1), a 75° modified arrow wing (W_2), and a 70°-80° cranked wing (W_3) - were tested. Each wing incorporated modified wedge airfoil sections with the maximum thickness at the 75-percent wing-chord station. Two nacelles representing those for turboramjet engines (designed for $M = 8$) were attached to the wing with the inlets located in a position below and aft of the wing leading edge so as to operate in a flow field of reduced Mach number. Longitudinal control was provided by an all-movable horizontal stabilizer located near the engine exits with provisions for position of the stabilizer at anhedral angles of either 30°, 60°, or 90°. Each wing configuration was tested with a vertical tail (V) located on the body center line. The 75° modified arrow wing configuration was tested with additional vertical tails (V_o) located at the wing tips. The center-line vertical tail, which had a flat-plate airfoil section with rounded leading edge and beveled trailing edge, had a 68° sweptback leading edge and an exposed area equivalent to 0.225 of the W_1 planform area. The auxiliary vertical tails had half-wedge airfoil sections and a total area equivalent to 0.136 of the W_1 planform area.

Tunnel

Tests were conducted in both the low and high Mach number test sections of the Langley Unitary Plan wind tunnel which is a variable-pressure, continuous-flow system. The test sections are 4 feet square and 7 feet long. The nozzles leading to the test sections are of the asymmetric, sliding-block type which permits a continuous variation in Mach number from about 1.5 to 2.9 in the low Mach number test section, and from about 2.3 to 4.7 in the high Mach number test section.

TEST CONDITIONS

The following table presents conditions at which the tests were performed:

M	T_t, °F	p_t, lb/sq in. abs
1.60	150	11.88
1.90	150	13.22
2.36	150	16.39
2.86	150	21.35
3.96	175	40.11
4.65	175	55.08

The tests were made over an angle-of-attack range from -6° to 20° at sideslip angles from -4° to 6°. The test Reynolds number per foot was 3.0×10^{6}.

In order to assure turbulent flow over the model, a 1/16-inch-wide transition strip of No. 60 carborundum grains was fixed on the wings, horizontal stabilizers, and vertical tails at the 10-percent streamwise chord stations and around the forebody 1 inch aft of the nose. The dewpoint, measured at stagnation pressure, was maintained below -30° F in order to assure negligible condensation effects.

Aerodynamic forces and moments on the model were measured by means of a six-component, internally mounted, electrical strain-gage balance. The balance was attached to a sting which was rigidly secured to the tunnel support system. Pressures in the balance chamber at the nacelle base were measured by means of static-pressure orifices.

CORRECTION AND ACCURACY

The angles of attack have been corrected for both tunnel flow angularity and deflection of model and sting support system due to aerodynamic loads. The drag coefficients have been corrected for internal skin friction in the nacelles and adjusted to correspond to free-stream static pressure in the balance chamber and at the base of the nacelles.

Based on balance calibrations and repeatability of data, it is estimated that the various measured quantities are accurate within the following limits:

C_L	±0.0037
C_D	±0.0004
C_m	±0.0006
C_l	±0.0001
C_n	±0.0005
α	±0.10
β	±0.10
$M < 3.96$	±0.015
$M > 3.96$	±0.05

PRESENTATION OF RESULTS

The results of this investigation are presented in the following figures:

	Figure
Effect of horizontal-stabilizer anhedral angle on aerodynamic characteristics in pitch. W_2, $i_t = 0^{\circ}$	4
Effect of wing planform on aerodynamic characteristics in pitch. $\Gamma_t = 60^{\circ}$, $i_t = 0^{\circ}$	5

Figure

Effect of horizontal-stabilizer deflection on aerodynamic characteristics in pitch. W_2, $\Gamma_t = 30^\circ$ 6

Effect of horizontal-stabilizer deflection on aerodynamic characteristics in pitch. W_2, $\Gamma_t = 60^\circ$ 7

Effect of vertical tails on aerodynamic characteristics in pitch. W_2, $\Gamma_t = 60^\circ$, $i_t = 0^\circ$ 8

Variation of longitudinal parameters with Mach number and horizontal-stabilizer anhedral 9

Variation of longitudinal parameters with Mach number for three wing planform configurations 10

Aerodynamic characteristics in sideslip. W_2, $\Gamma_t = 30^\circ$, $i_t = 0^\circ$ 11

Aerodynamic characteristics in sideslip. W_2, $\Gamma_t = 60^\circ$, $i_t = 0^\circ$ 12

Effect of components on sideslip parameters. W_2 13

Effect of horizontal-stabilizer anhedral angle on sideslip parameters. W_2, $i_t = 0^\circ$ 14

Effect of outboard vertical tails on sideslip parameters. W_2, $\Gamma_t = 60^\circ$, $i_t = 0^\circ$ 15

Comparison of the sideslip parameters for configurations with W_1 and W_2 wings. $\Gamma_t = 60^\circ$, $i_t = 0^\circ$ 16

DISCUSSION

Longitudinal Characteristics

The longitudinal aerodynamic characteristics of the 75° modified arrow wing configuration with the horizontal stabilizer at anhedral angles of 30°, 60°, and 90° are presented in figure 4 for each test Mach number. Data for the configuration without the horizontal stabilizer are also included for Mach numbers to 2.86. These results show that the tail-on configuration is longitudinally stable about the moment reference point at all test Mach numbers, and is stable even with the horizontal stabilizer off, to a Mach number of 2.86. Increasing the stabilizer anhedral angle results in a decrease in longitudinal stability level and lift-curve slope, particularly at the lower test Mach numbers. The stability decrease with Mach number (fig. 9) corresponds to a forward shift in the center of pressure of about 4 percent of the wing root chord for all stabilizer anhedral angles tested.

The effect of wing planform on the pitch characteristics is presented in figure 5. Generally, the lift-curve slope for the 75° modified arrow wing configuration (W_2) is the greatest and that for the 70°-80° cranked wing configuration (W_3) is the lowest of the three wing planforms tested. At the lower test Mach numbers, all the planform configurations exhibit a noticeable increase in C_{L_α} at the lower values of lift coefficient. The maximum lift-drag ratios for the W_1 and W_2 configurations are about the same, and greater than those for

the W_3 configuration. The value of maximum untrimmed L/D for the W_2 configuration varies from about 4.4 at $M = 1.60$ to about 3.9 at $M = 4.65$. (See fig. 10.)

Pitch control data for the horizontal stabilizer at anhedral angles of 30° and 60° are shown in figures 6 and 7, respectively, and summary data may be found in figure 9. Deflection of the horizontal stabilizer provides an effective means of control with $\Gamma_t = 30^\circ$ (fig. 6), although the results indicate a substantial decrease in L/D due to trimming. At Mach numbers from 1.60 to 2.36 the control effectiveness is essentially constant throughout the lift range; however, at Mach numbers from 2.86 to 4.65 the control effectiveness increases with increasing lift as a result of an increase in dynamic pressure at the horizontal stabilizer that is induced by the flow field below the wing. Primarily as a result of the increased effectiveness of the horizontal stabilizer, the -20° deflection of the stabilizer provides a higher trim lift at $M = 4.65$ than at the lower Mach numbers. With the stabilizer anhedral increased to 60° (fig. 7), the pitch control provided by the stabilizer is relatively ineffective.

The addition of the wing-tip vertical tails to the W_2 configuration has little effect on the pitch characteristics, other than a small penalty in drag coefficient and $(L/D)_{max}$. (See fig. 8.)

Sideslip Characteristics

Typical aerodynamic characteristics in sideslip of the configuration with the 75° modified arrow wing (W_2) are presented in figures 11 and 12 to show the linearity of the basic data. All the sideslip parameter data were obtained from pitch tests at sideslip angles of 0° and 5°.

The W_2 configuration exhibits directional instability which increases rapidly with increasing angle of attack (fig. 13). Addition of the center-line vertical tail significantly increases C_{n_β}; however, at $M = 1.60$ the configuration is directionally stable only to an angle of attack of about 6°, and at $M = 2.86$ directional instability occurs throughout most of the positive angle-of-attack range. Figure 14 indicates that an increase in horizontal-stabilizer anhedral angle generally provides an increase in C_{n_β}. With an anhedral angle of 90°, however, the configuration is directionally stable only to about $\alpha = 8^\circ$ at $M = 1.60$, and directional instability occurs at all positive angles of attack at the two highest test Mach numbers. Addition of the tip vertical tails to the configuration having $\Gamma_t = 60^\circ$ generally improves the directional stability (fig. 15), although directional instability still occurs at all positive angles of attack at the highest test Mach number. There are only small differences in the sideslip parameters for the configurations with the 75° delta and 75° modified arrow wings (fig. 16). All configurations exhibited positive effective dihedral through the test angle-of-attack and Mach number ranges.

CONCLUSIONS

The results of an investigation to determine the aerodynamic characteristics of a manned, recoverable booster configuration at Mach numbers from 1.60 to 4.65 may be summarized by the following conclusions:

1. The 75° modified arrow wing configuration with the horizontal stabilizer set at an anhedral of 30° was longitudinally stable throughout the test Mach number range. The maximum untrimmed lift-drag ratio varied from about 4.4 at a Mach number of 1.60 to about 3.9 at Mach 4.65.

2. Effective trim control was obtained with deflection of the horizontal stabilizer having a 30° anhedral angle, although a substantial decrease in lift-drag ratio occurs as a result of trimming.

3. A substantial increase in control effectiveness occurred with increasing lift at the higher Mach numbers as a result of an increase in dynamic pressure induced on the horizontal stabilizer by the wing flow field.

4. Increasing the anhedral angle of the horizontal stabilizer provided an increase in directional stability, although, even with a stabilizer anhedral angle of 90°, the configuration was directionally unstable throughout the angle-of-attack range at the higher test Mach numbers.

Langley Research Center,
National Aeronautics and Space Administration,
Langley Station, Hampton, Va., May 28, 1964.

REFERENCE

1. Spencer, Bernard, Jr., Henry, Beverly Z., Jr., and Phillips, W. Pelham: Transonic Aerodynamic Characteristics of a Horizontal Take-Off and Landing Reusable Booster Having Variations in Wing Planform. NASA TM X-982, 1964.

Wing Geometry

Wing	A	b, in.	S, ft^2	c_r, in.
1	1.080	10.80	0.758	20.20
2	.894	9.88	.758	18.44
3	.836	9.24	.709	18.92

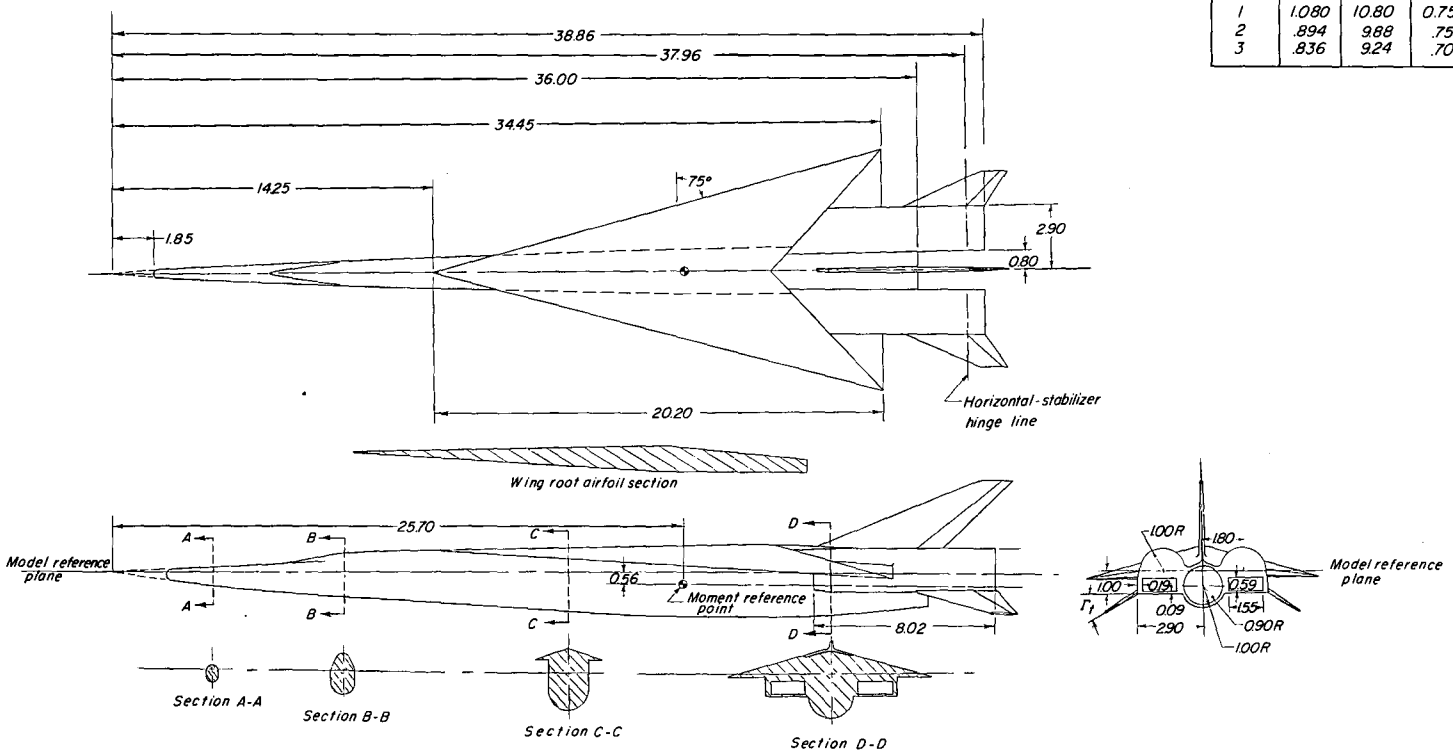

Figure 1.- Configuration with 75° delta wing (W_1). All dimensions are in inches.

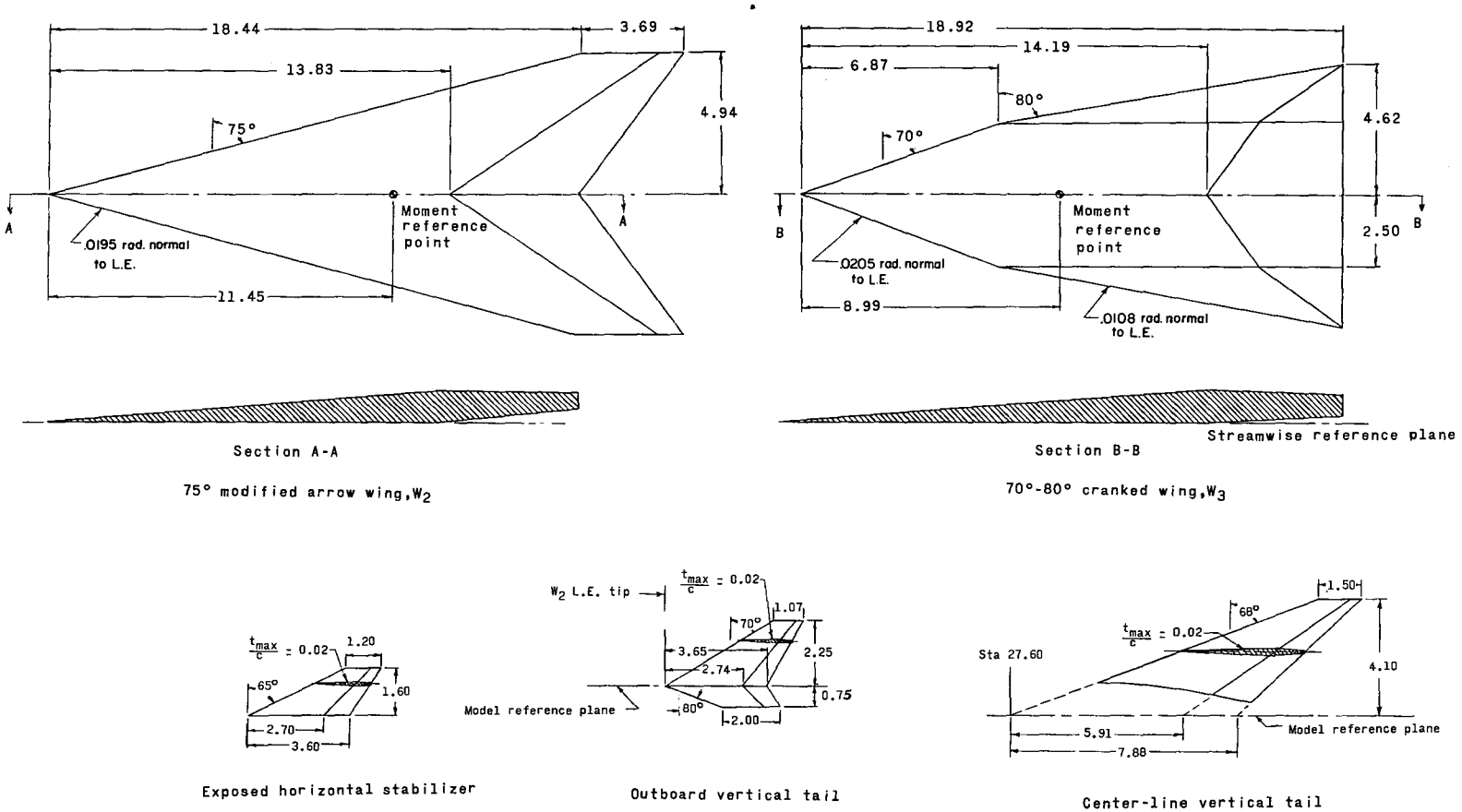

Figure 2.- 75° modified arrow wing (W_2), 70°-80° cranked wing (W_3), and control surfaces.

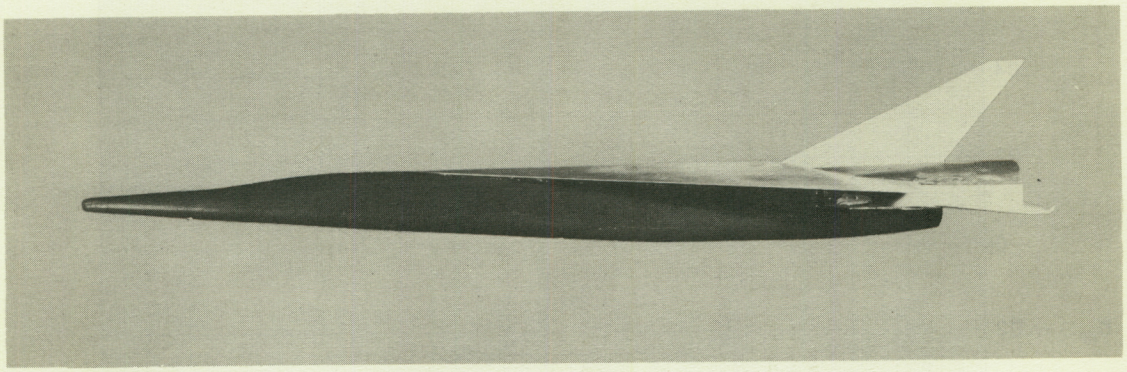

(a) Side view. L-63-5407

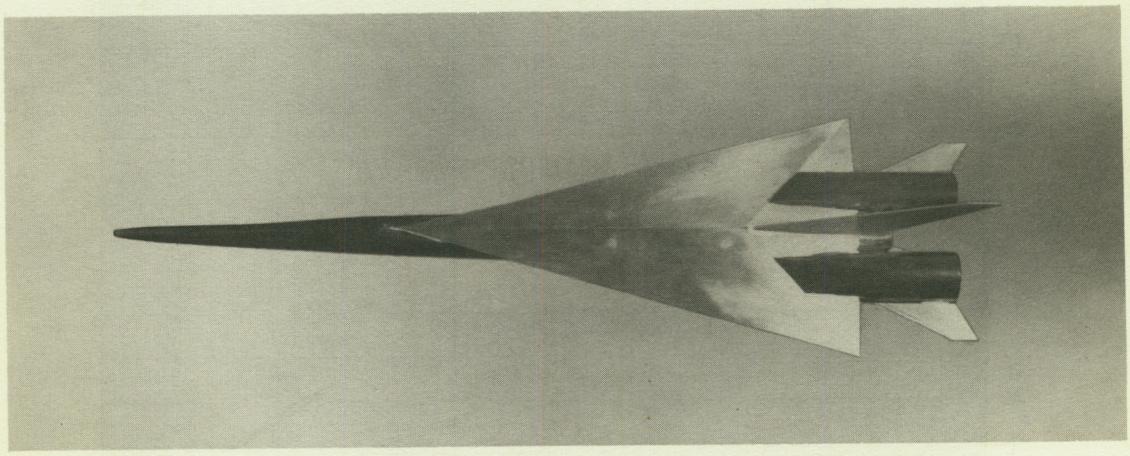

(b) Plan view. L-63-5408

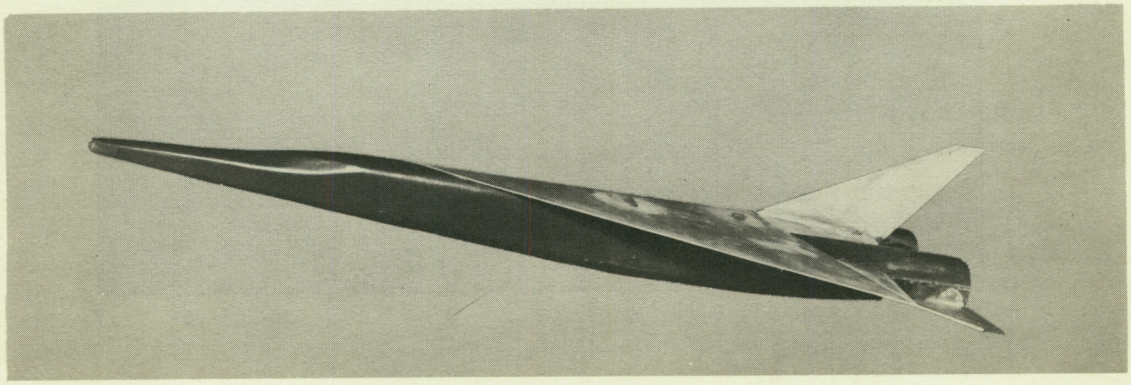

(c) Three-quarter side view. L-63-5406

Figure 3.- Photographs of configuration W_1BVH. $\Gamma_t = 30^\circ$, $i_t = 0^\circ$.

Reproduced from best available copy.

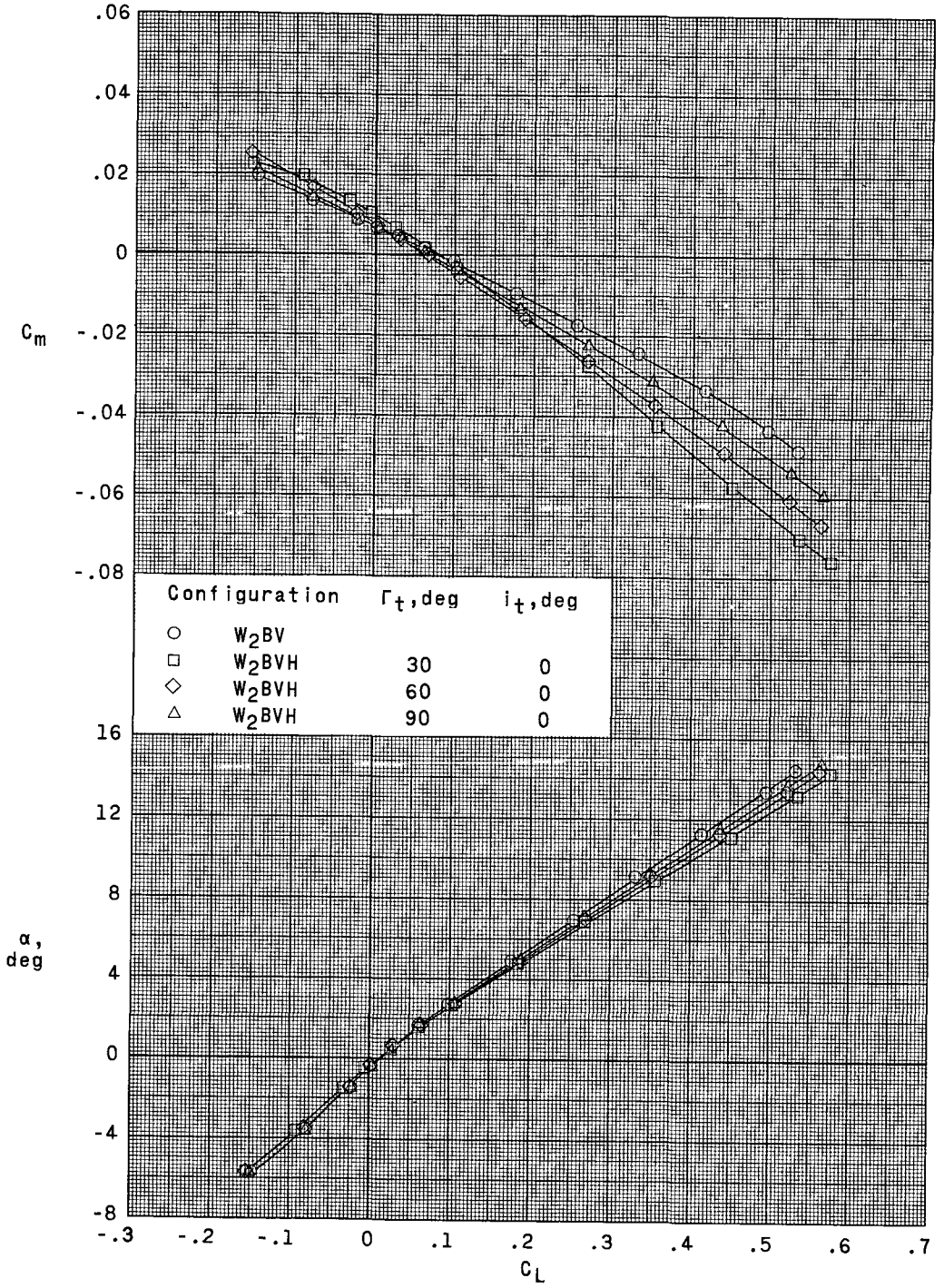

(a) M = 1.60.

Figure 4.- Effect of anhedral angle of the horizontal stabilizer on aerodynamic characteristics in pitch.

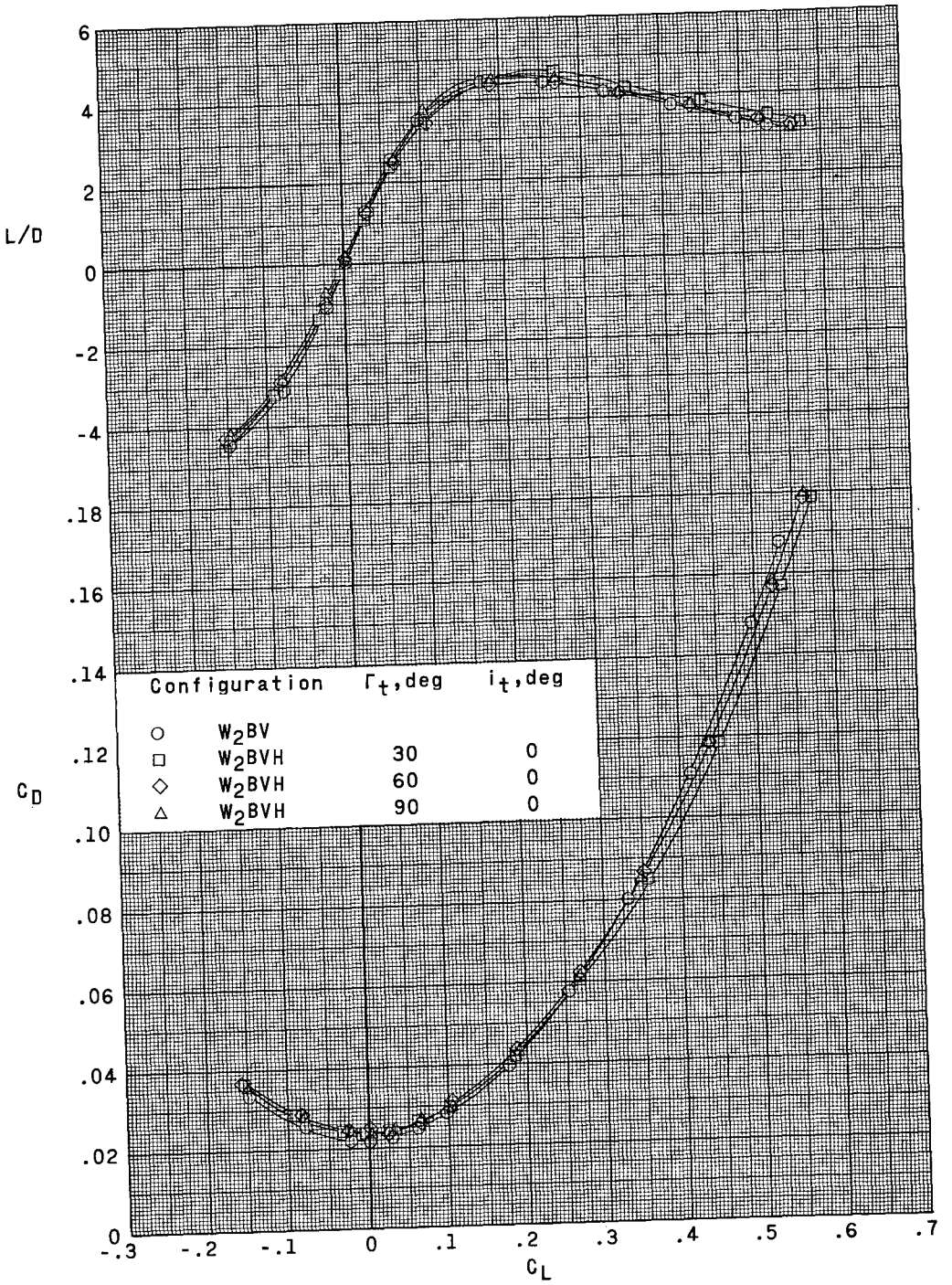

(a) Concluded.

Figure 4.- Continued.

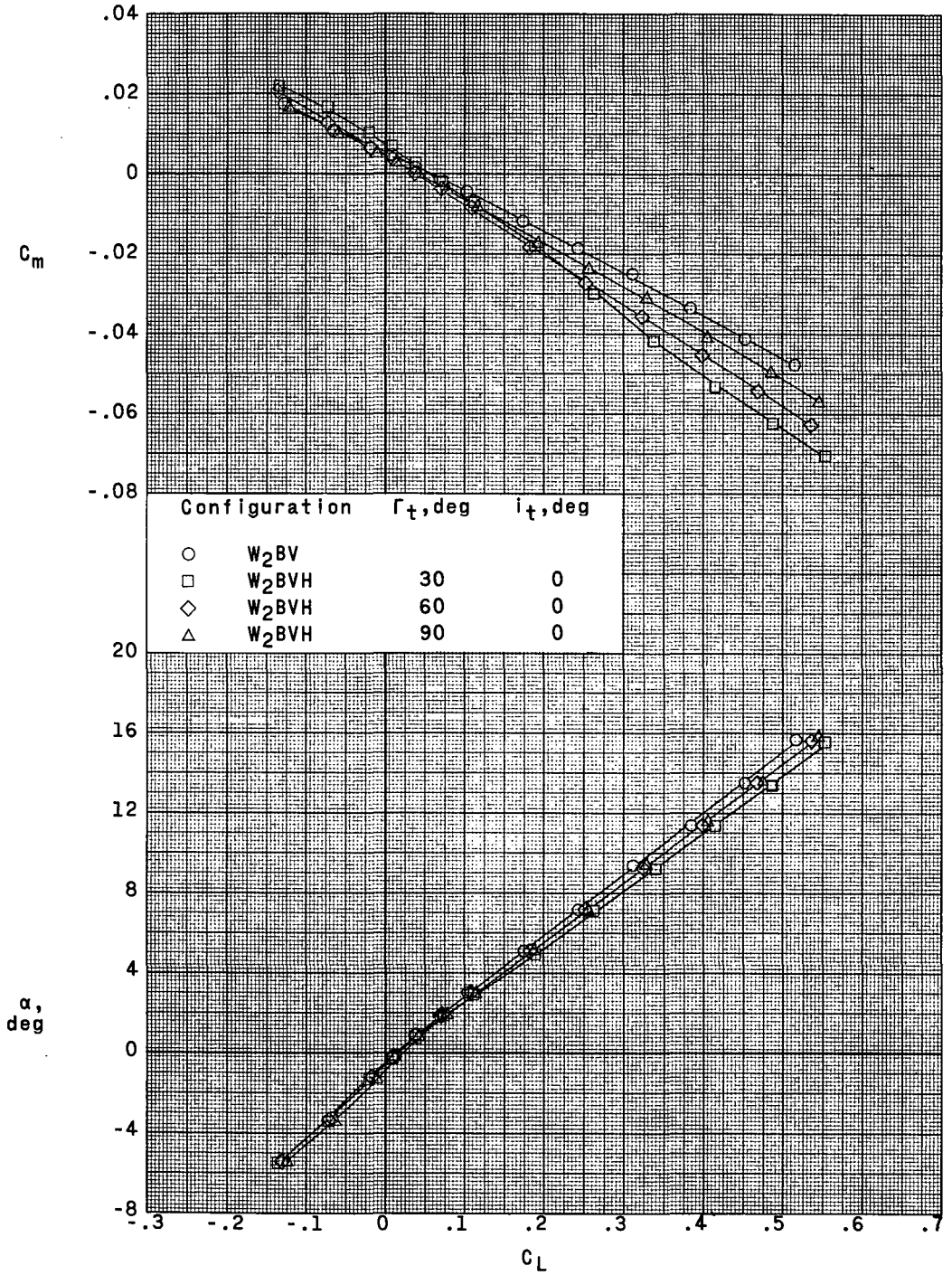

(b) M = 1.90.

Figure 4.- Continued.

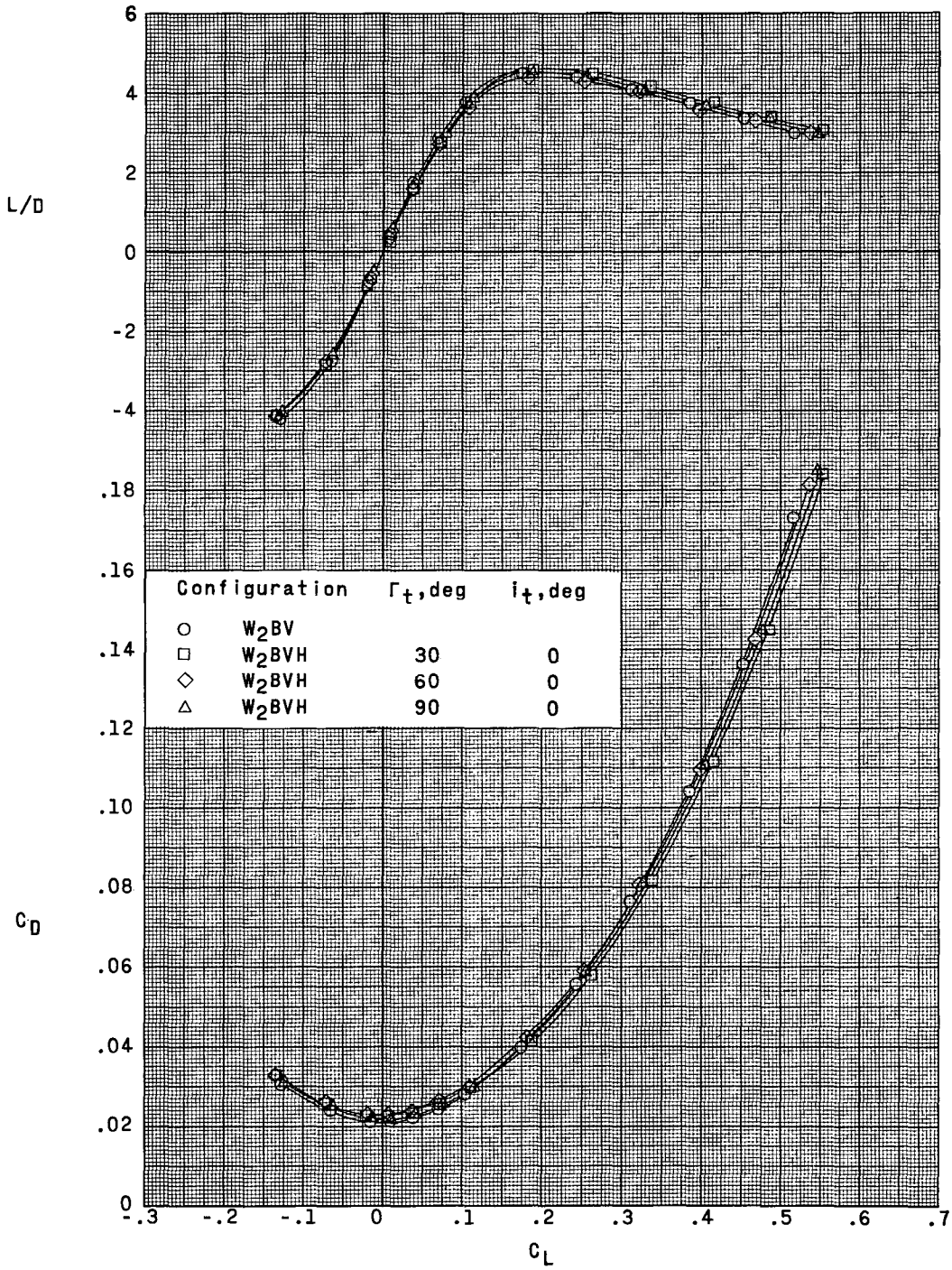

(b) Concluded.

Figure 4.- Continued.

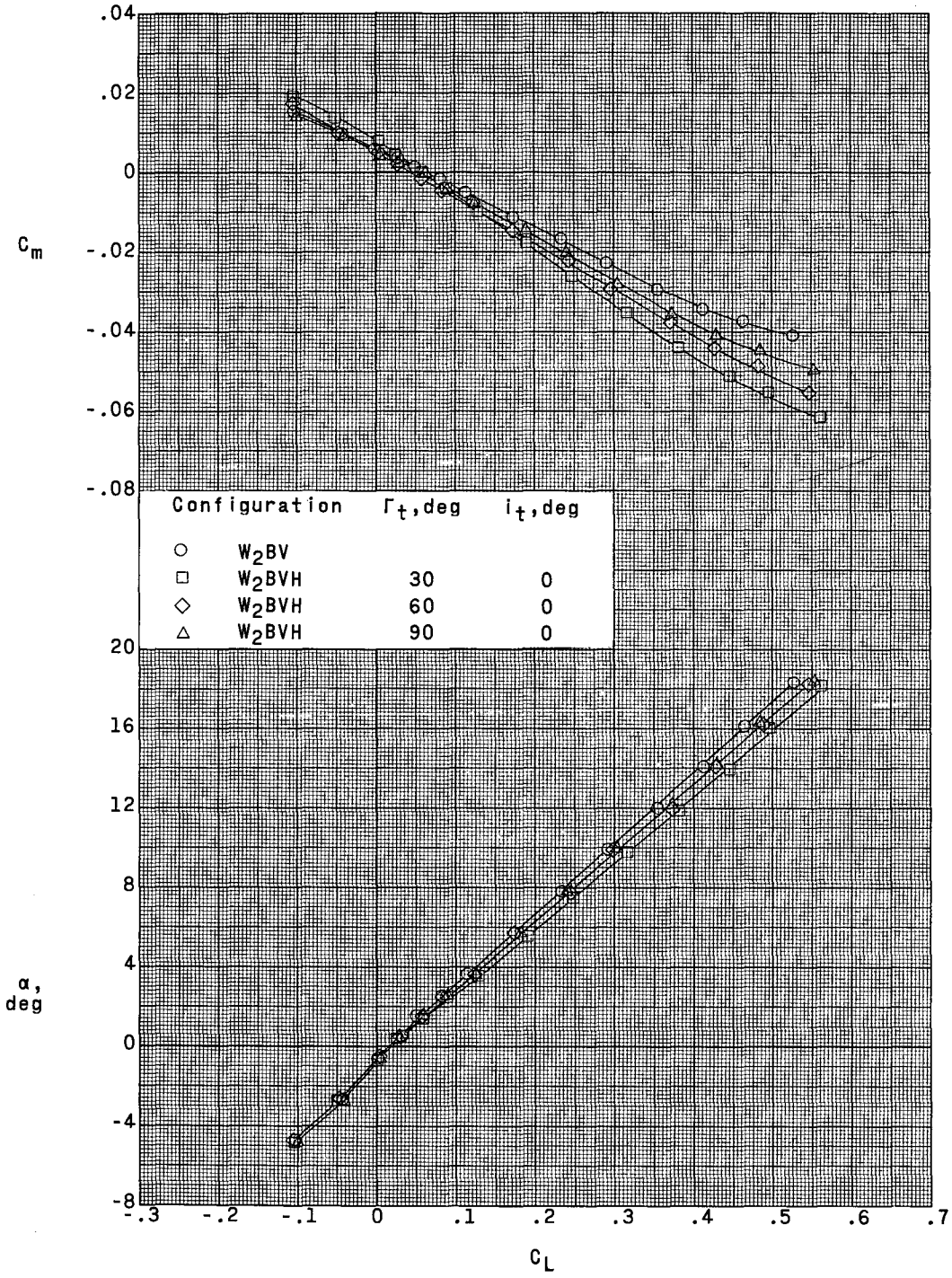

(c) M = 2.36.

Figure 4.- Continued.

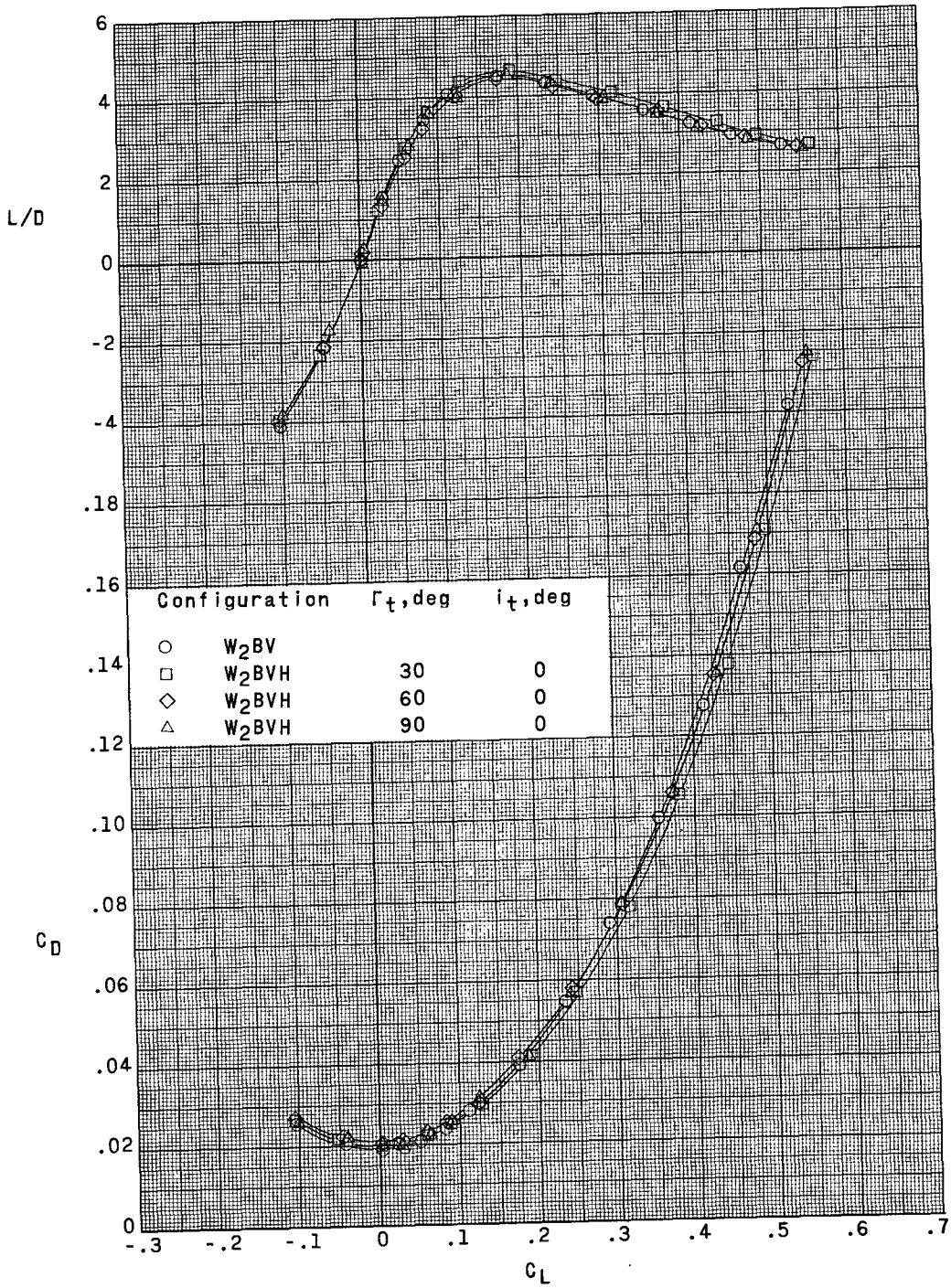

(c) Concluded.

Figure 4.- Continued.

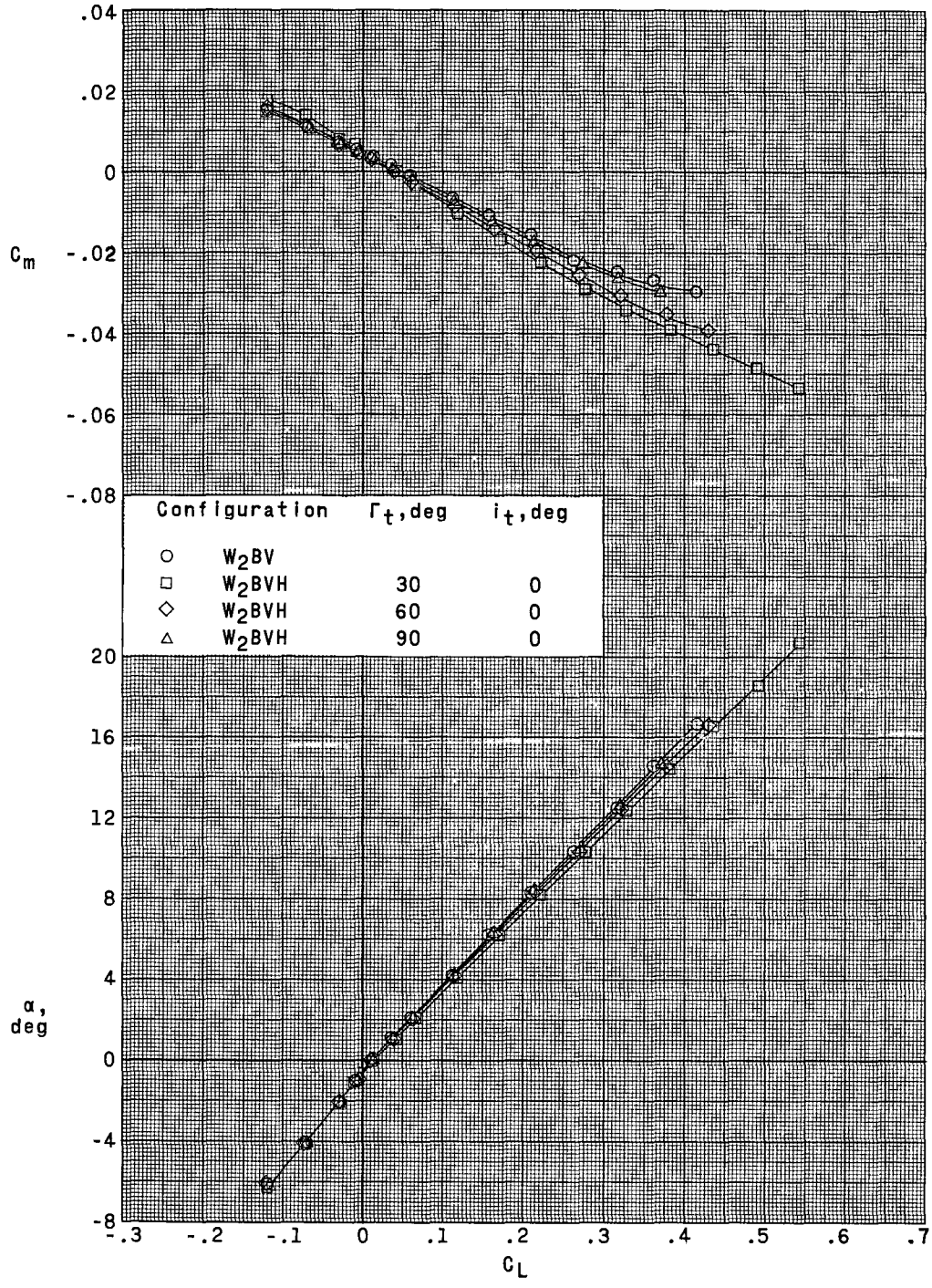

(d) M = 2.86.

Figure 4.- Continued.

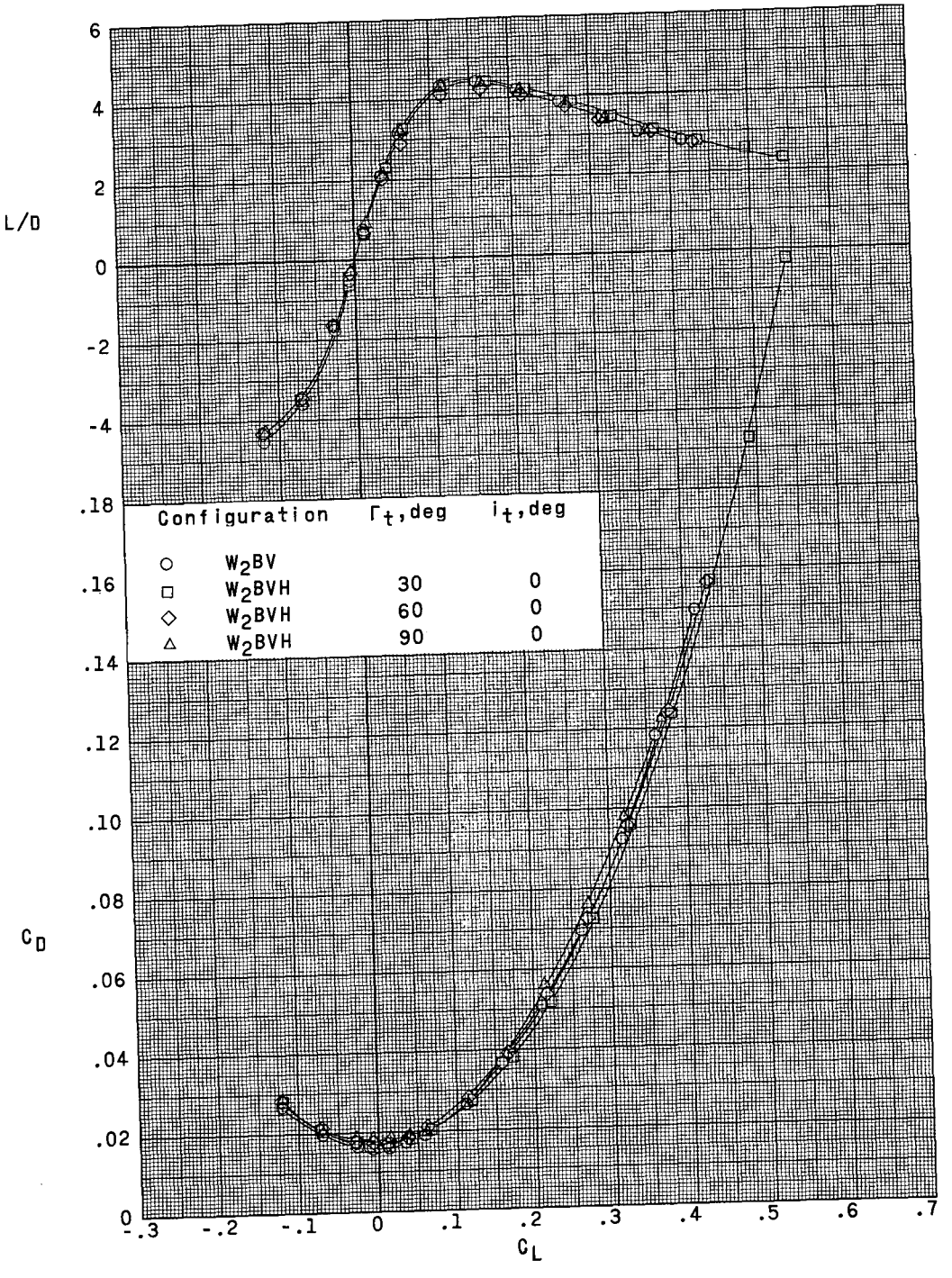

(d) Concluded.

Figure 4.- Continued.

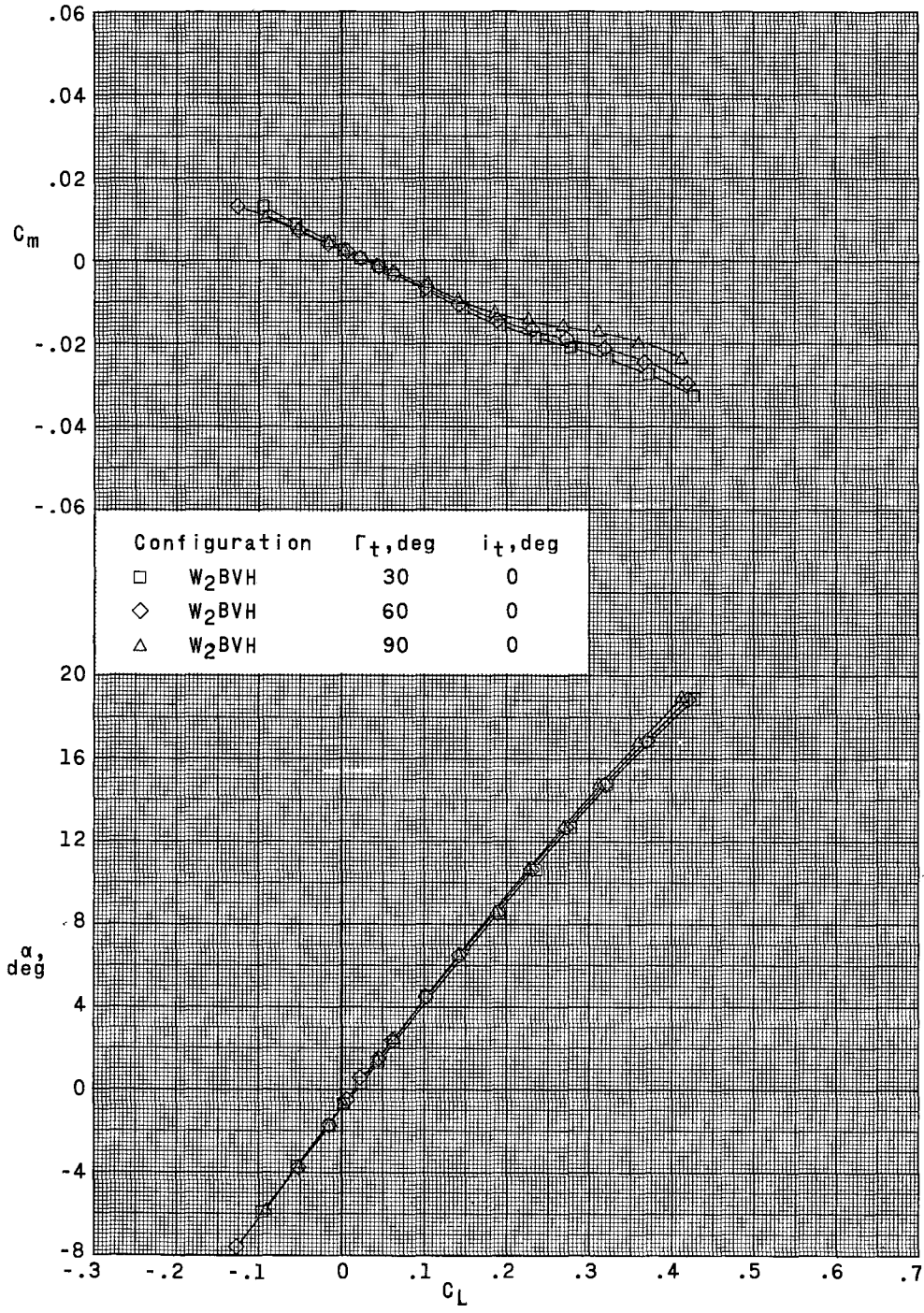

(e) M = 3.96.

Figure 4.- Continued.

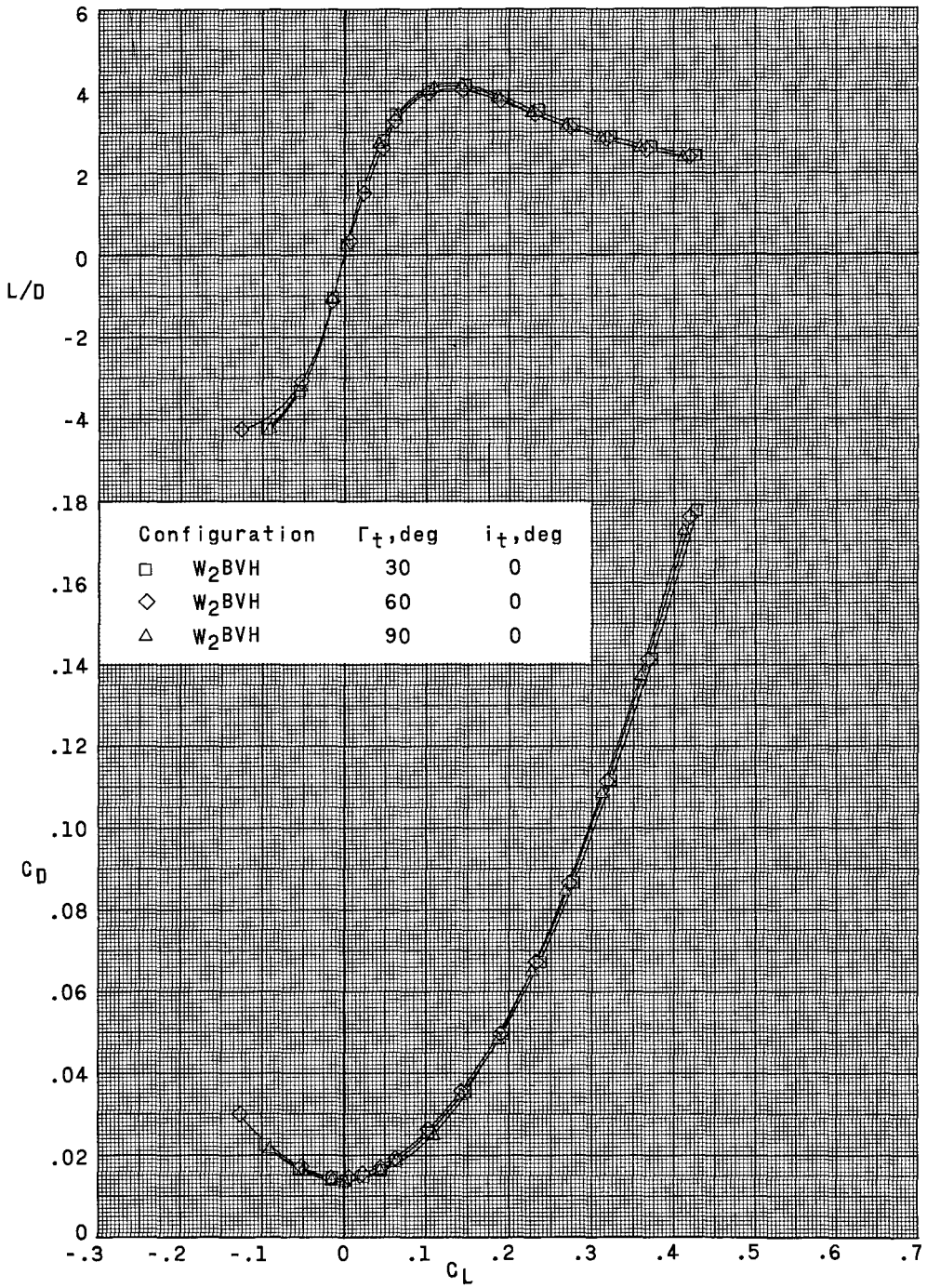

(e) Concluded.

Figure 4.- Continued.

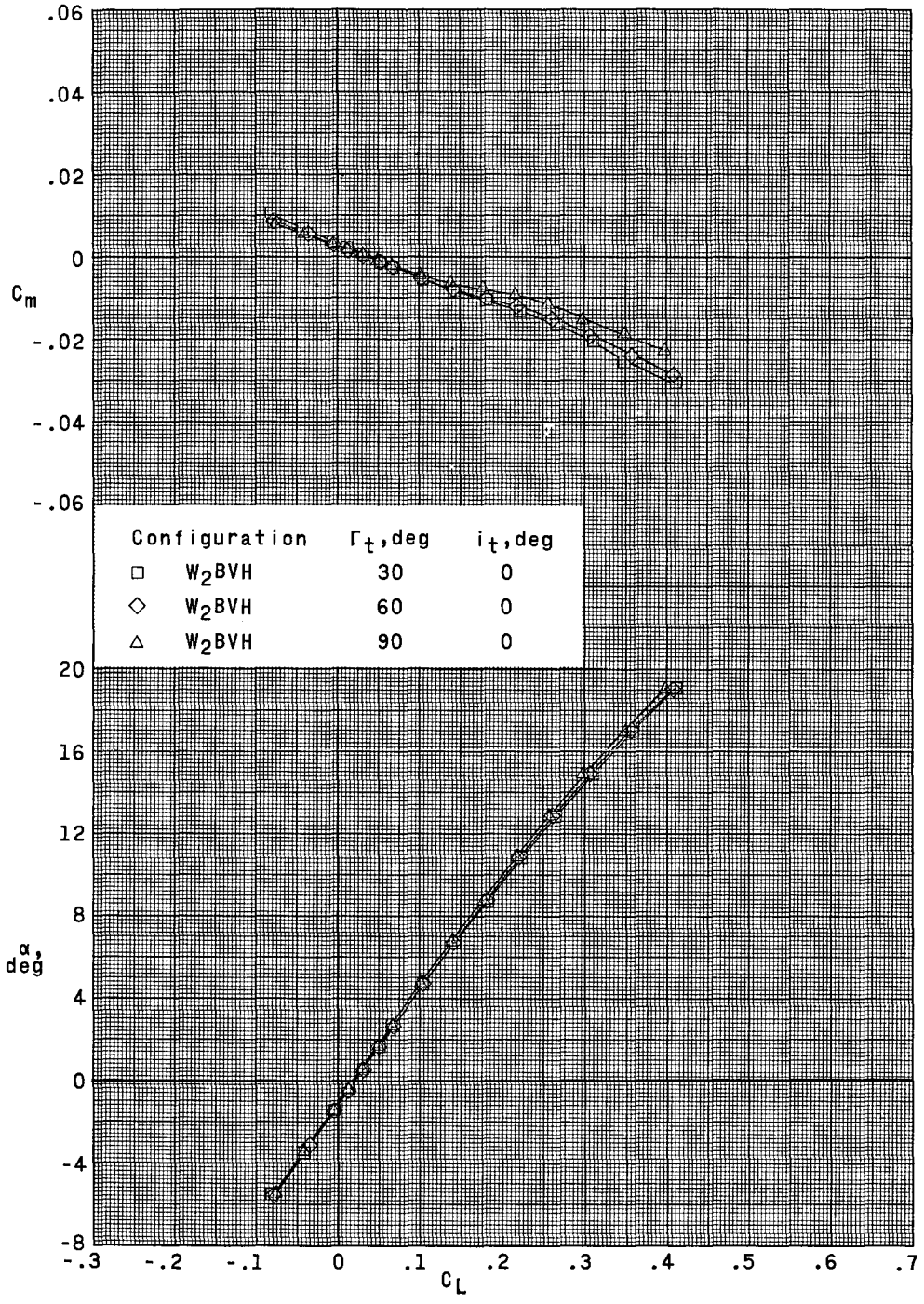

(f) M = 4.65.

Figure 4.- Continued.

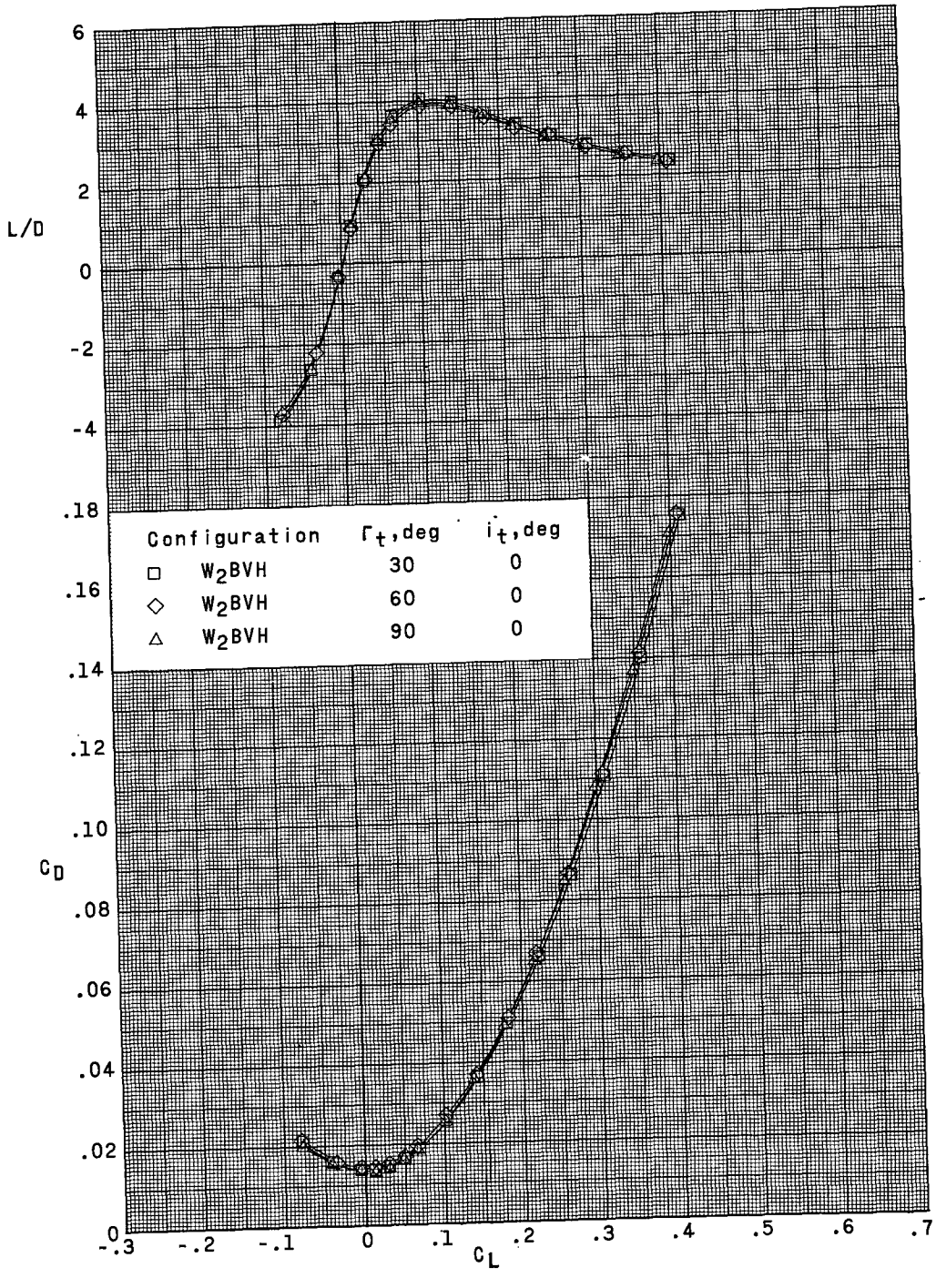

(f) Concluded.

Figure 4.- Concluded.

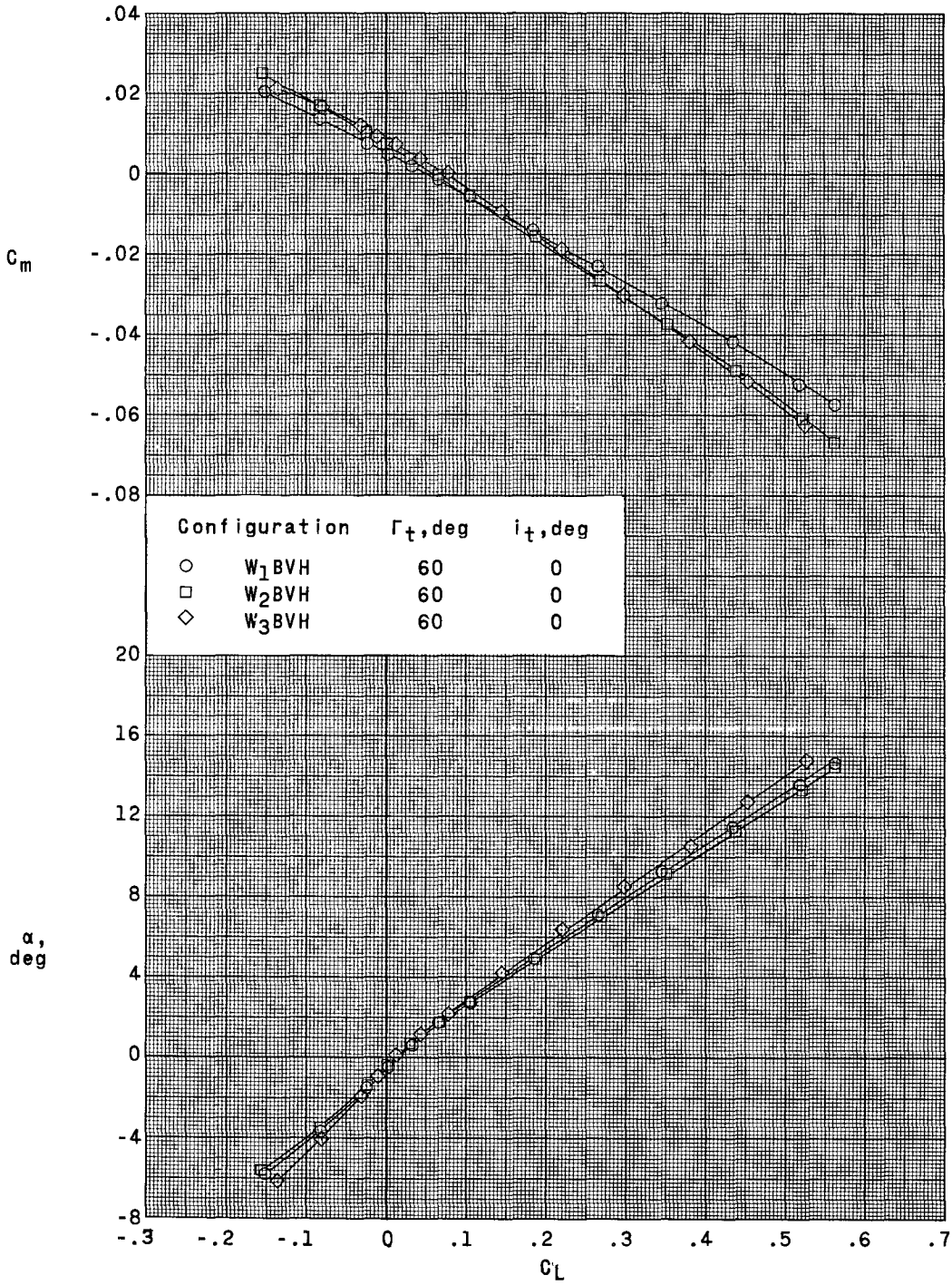

(a) M = 1.60.

Figure 5.- Effect of wing planform on aerodynamic characteristics in pitch.

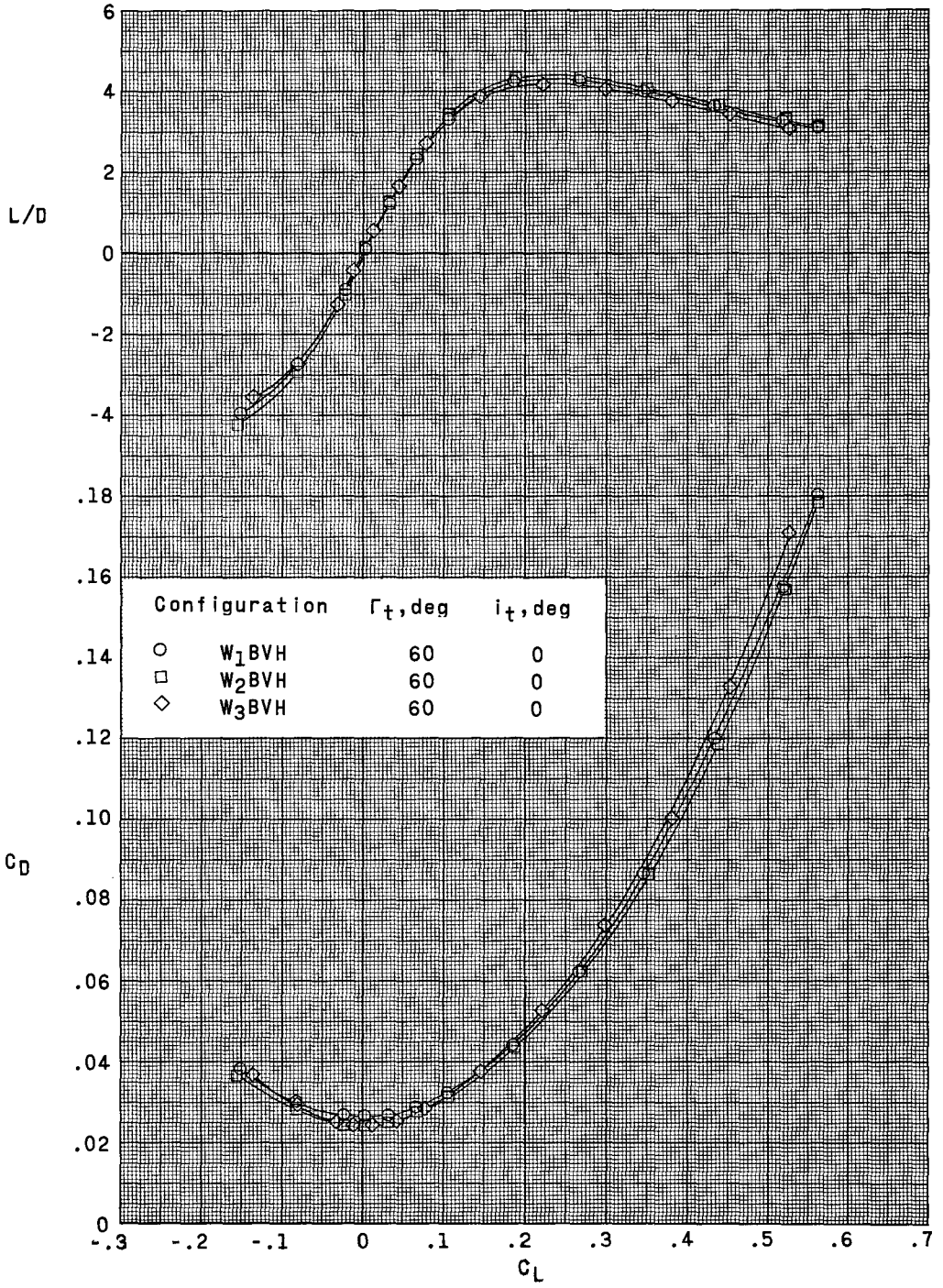

(a) Concluded.

Figure 5.- Continued.

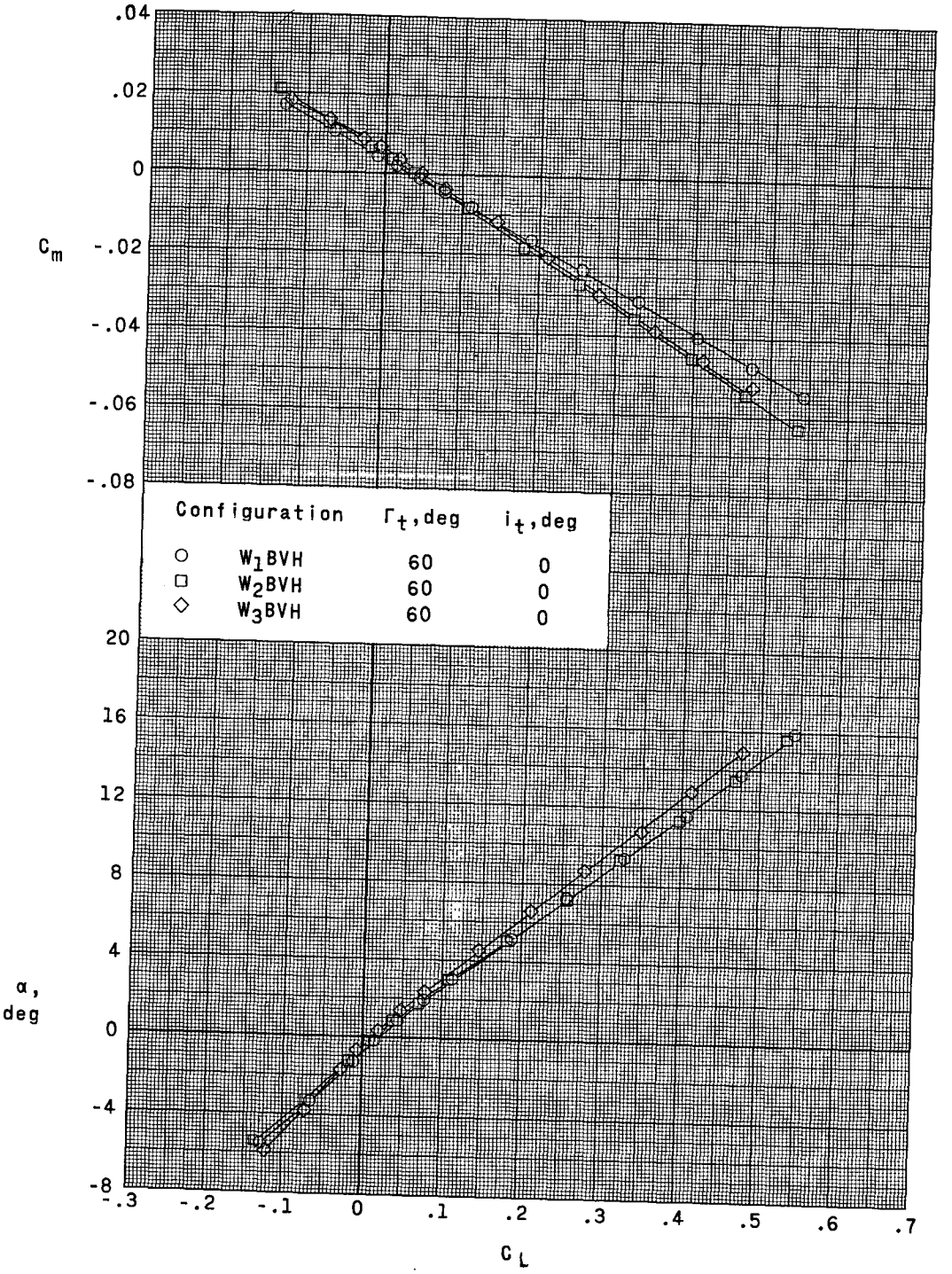

(b) M = 1.90.

Figure 5.- Continued.

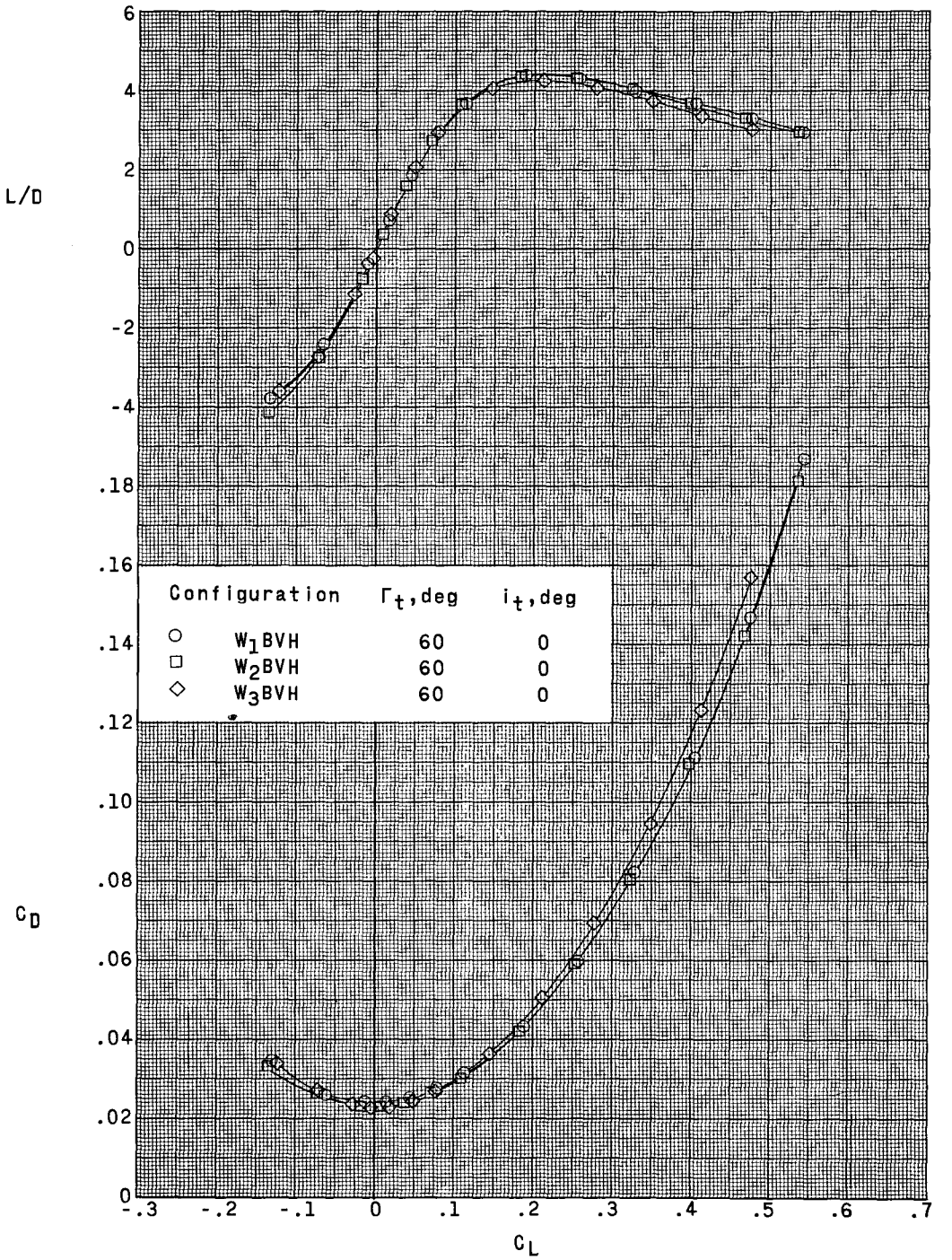

(b) Concluded.

Figure 5.- Continued.

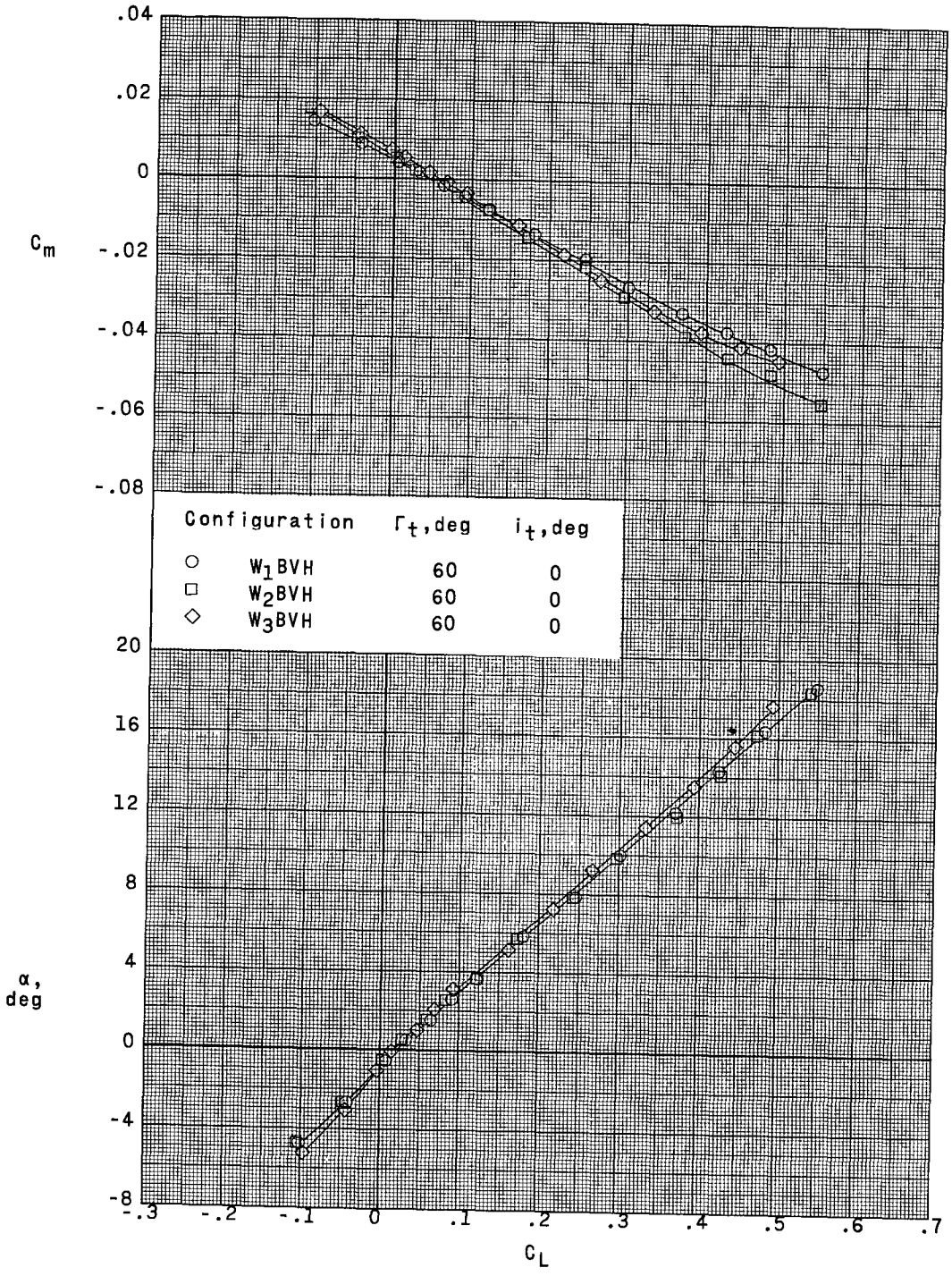

(c) M = 2.36.

Figure 5.- Continued.

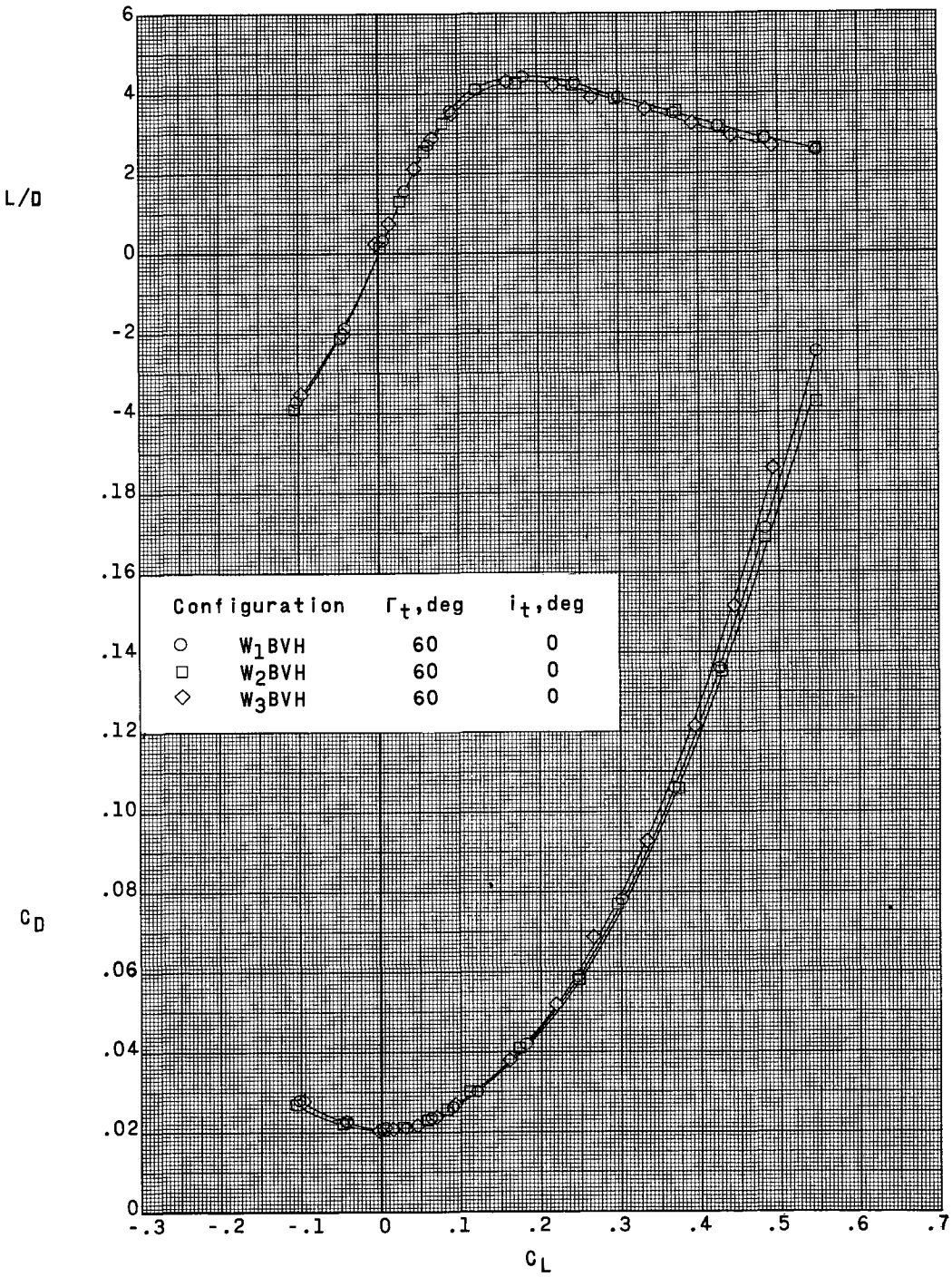

(c) Concluded.

Figure 5.- Continued.

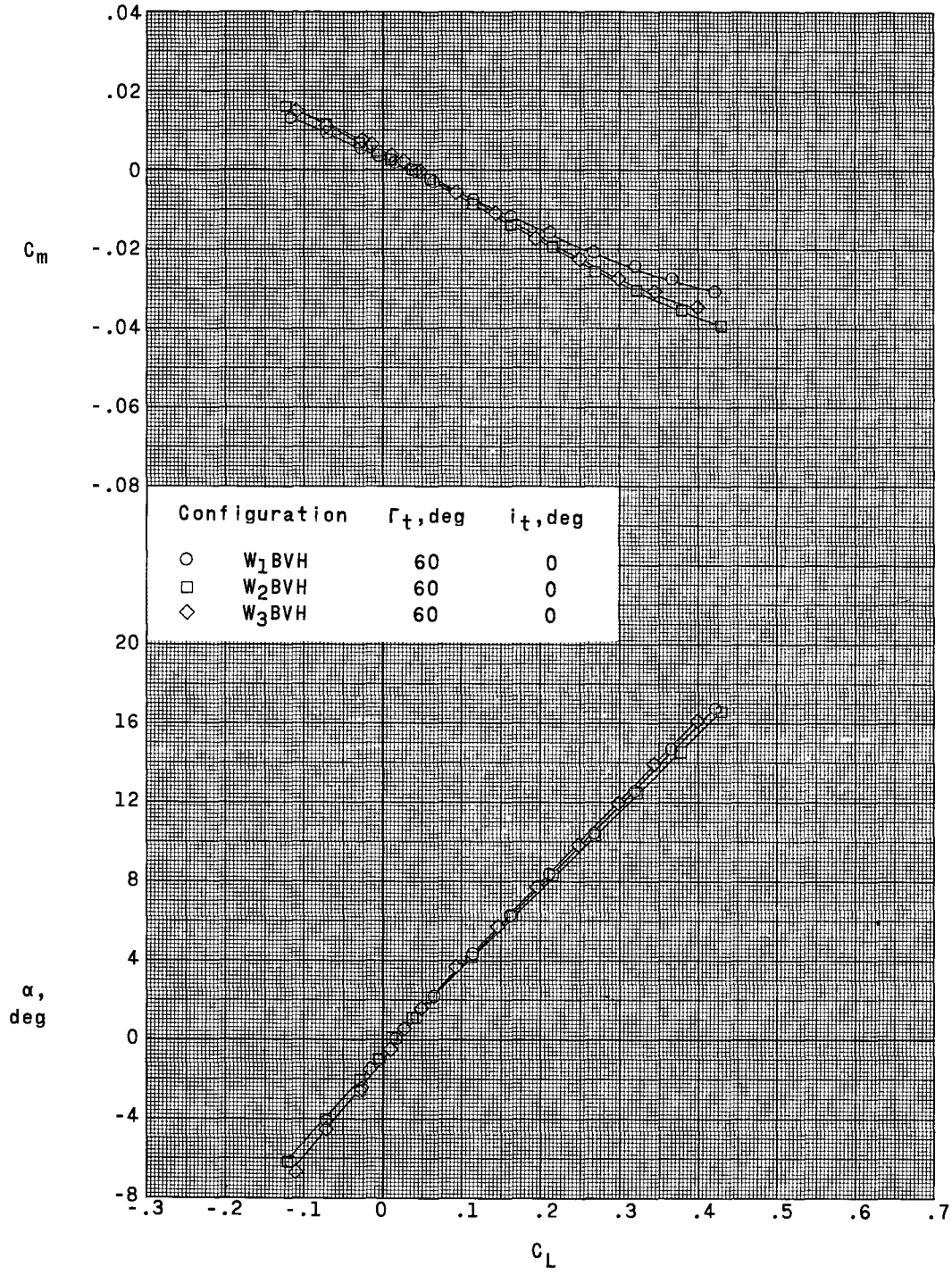

(d) M = 2.86.

Figure 5.- Continued.

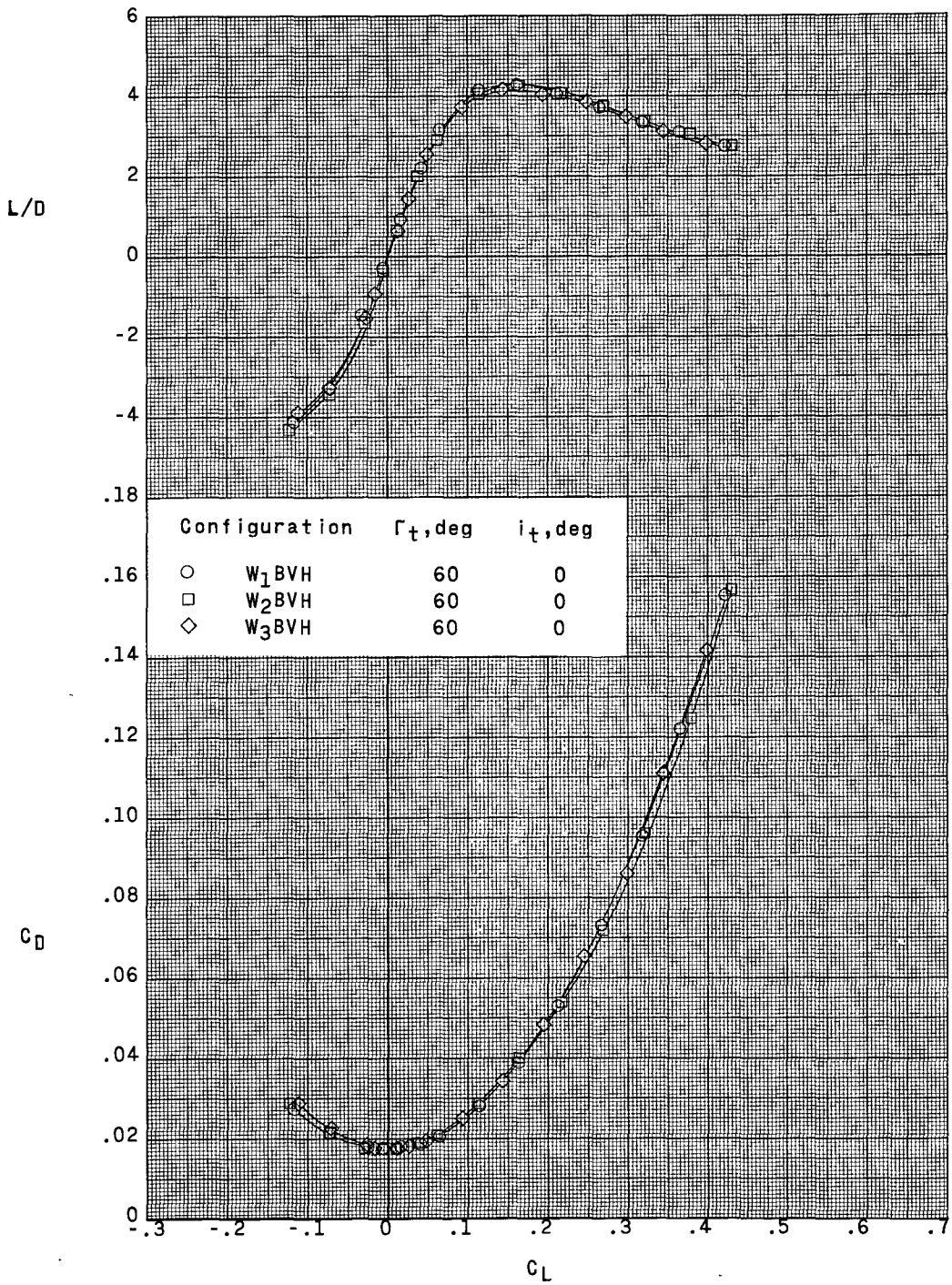

(d) Concluded.

Figure 5.- Continued.

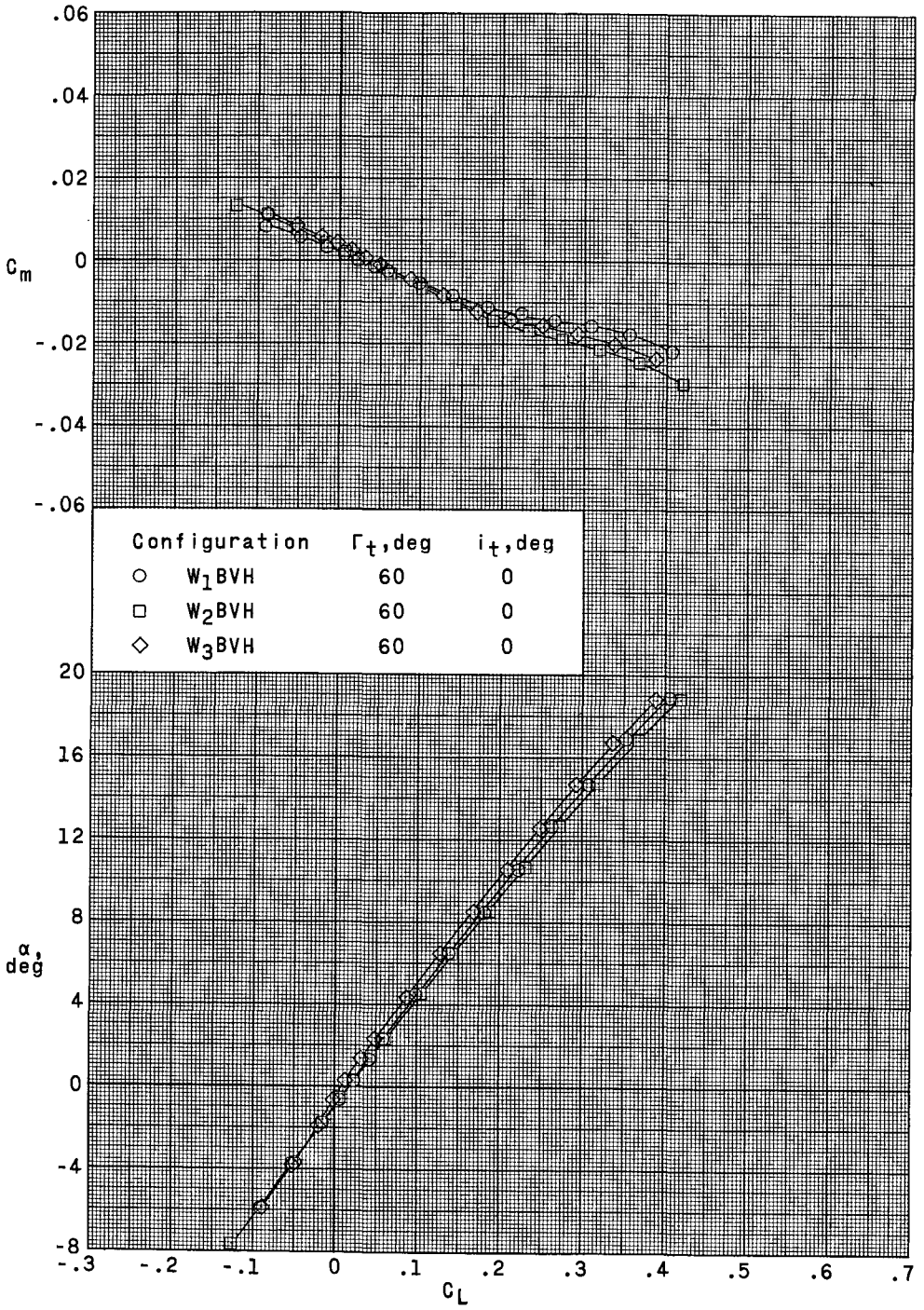

(e) M = 3.96.

Figure 5.- Continued.

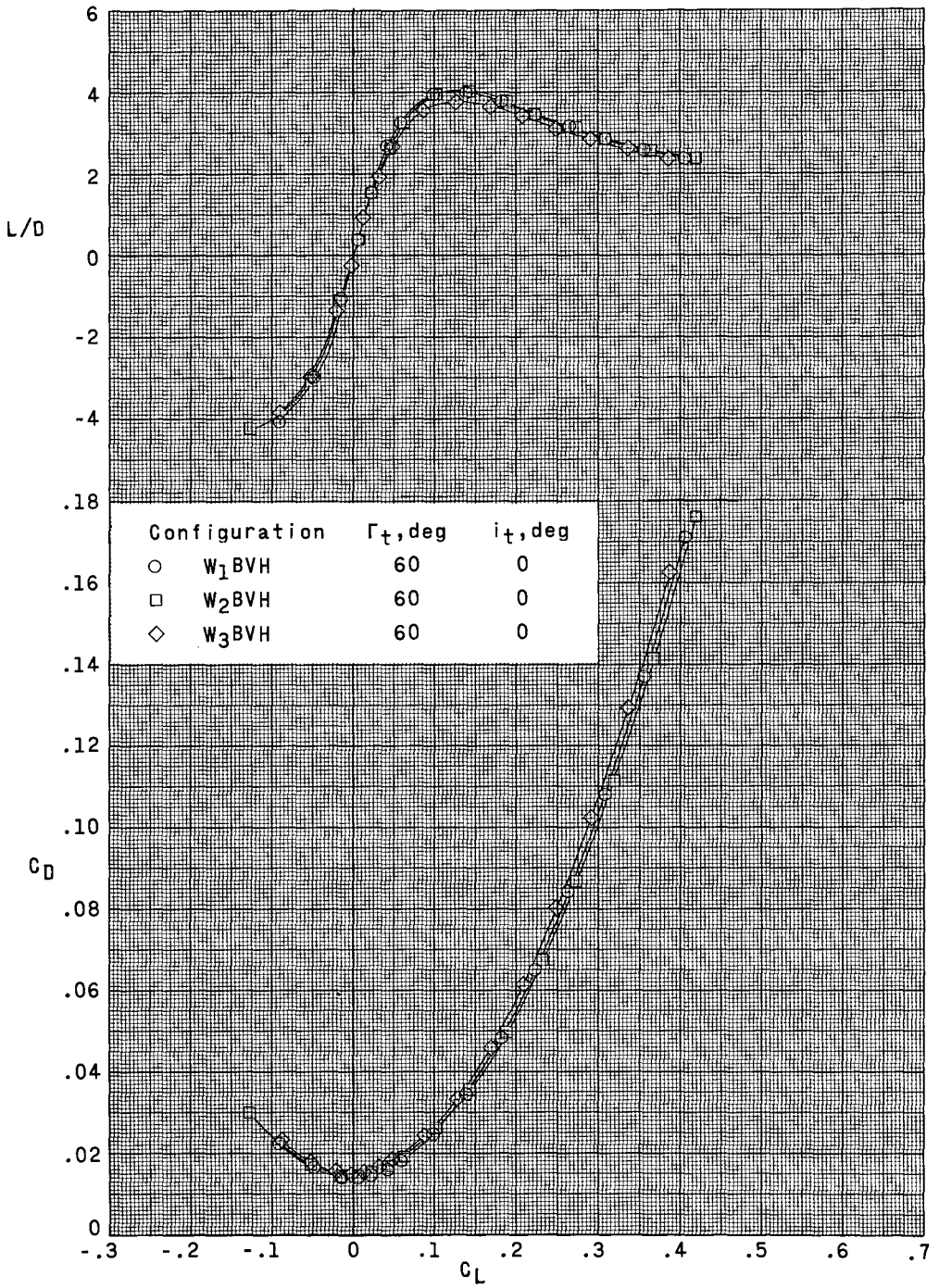

(e) Concluded.

Figure 5.- Continued.

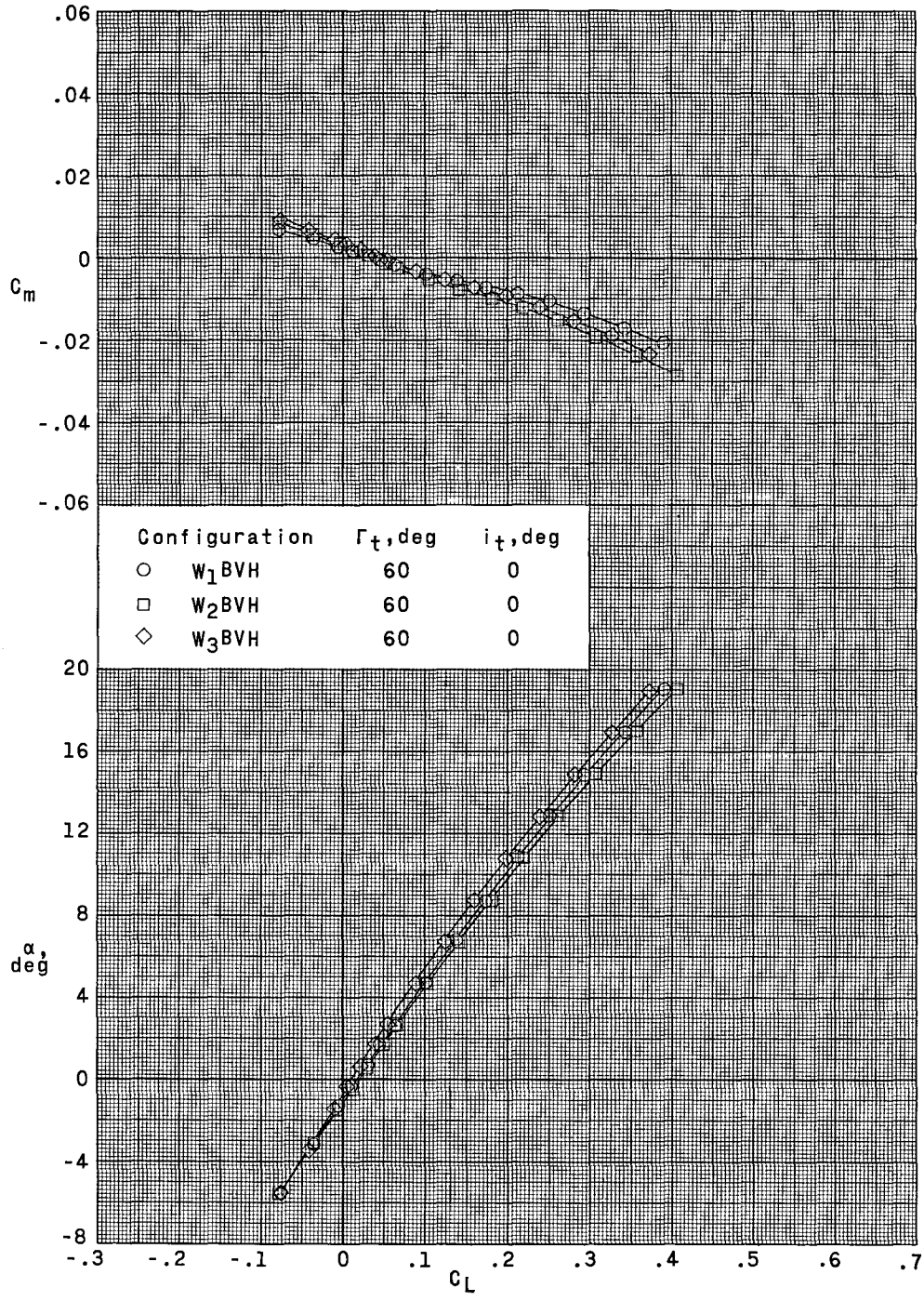

(f) M = 4.65.

Figure 5.- Continued.

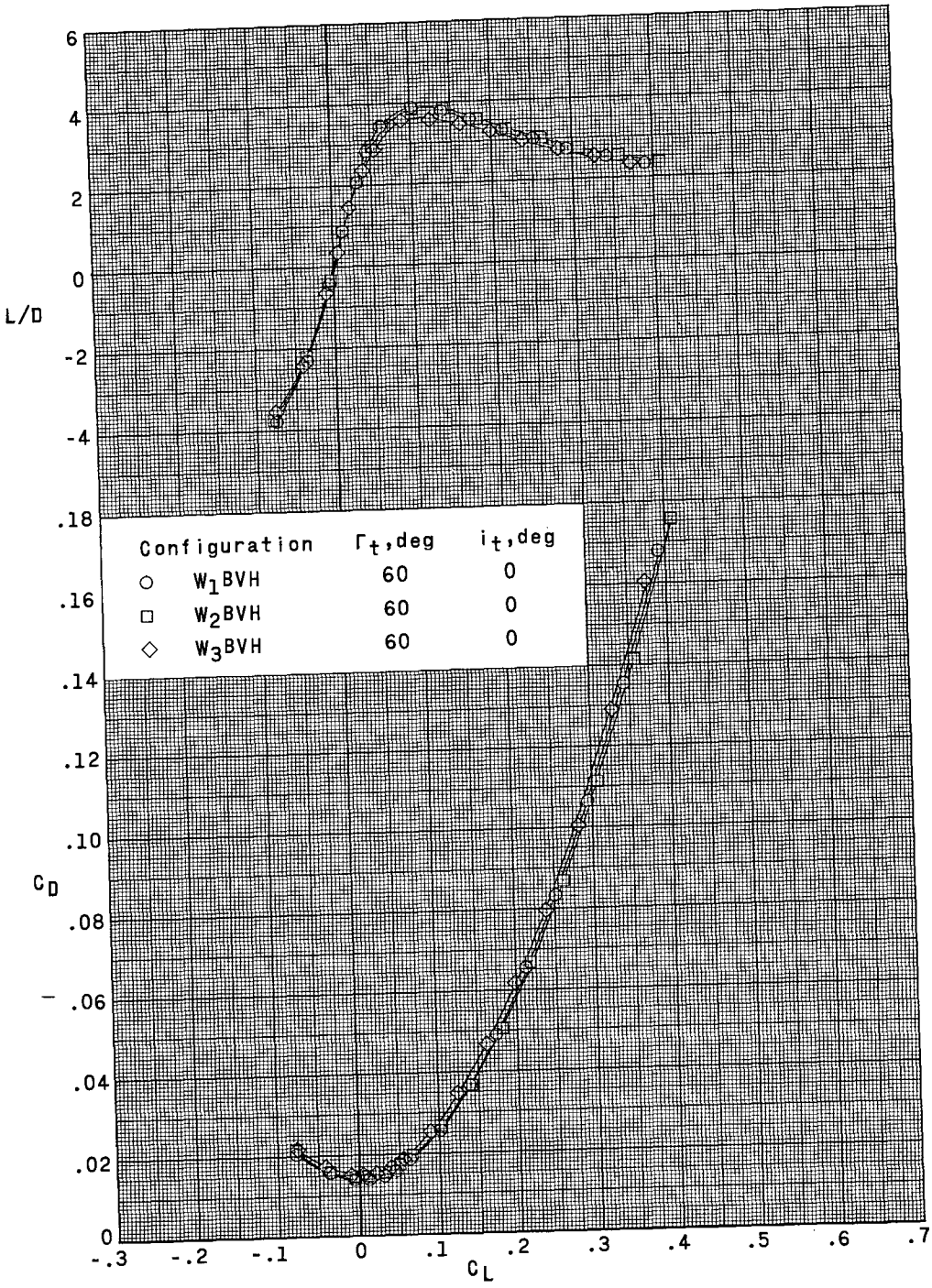

(f) Concluded.

Figure 5.- Concluded.

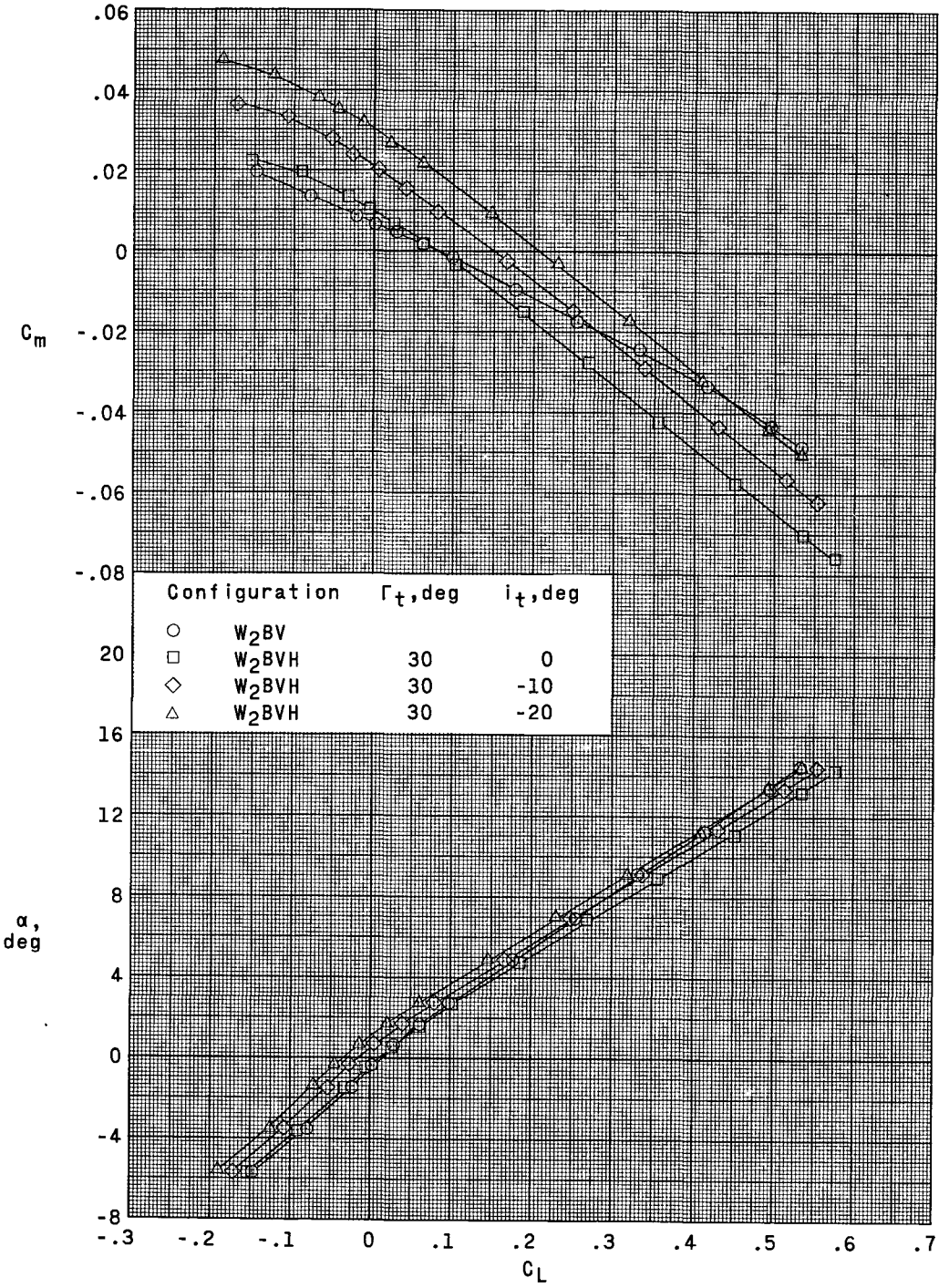

(a) M = 1.60.

Figure 6.- Effect of horizontal-stabilizer deflection on aerodynamic characteristics in pitch. $\Gamma_t = 30^{\circ}$.

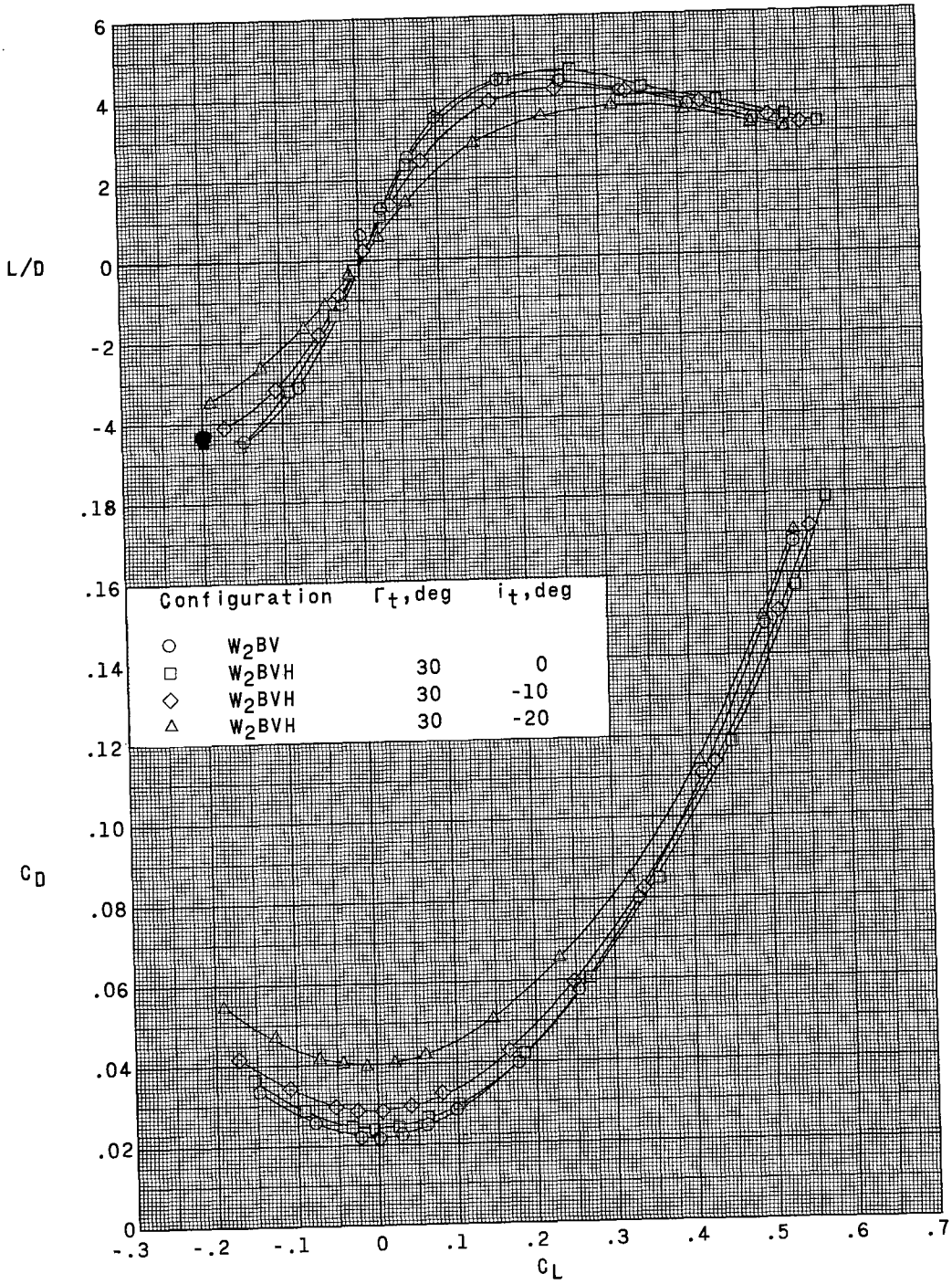

(a) Concluded.

Figure 6.- Continued.

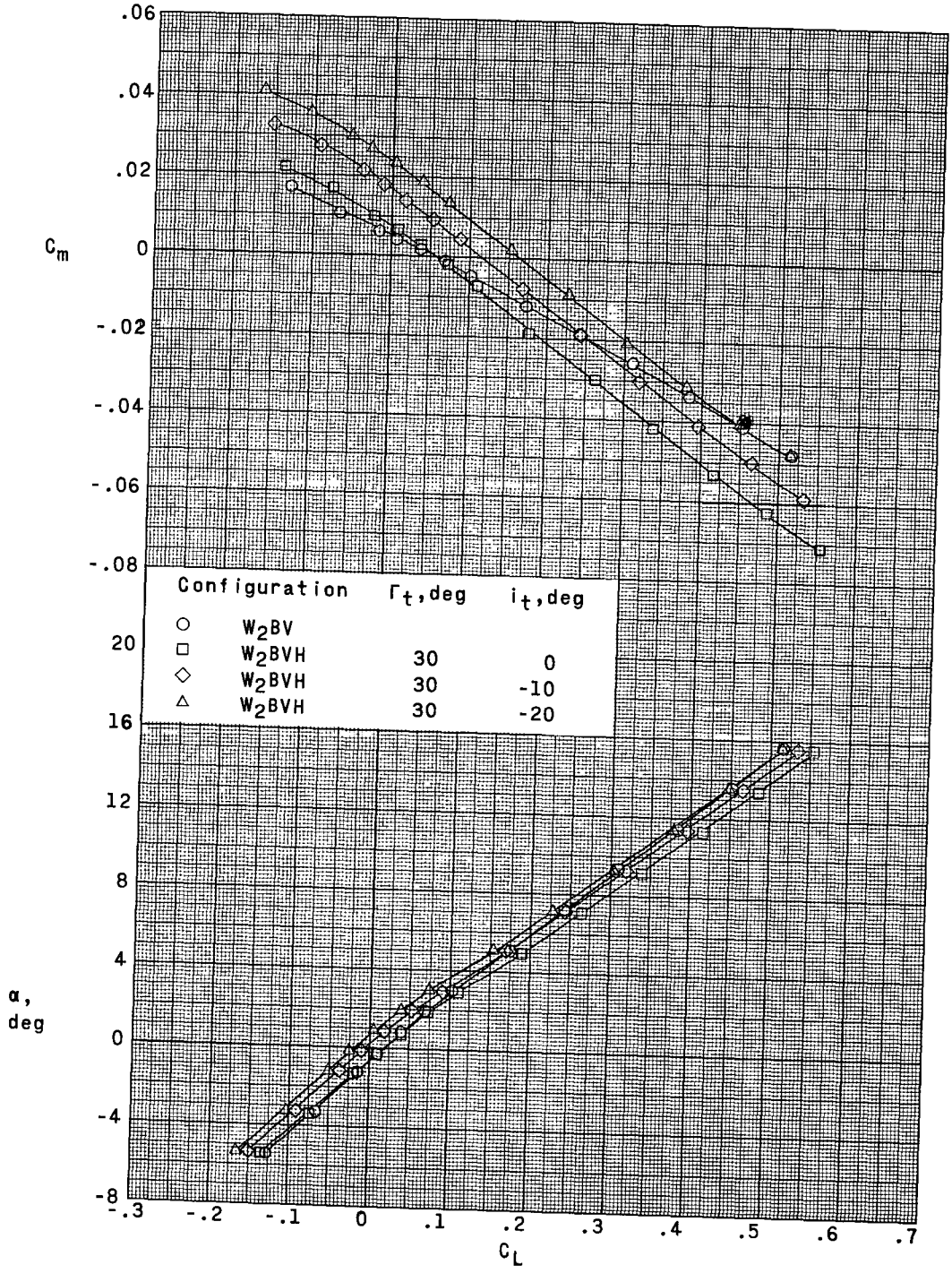

(b) M = 1.90.

Figure 6.- Continued.

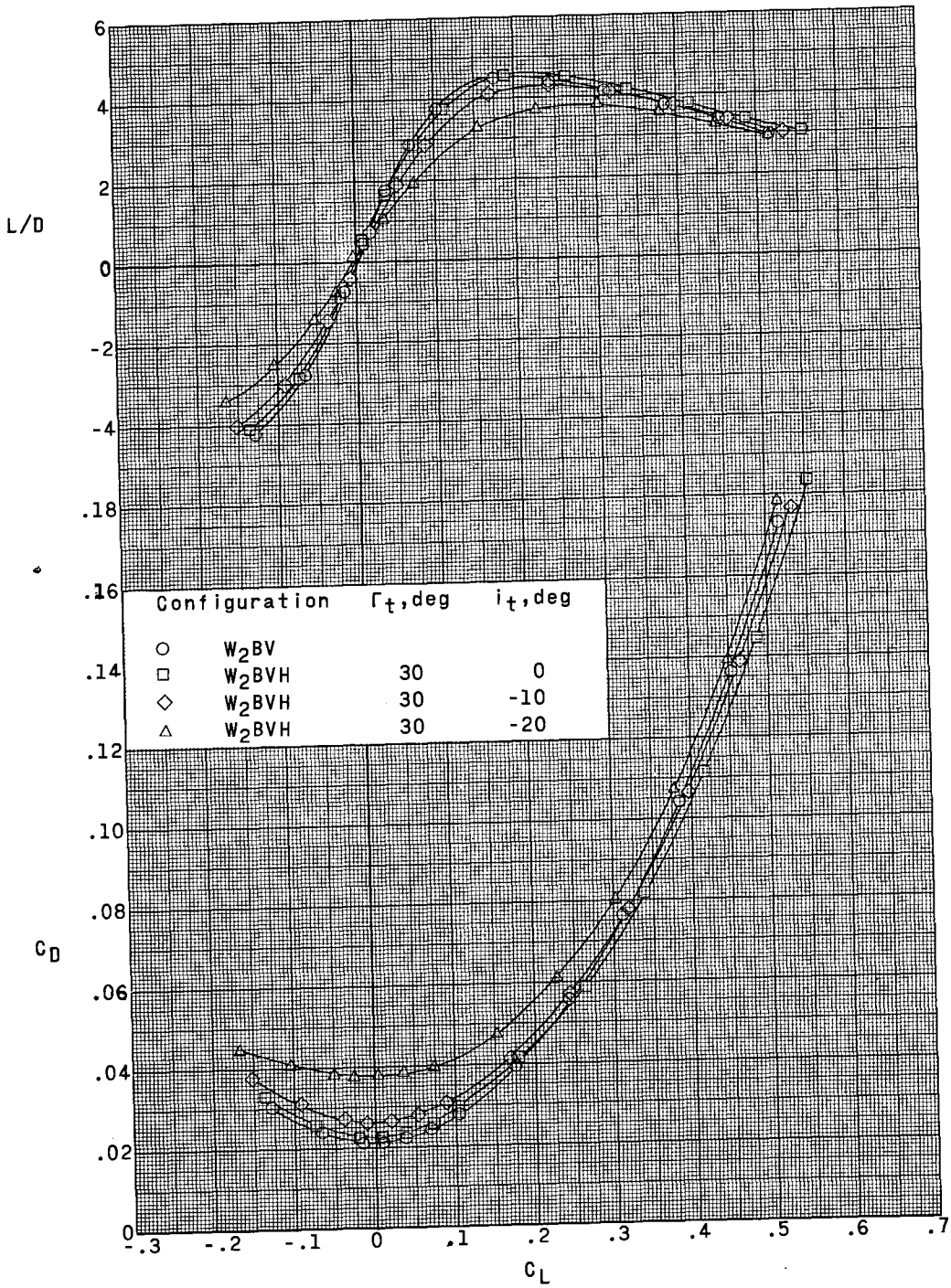

(b) Concluded.

Figure 6.- Continued.

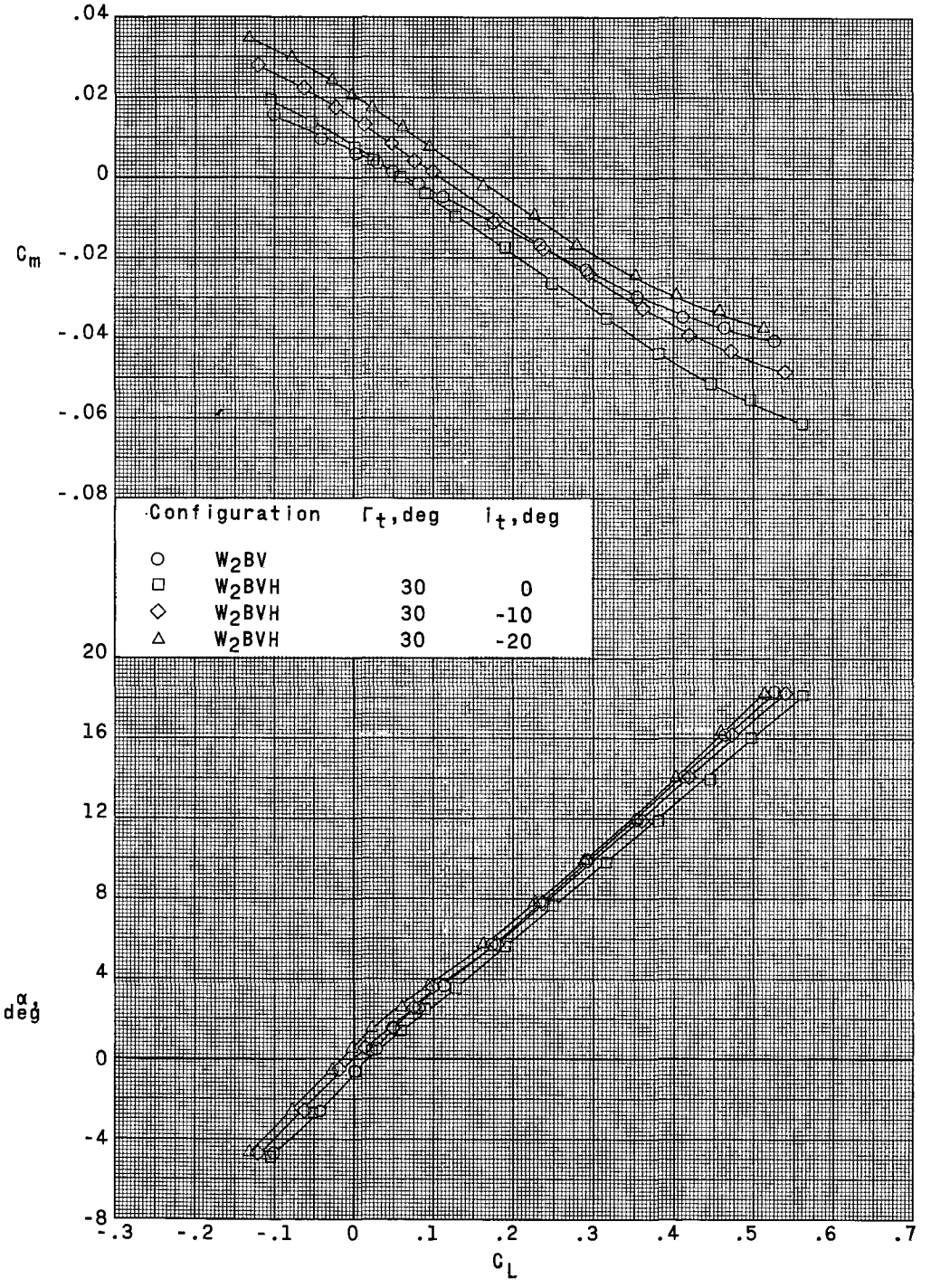

(c) M = 2.36.

Figure 6.- Continued.

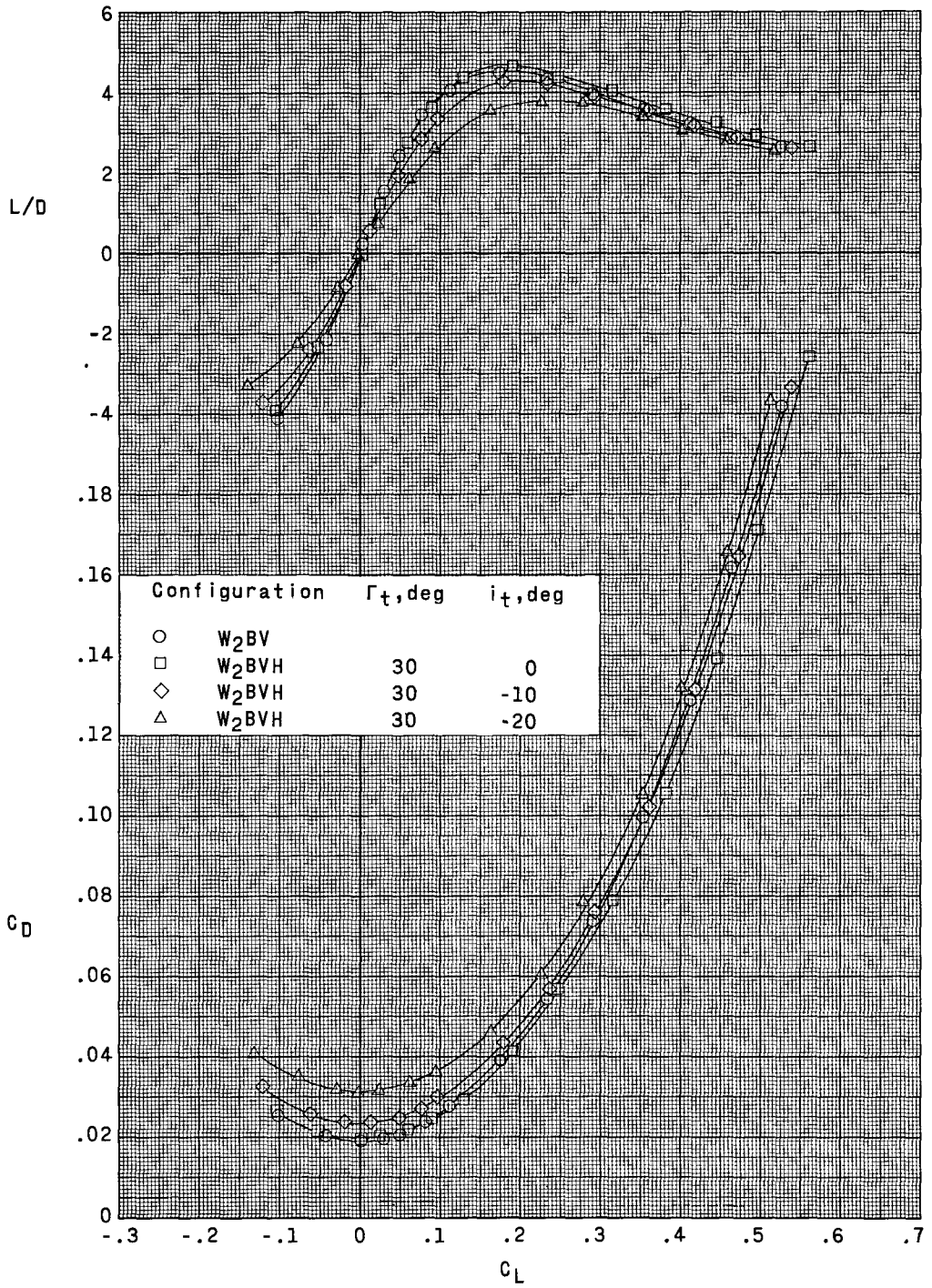

(c) Concluded.

Figure 6.- Continued.

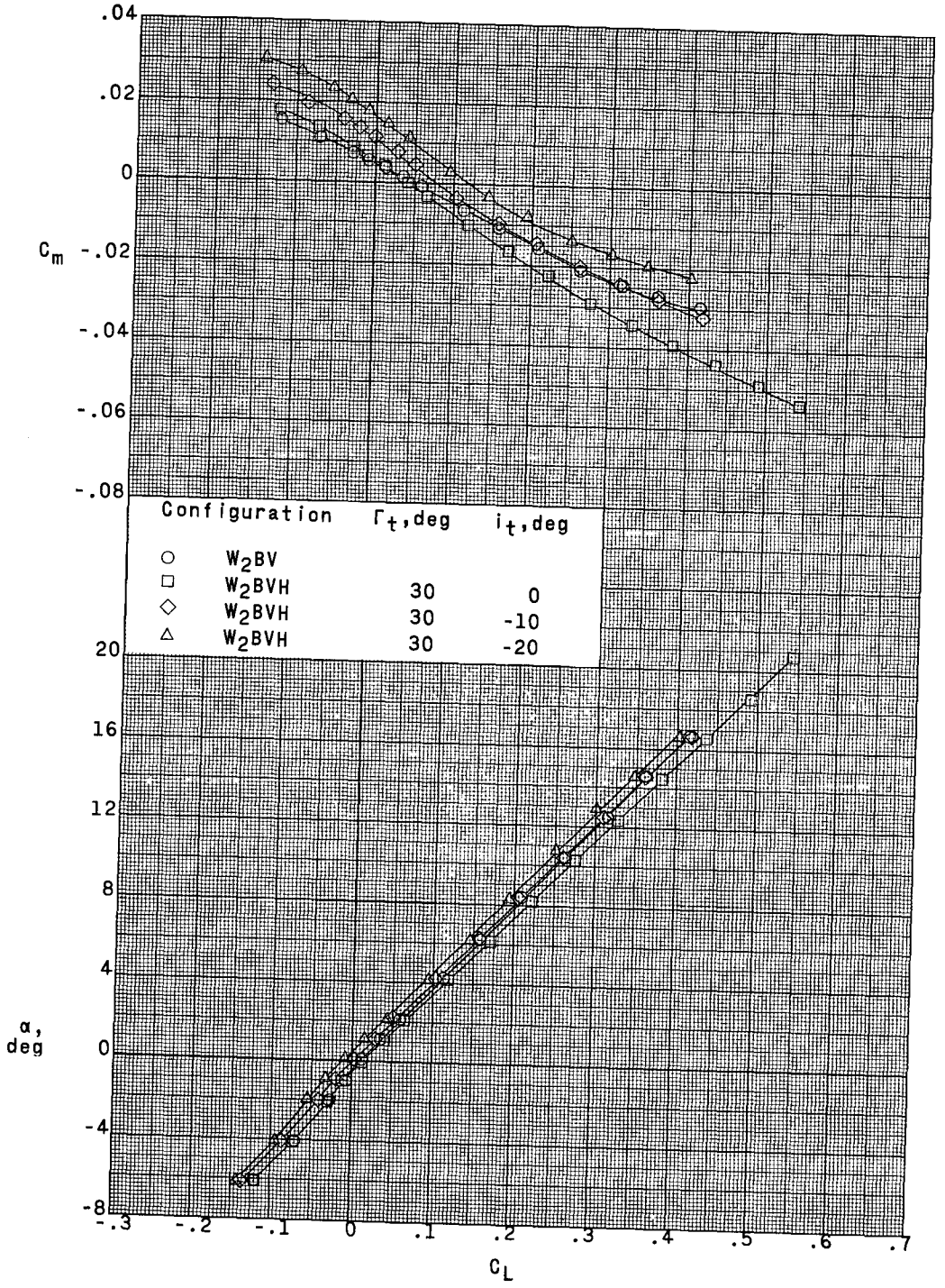

(d) M = 2.86.

Figure 6.- Continued.

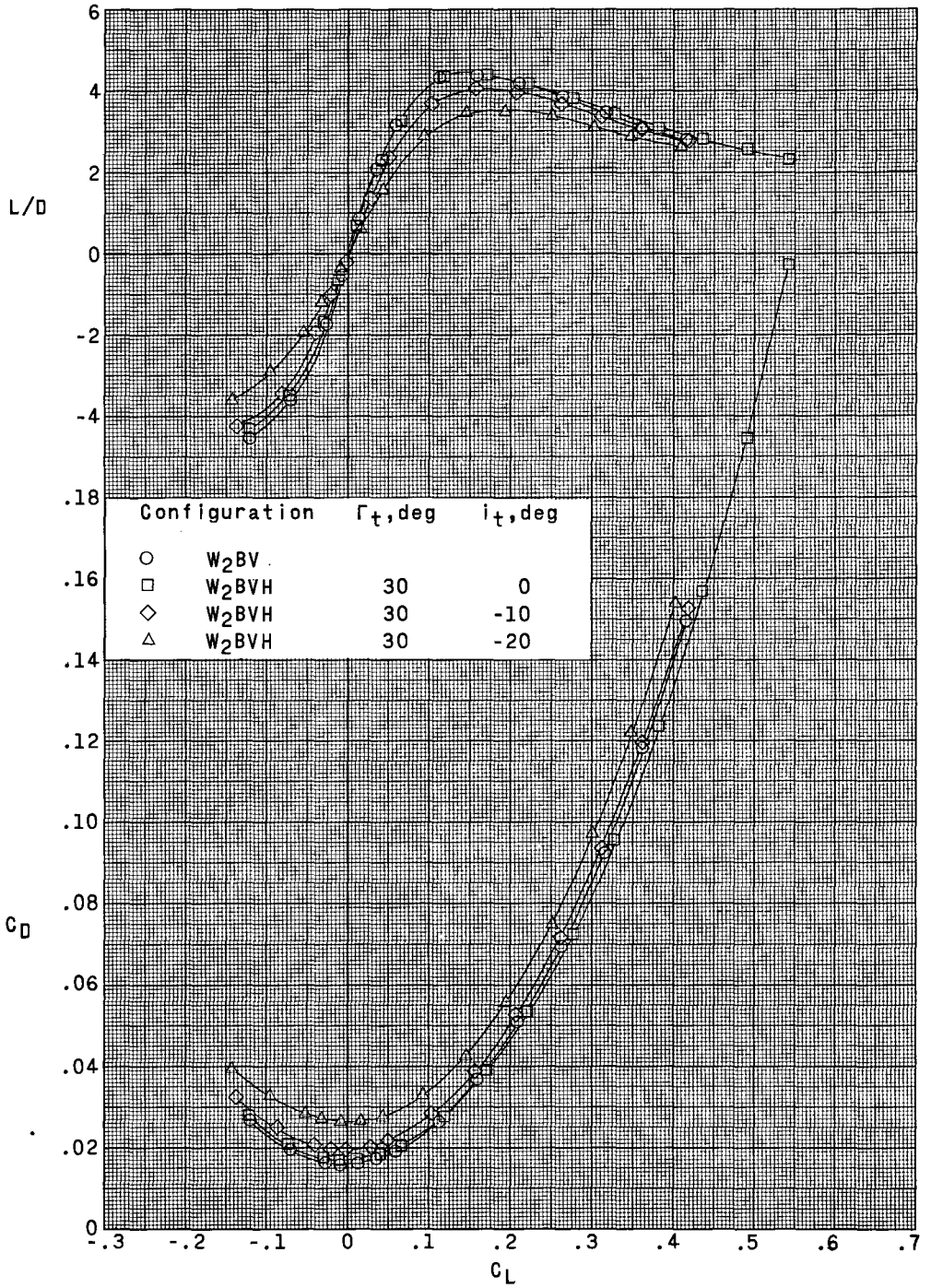

(d) Concluded.

Figure 6.- Continued.

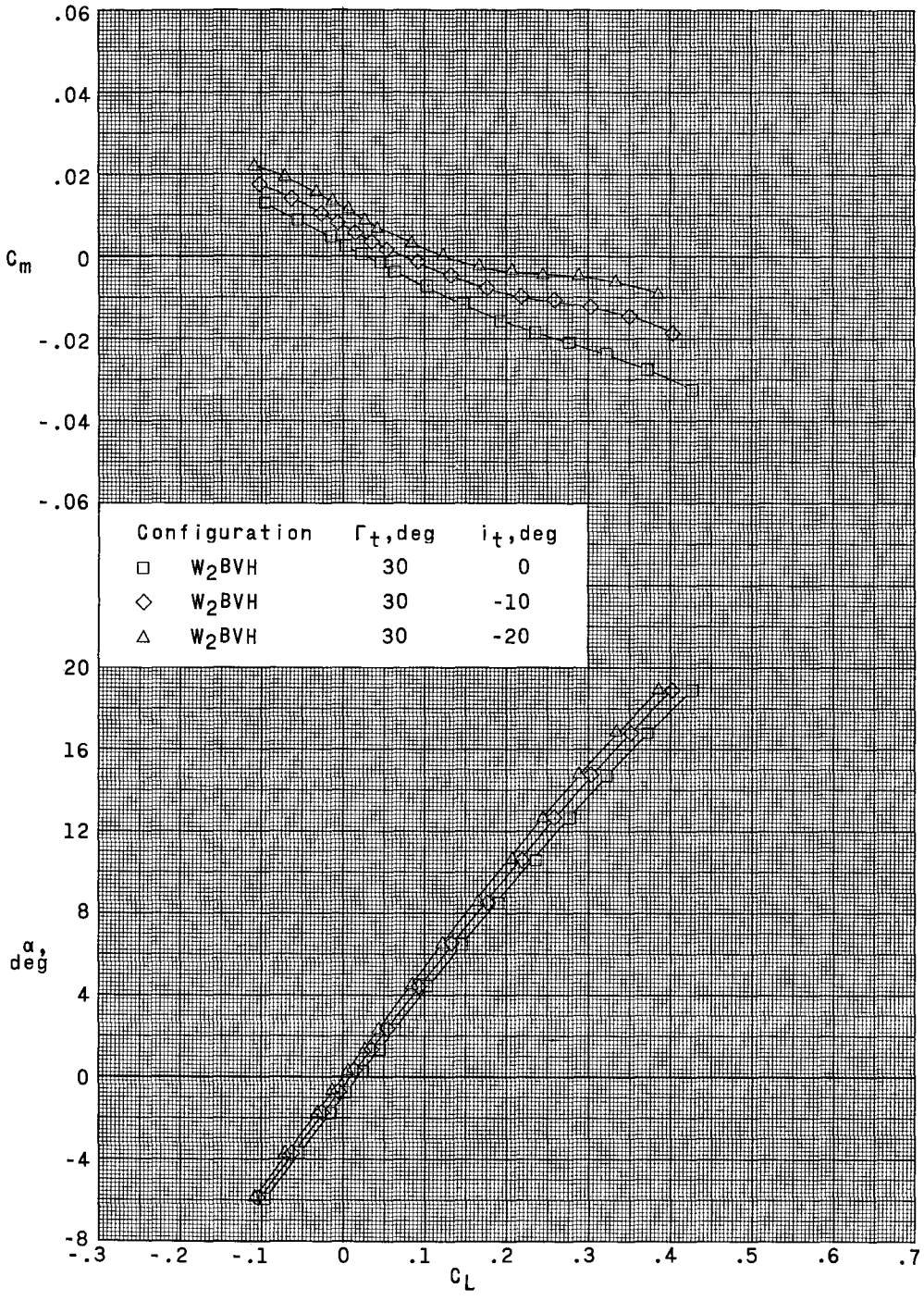

(e) M = 3.96.

Figure 6.- Continued.

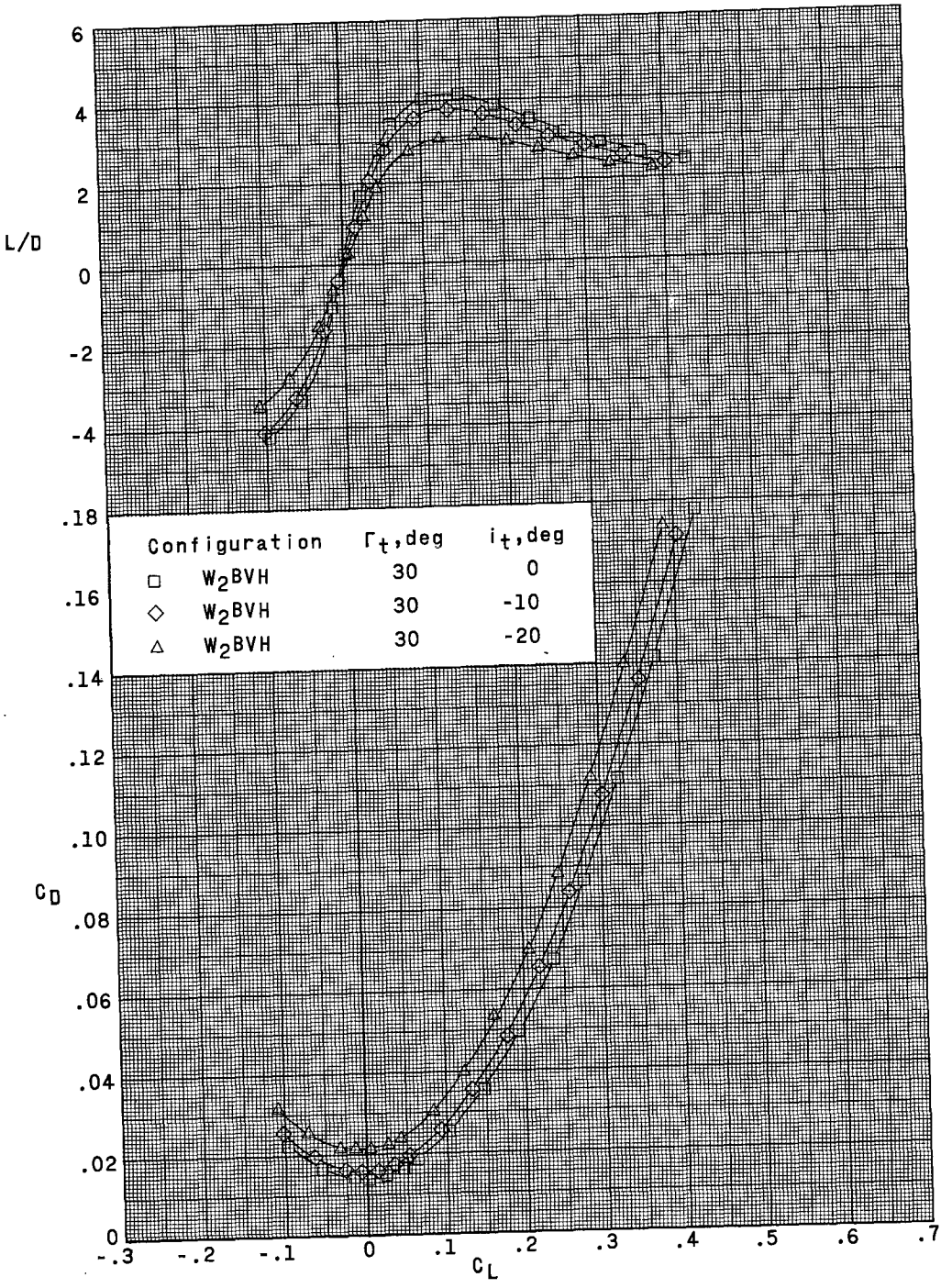

(e) Concluded.

Figure 6.- Continued.

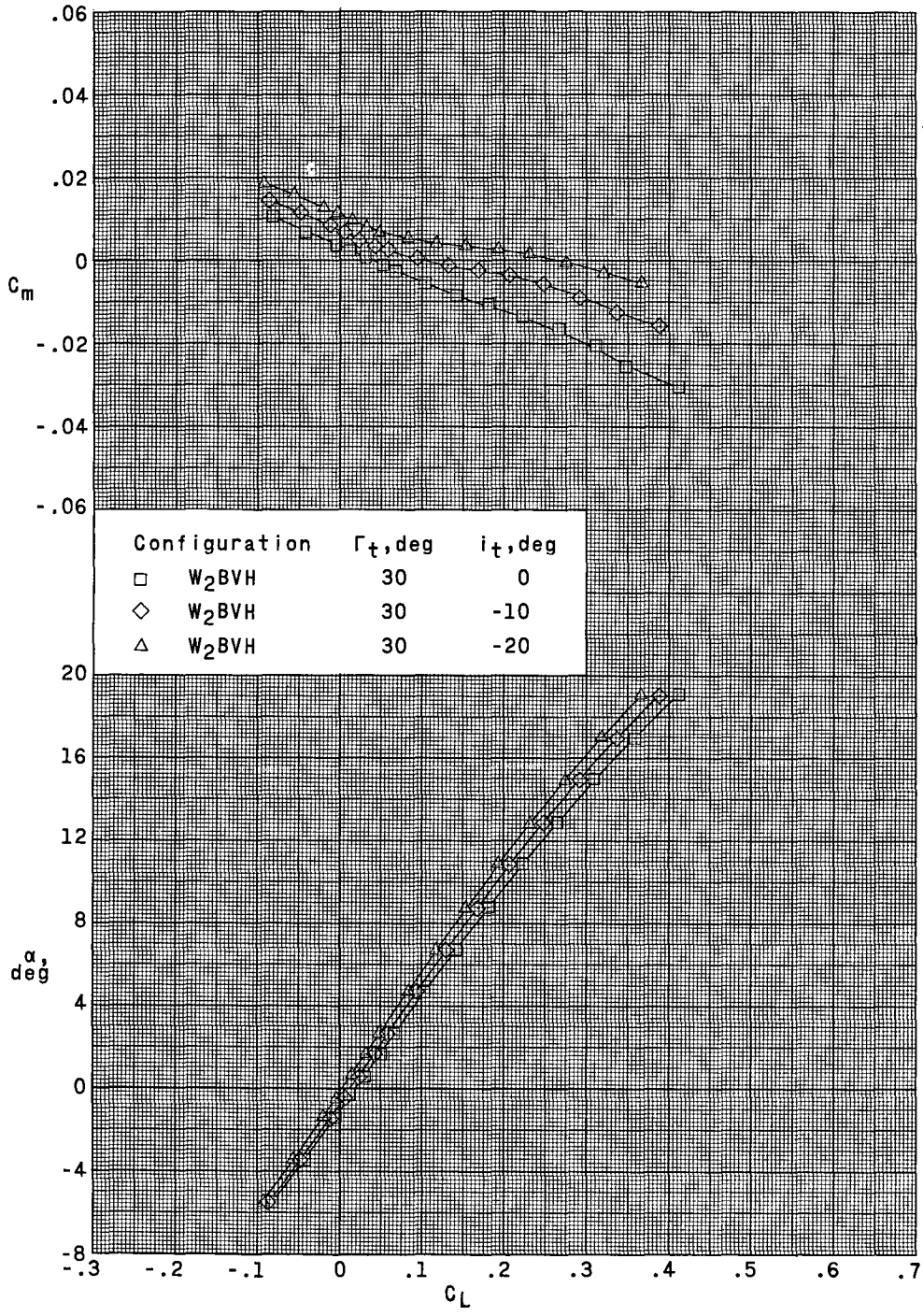

(f) M = 4.65.

Figure 6.- Continued.

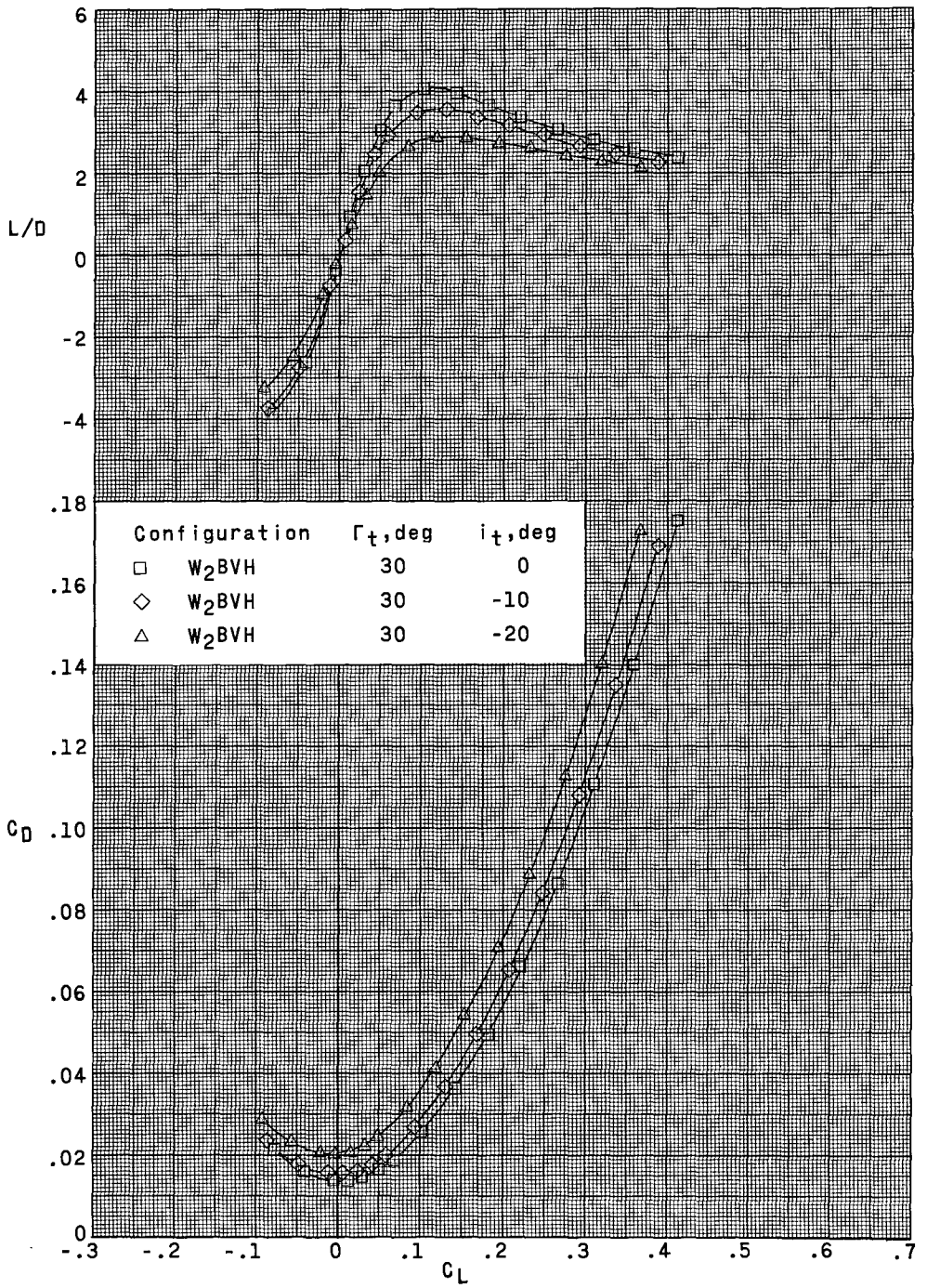

(f) Concluded.

Figure 6.- Concluded.

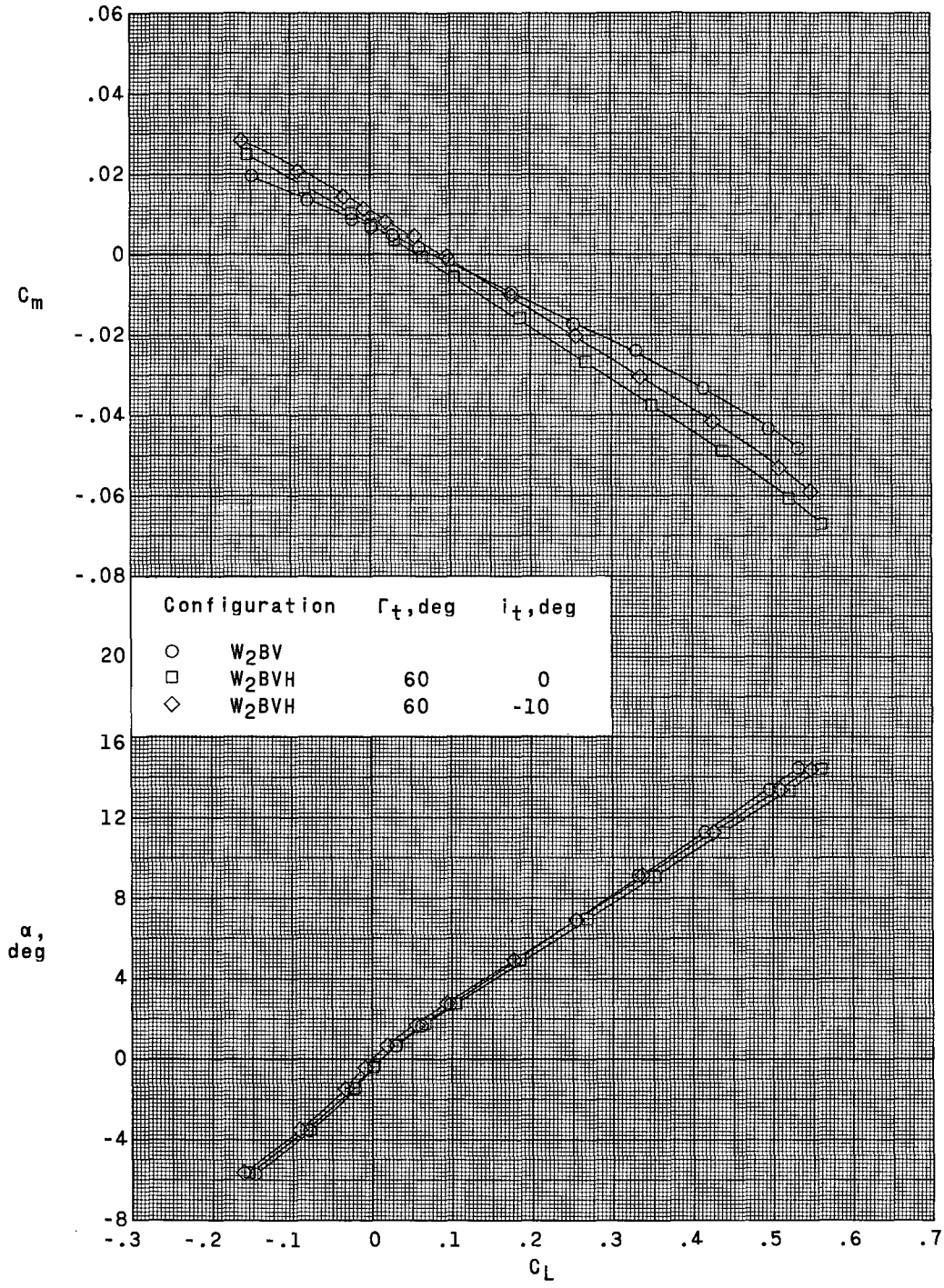

(a) M = 1.60.

Figure 7.- Effect of horizontal-stabilizer deflection on aerodynamic characteristics in pitch. $\Gamma_t = 60^\circ$.

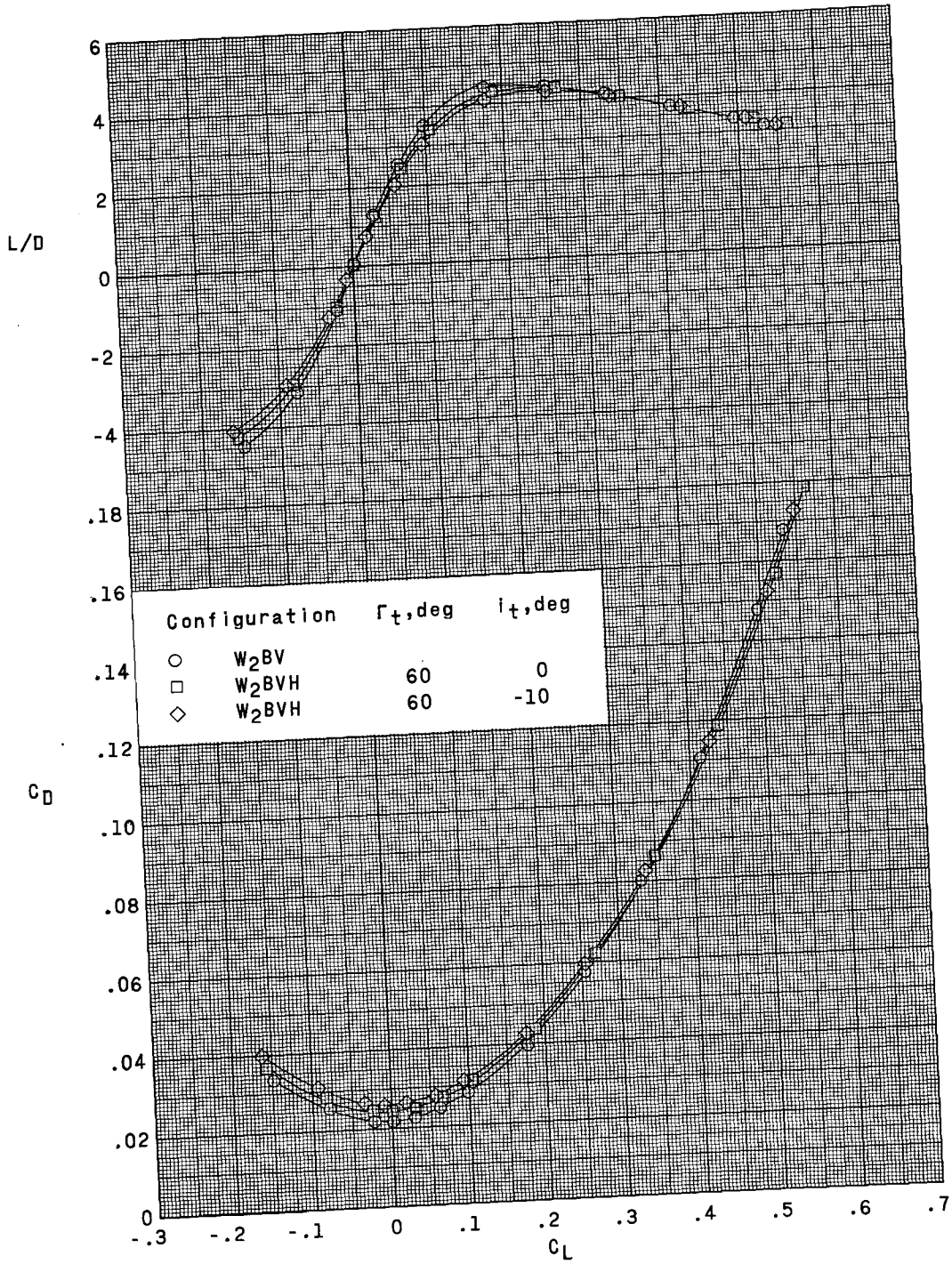

(a) Concluded.

Figure 7.- Continued.

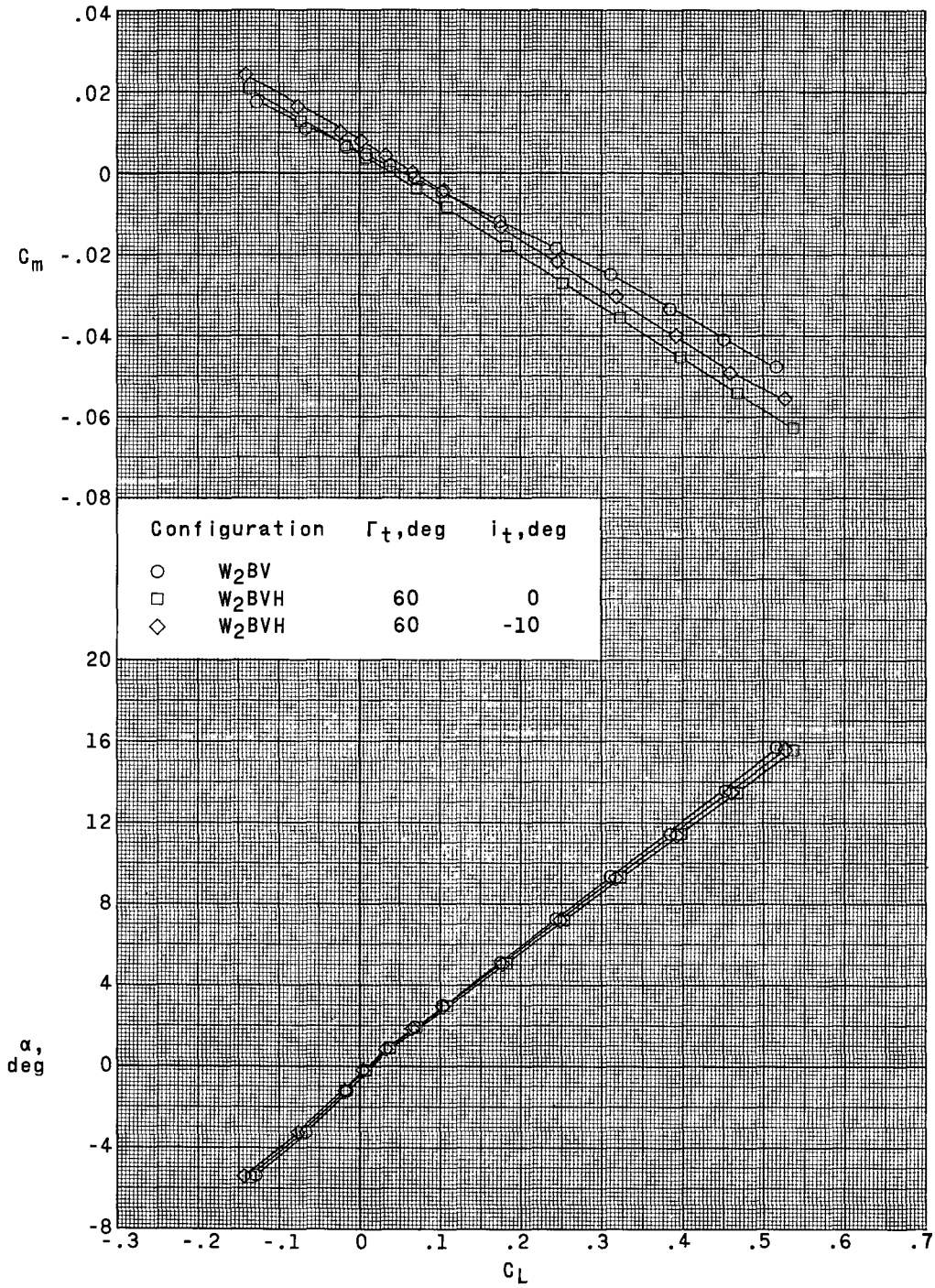

(b) M = 1.90.

Figure 7.- Continued.

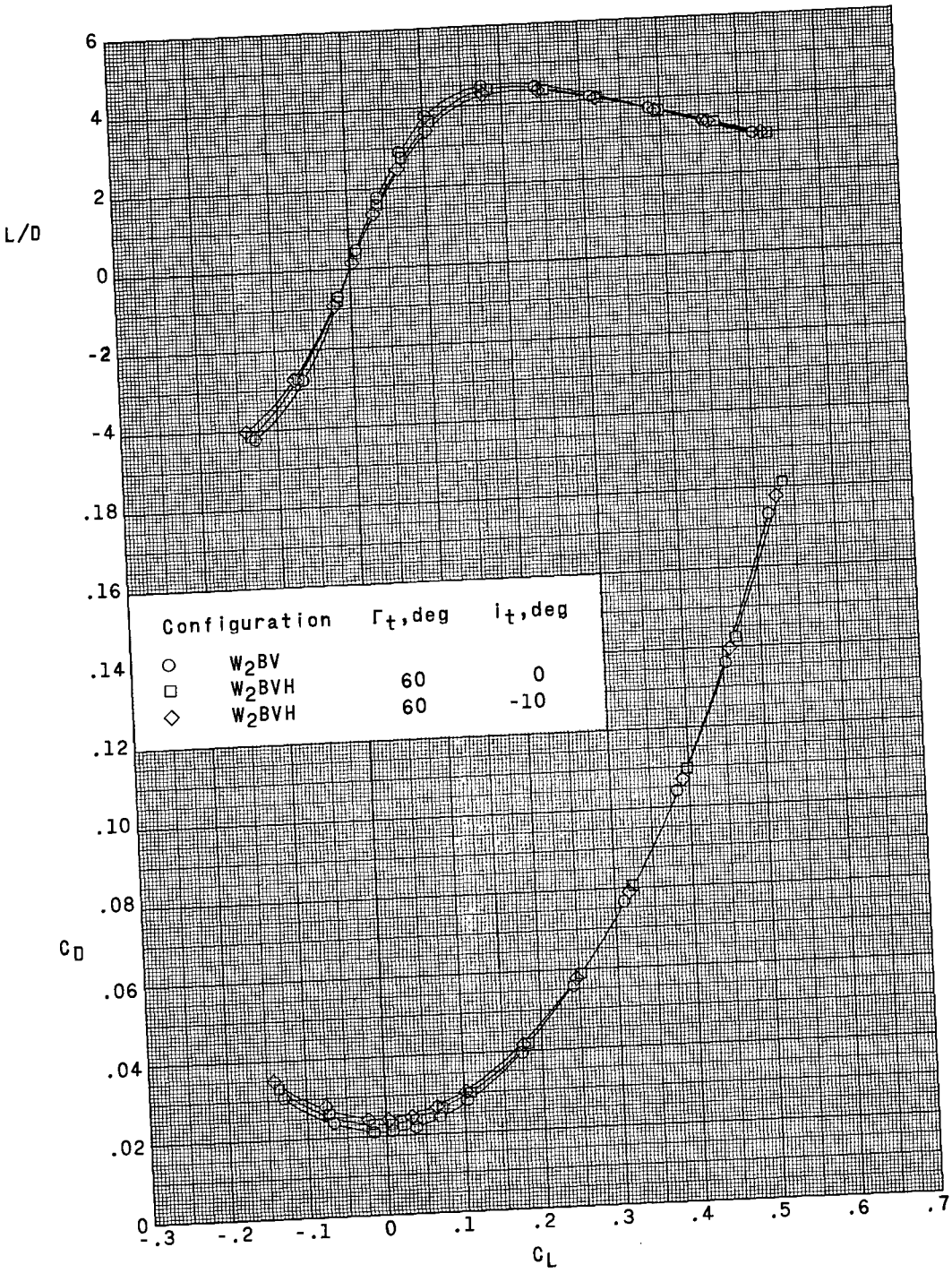

(b) Concluded.

Figure 7.- Continued.

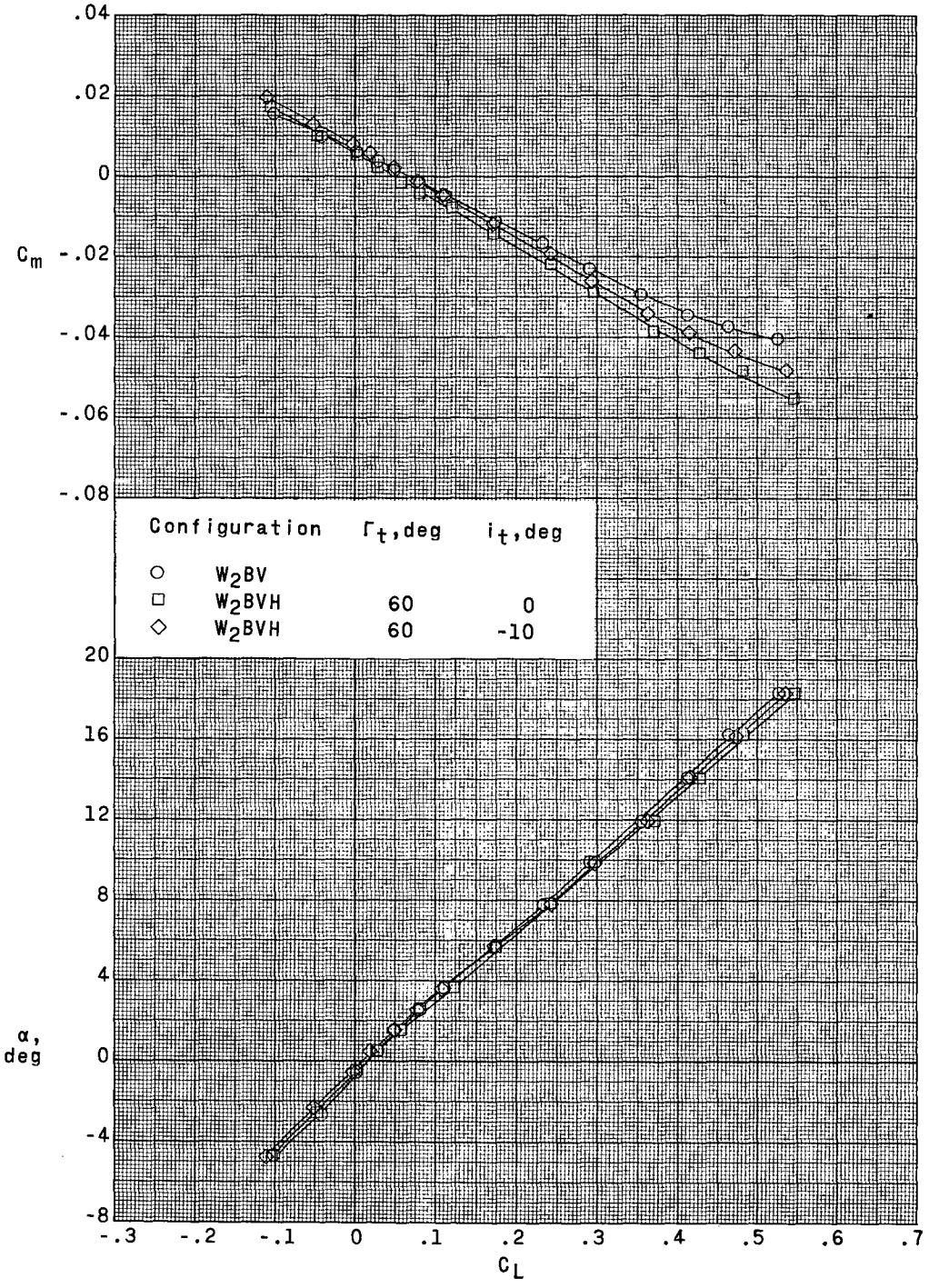

(c) M = 2.36.

Figure 7.- Continued.

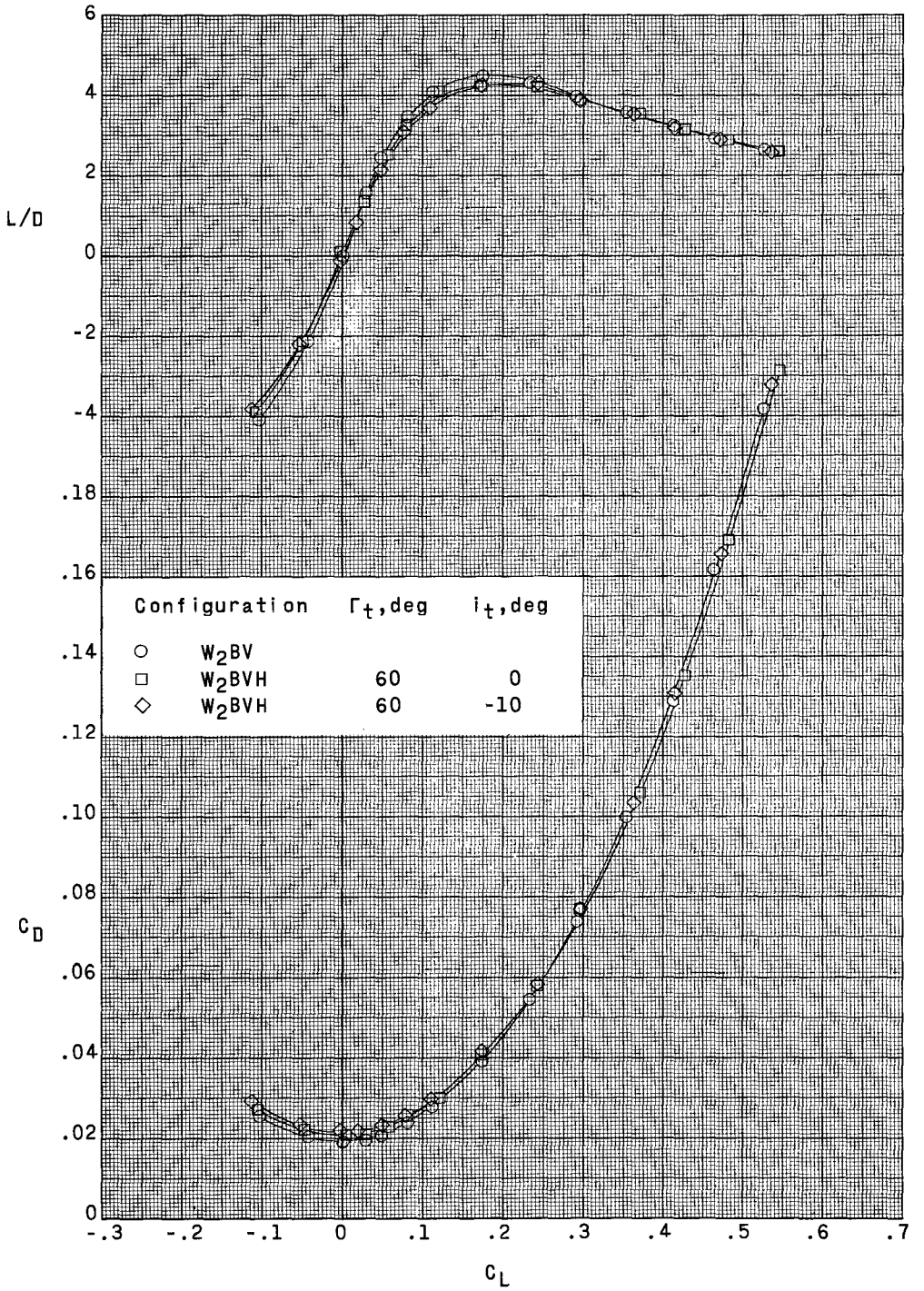

(c) Concluded.

Figure 7.- Continued.

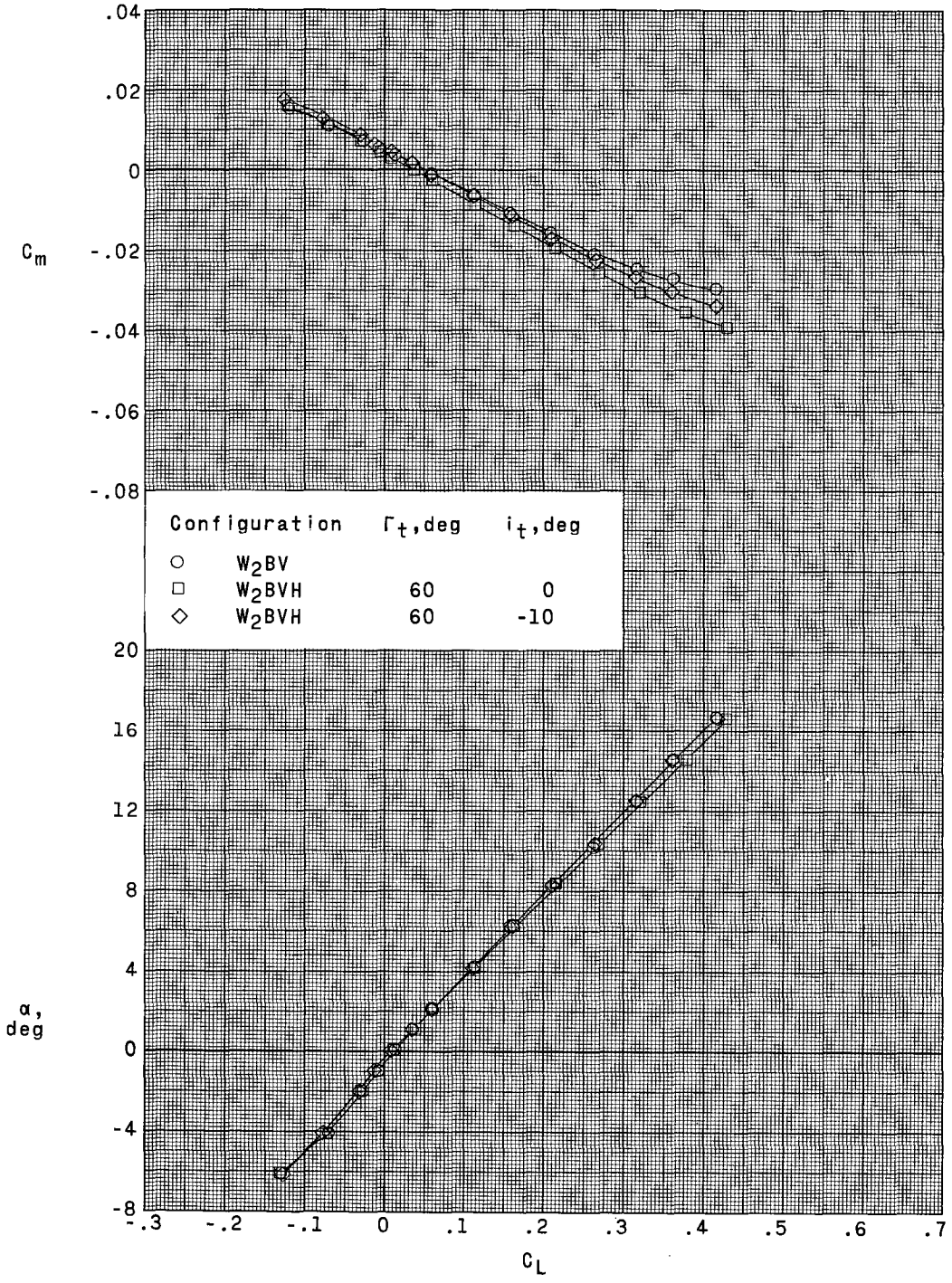

(d) M = 2.86.

Figure 7.- Continued.

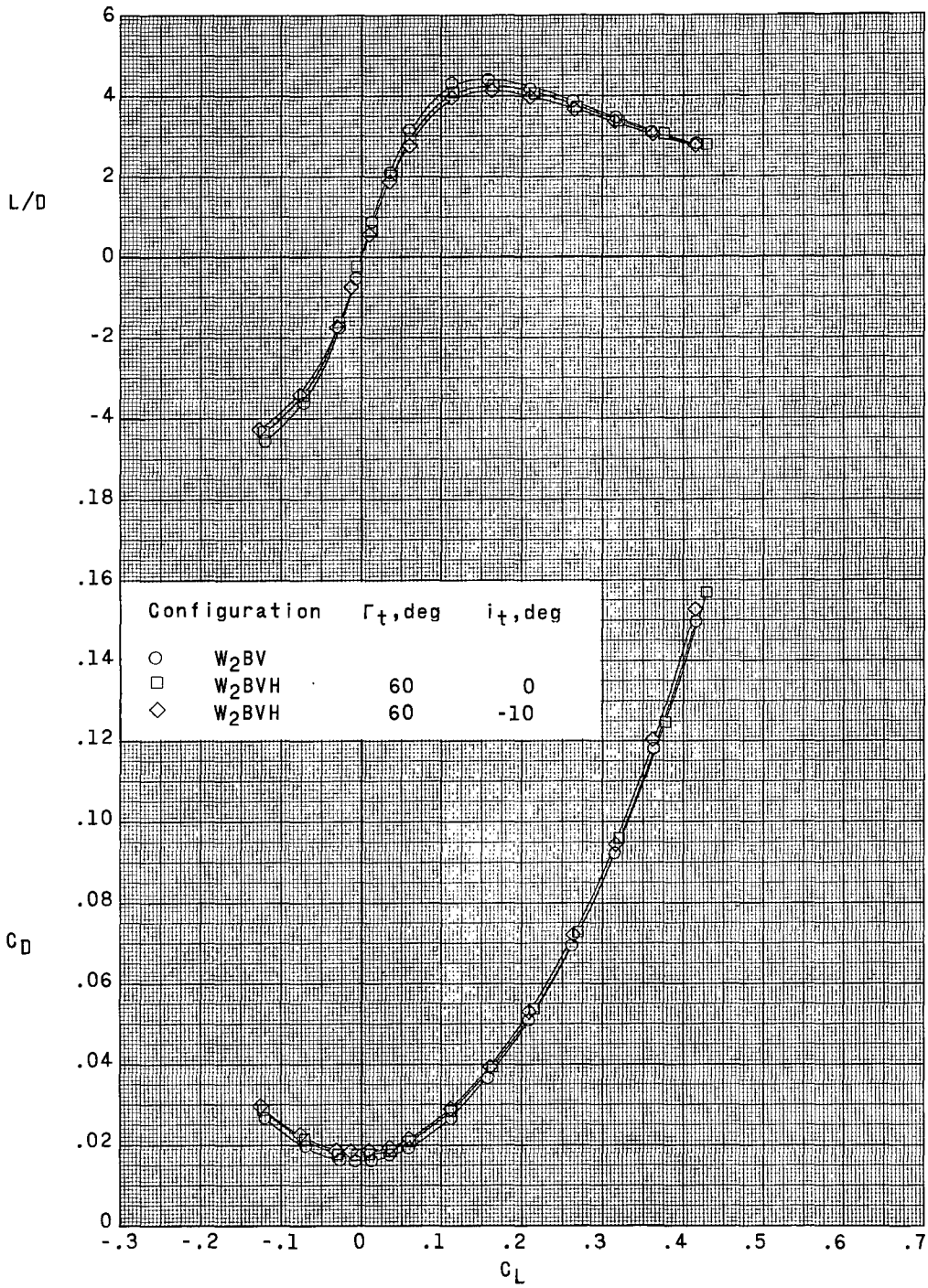

(d) Concluded.

Figure 7.- Continued.

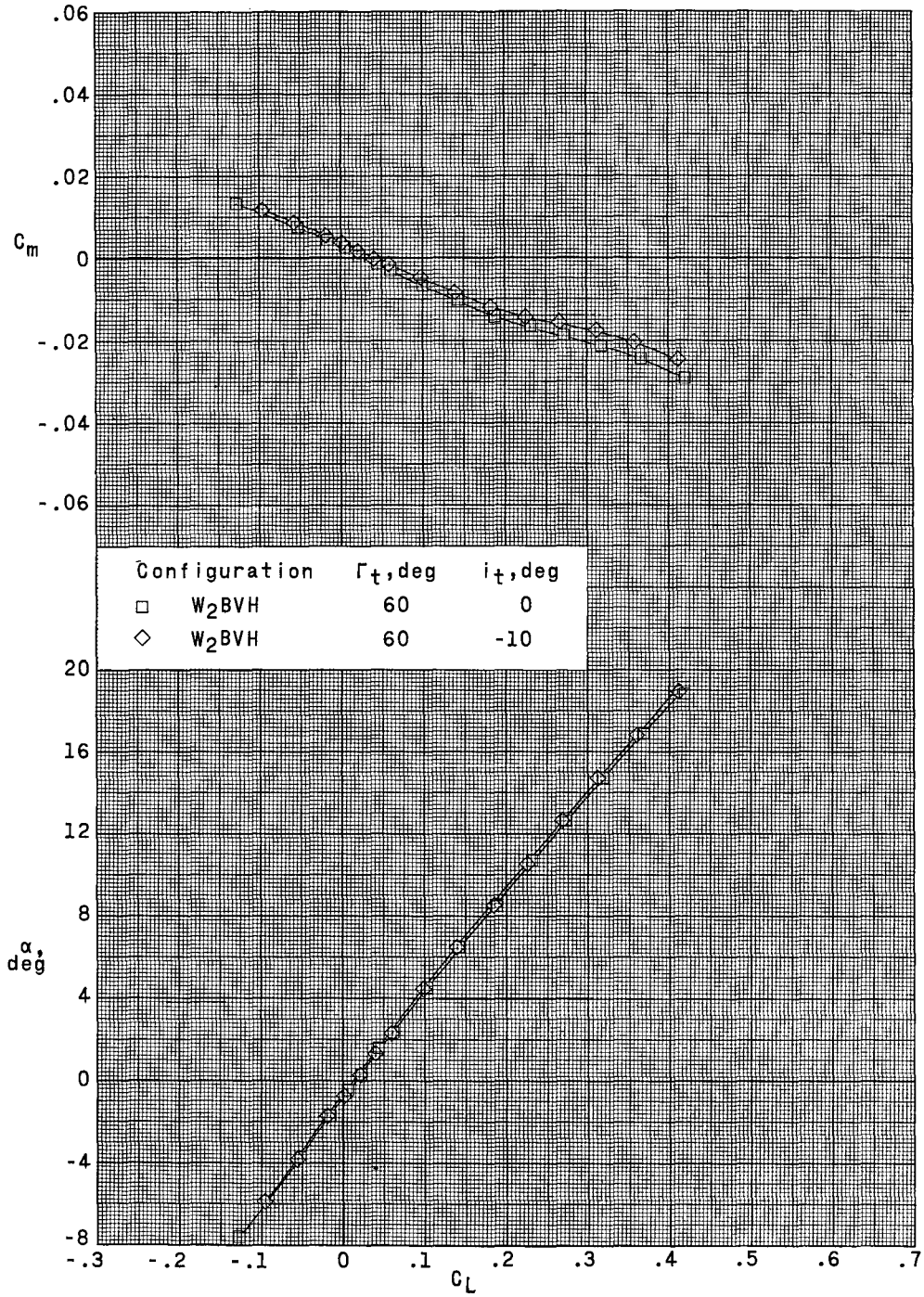

(e) M = 3.96.

Figure 7.- Continued.

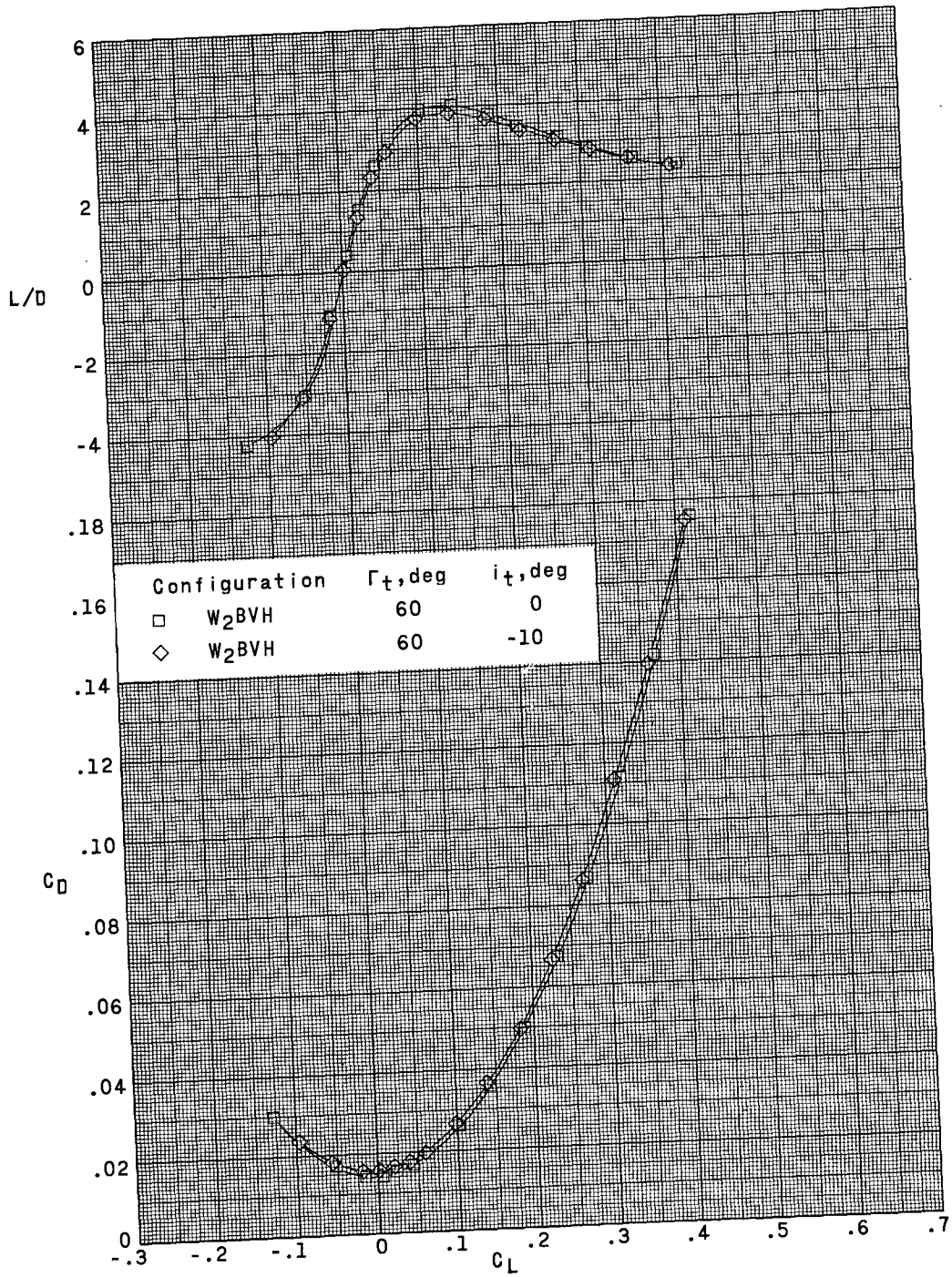

(e) Concluded.

Figure 7.- Continued.

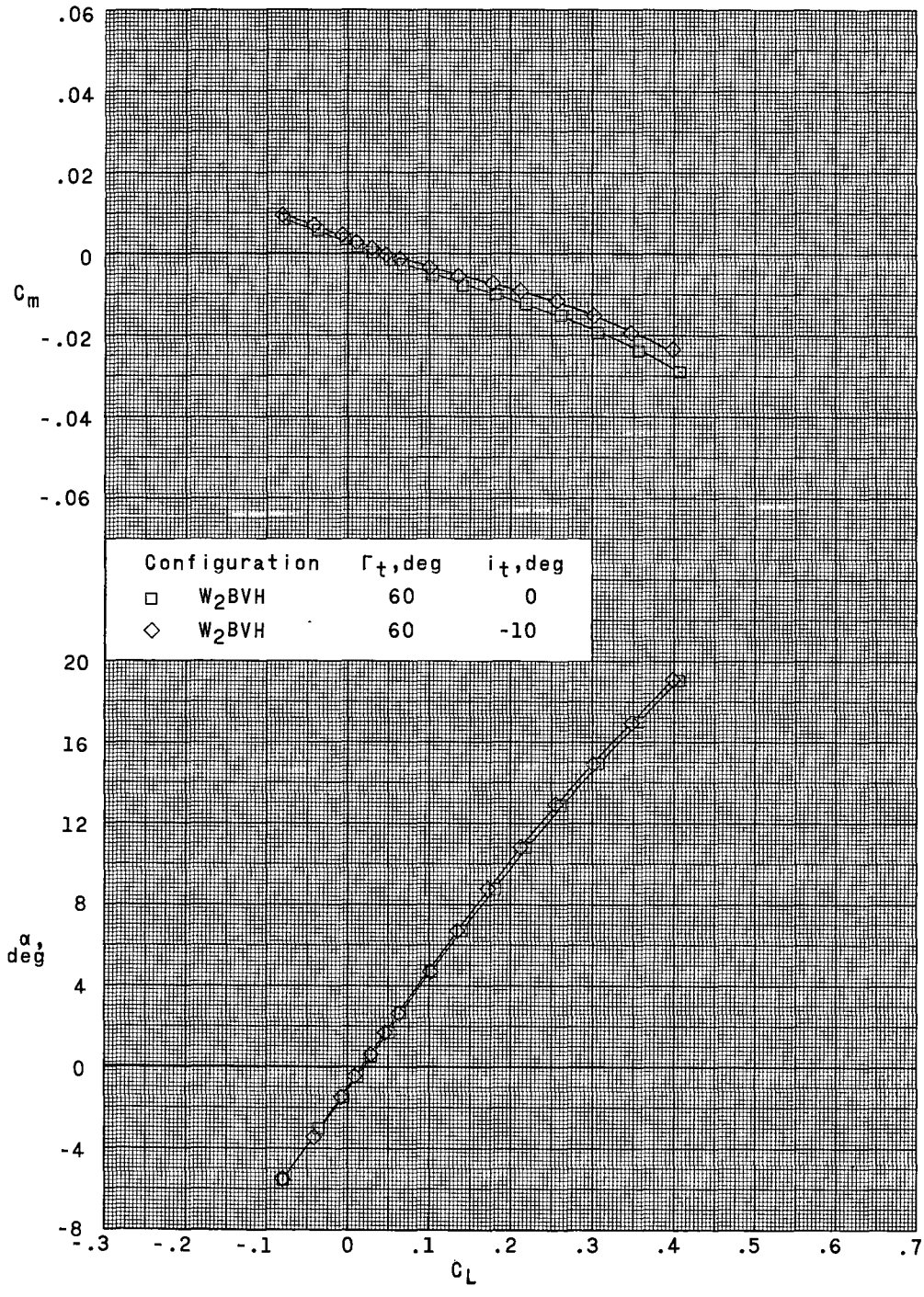

(f) M = 4.65.

Figure 7.- Continued.

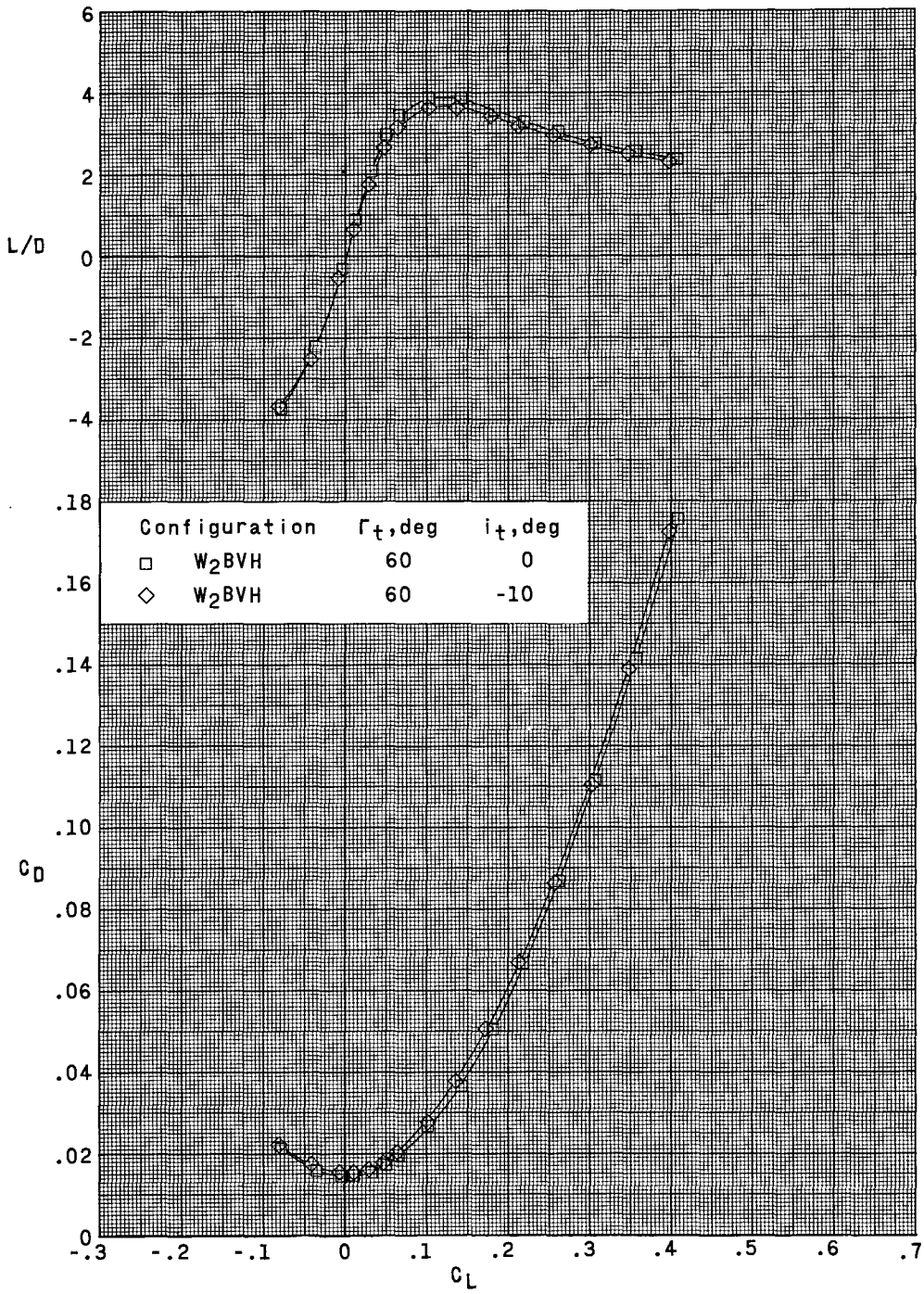

(f) Concluded.

Figure 7.- Concluded.

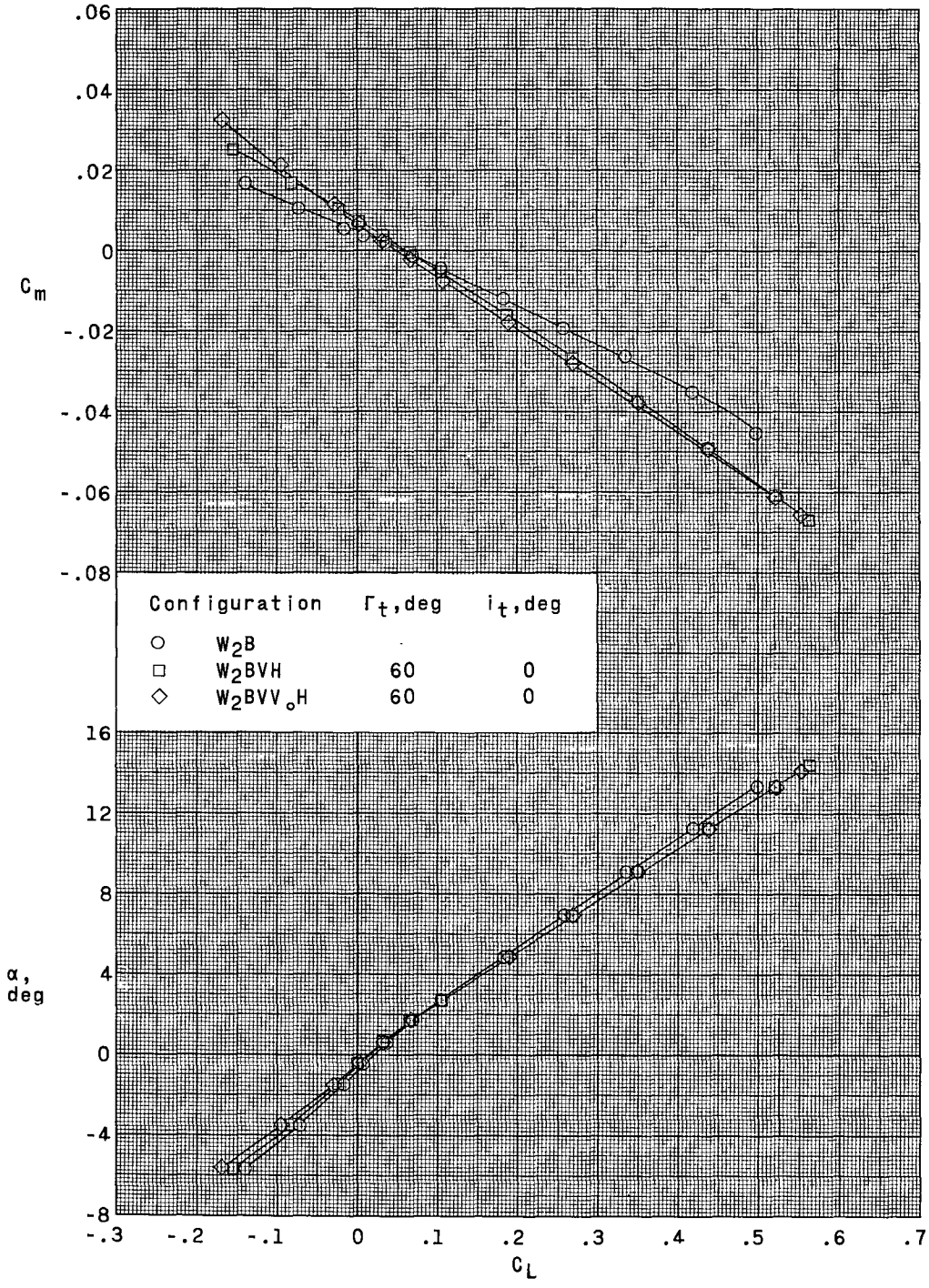

(a) M = 1.60.

Figure 8.- Effect of vertical tails on aerodynamic characteristics in pitch.

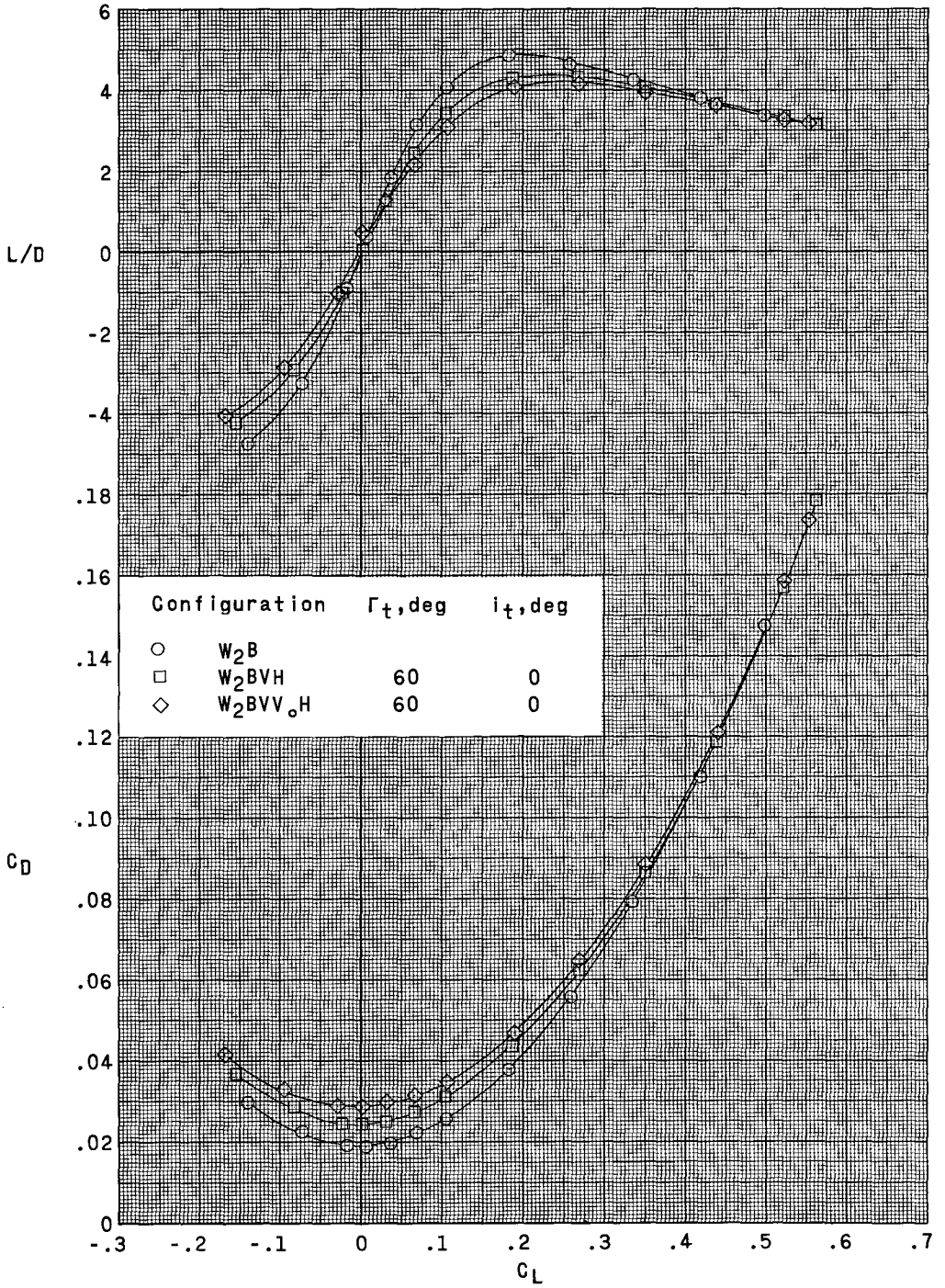

(a) Concluded.

Figure 8.- Continued.

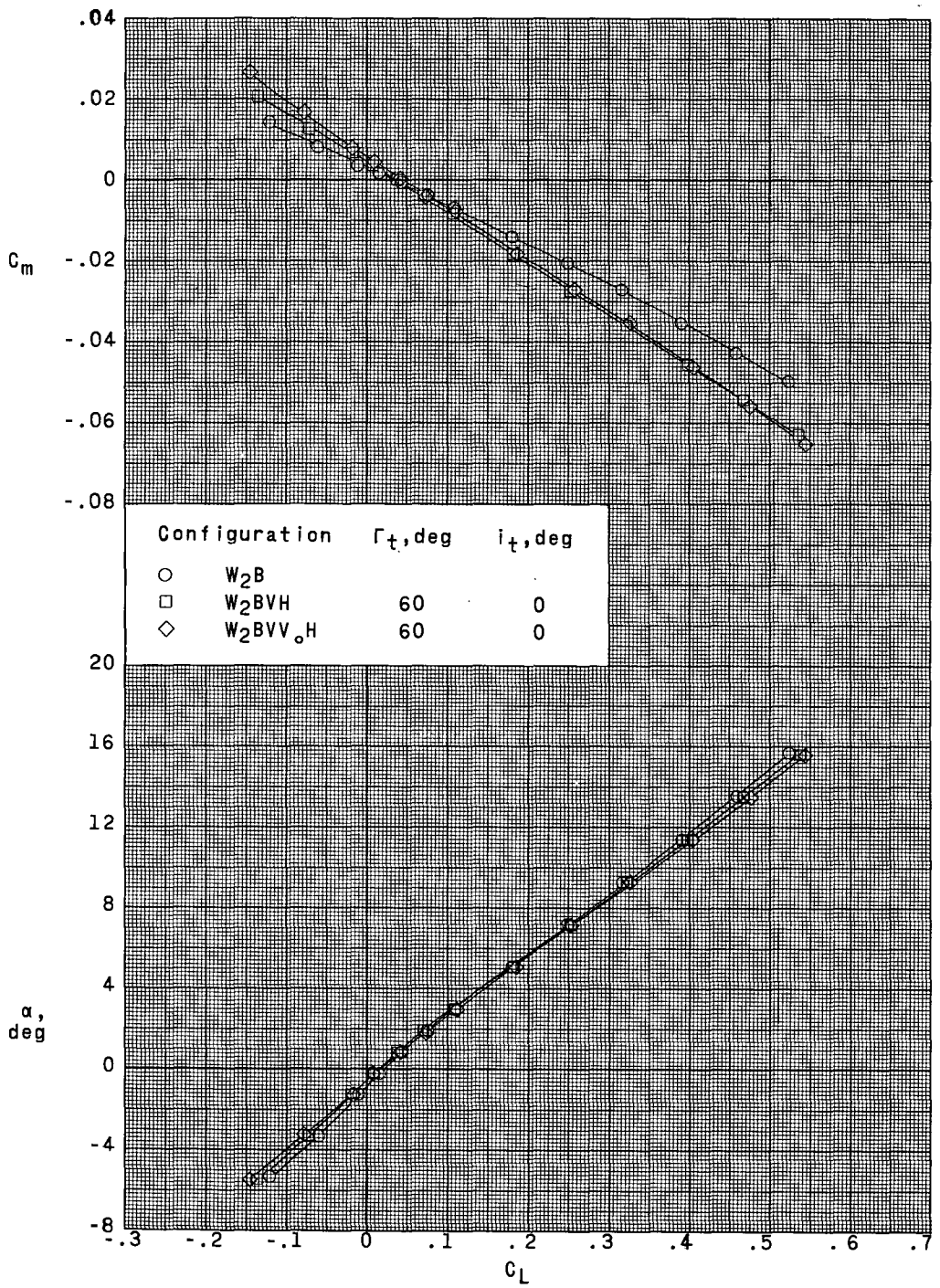

(b) M = 1.90.

Figure 8.- Continued.

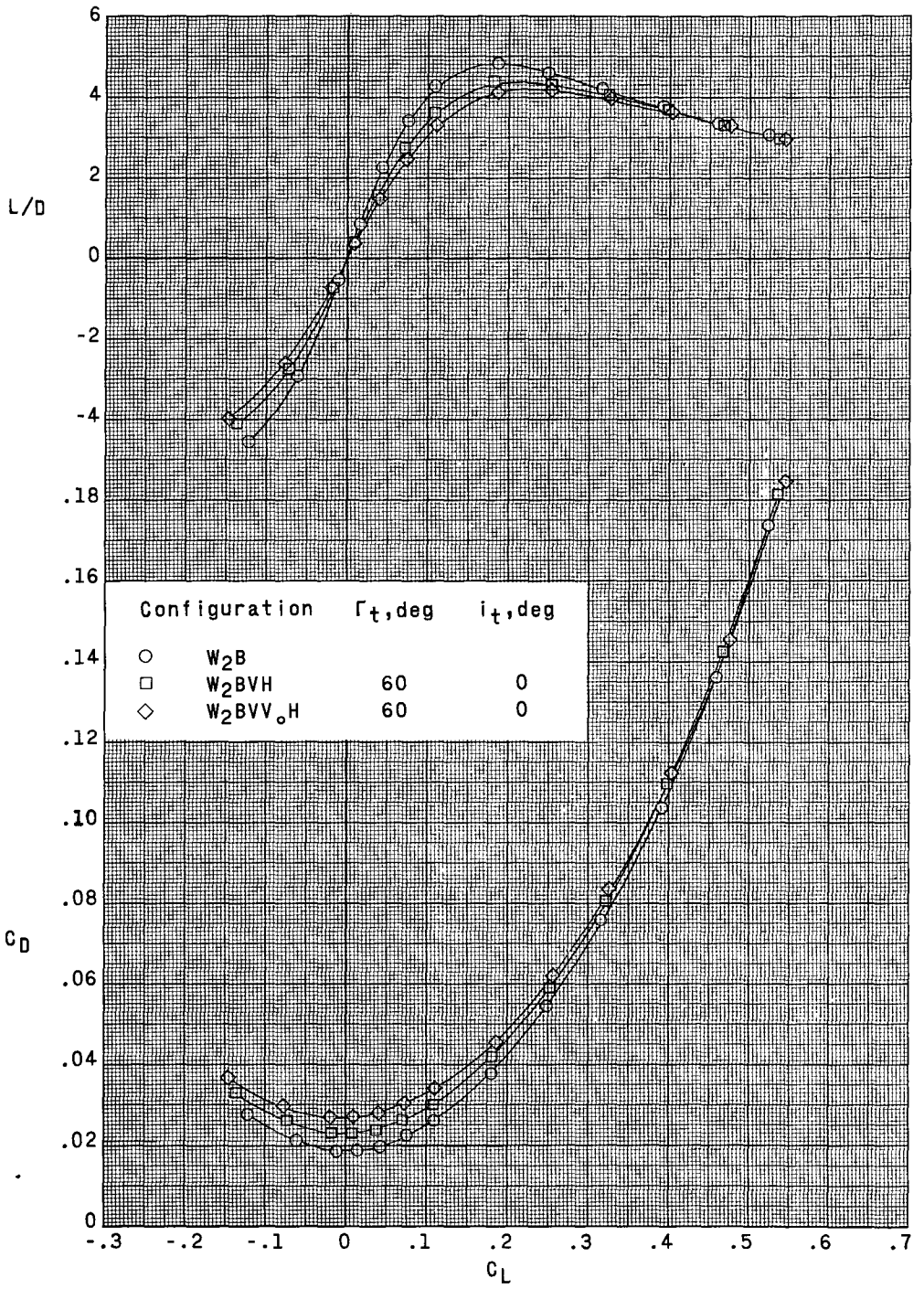

(b) Concluded.

Figure 8.- Continued.

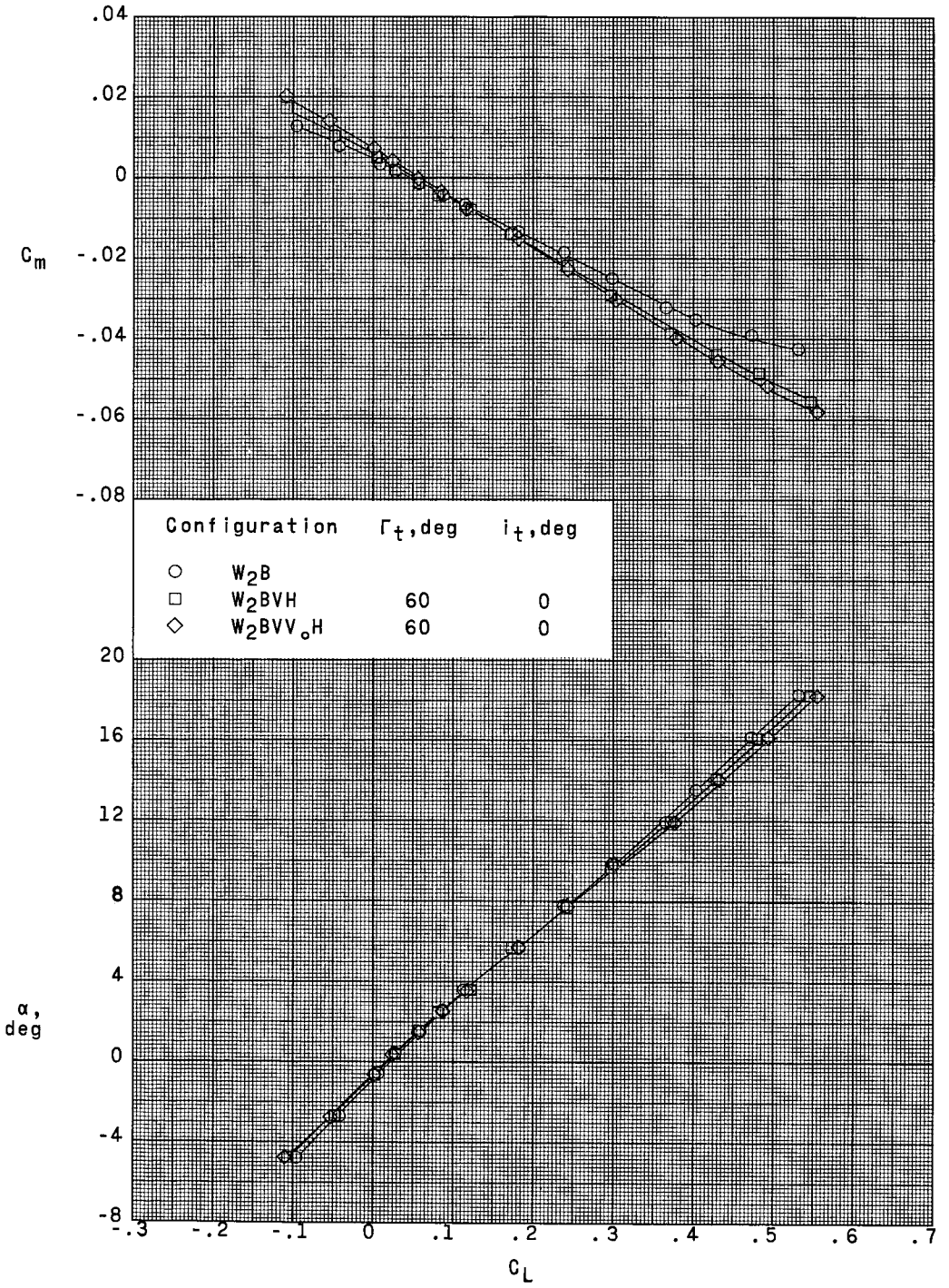

(c) M = 2.36.

Figure 8.- Continued.

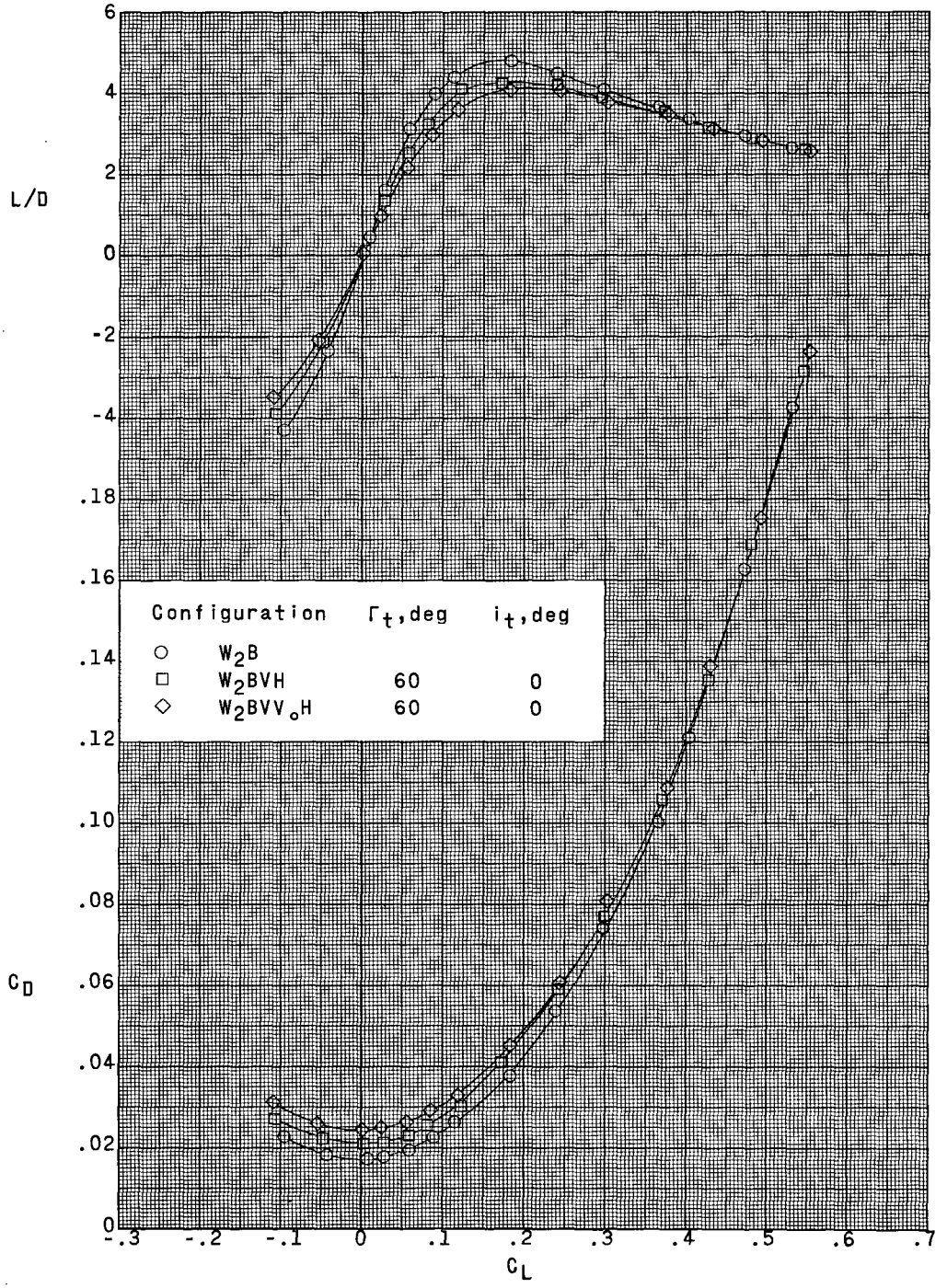

(c) Concluded.

Figure 8.- Continued.

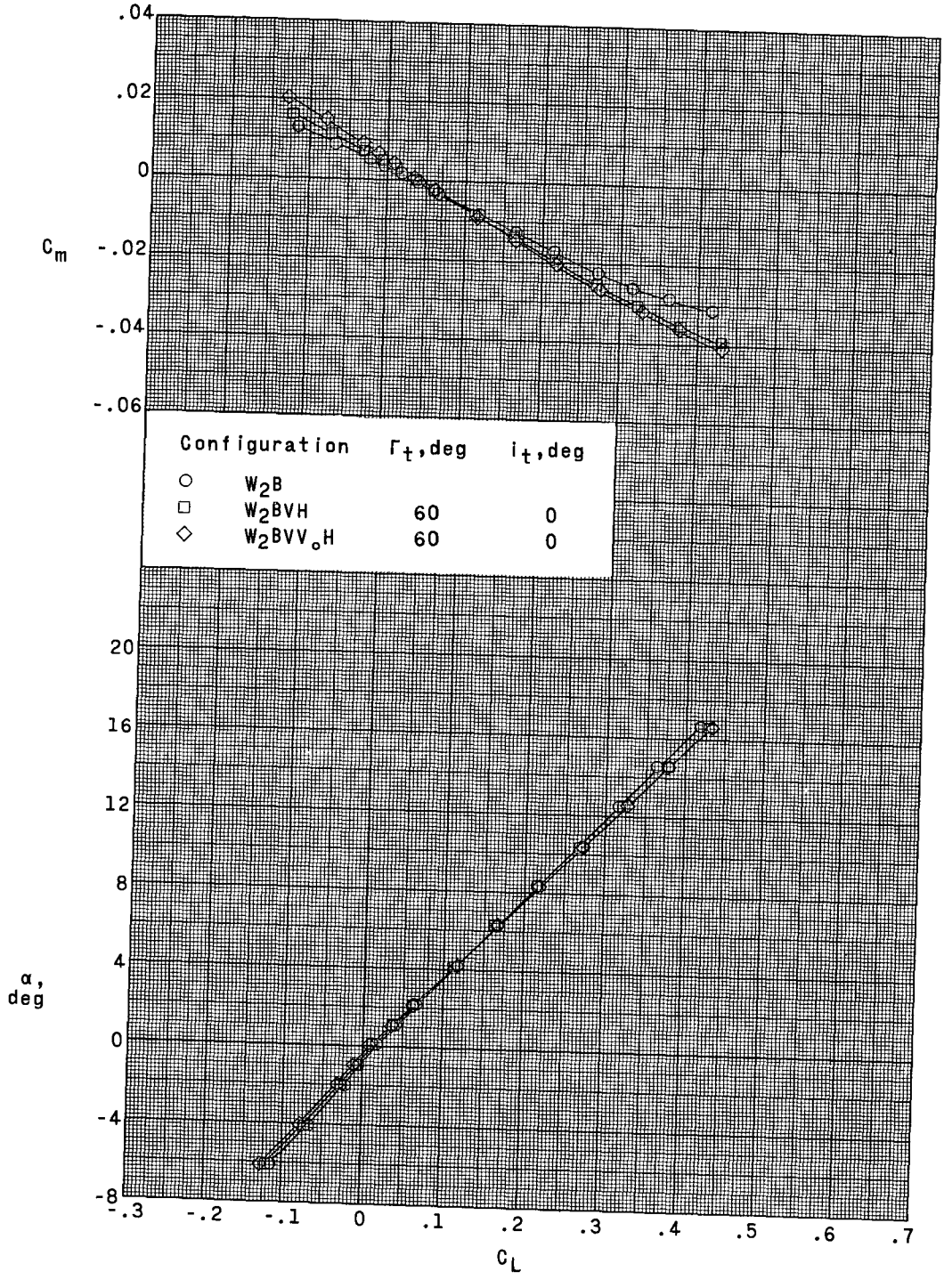

(d) M = 2.86.

Figure 8.- Continued.

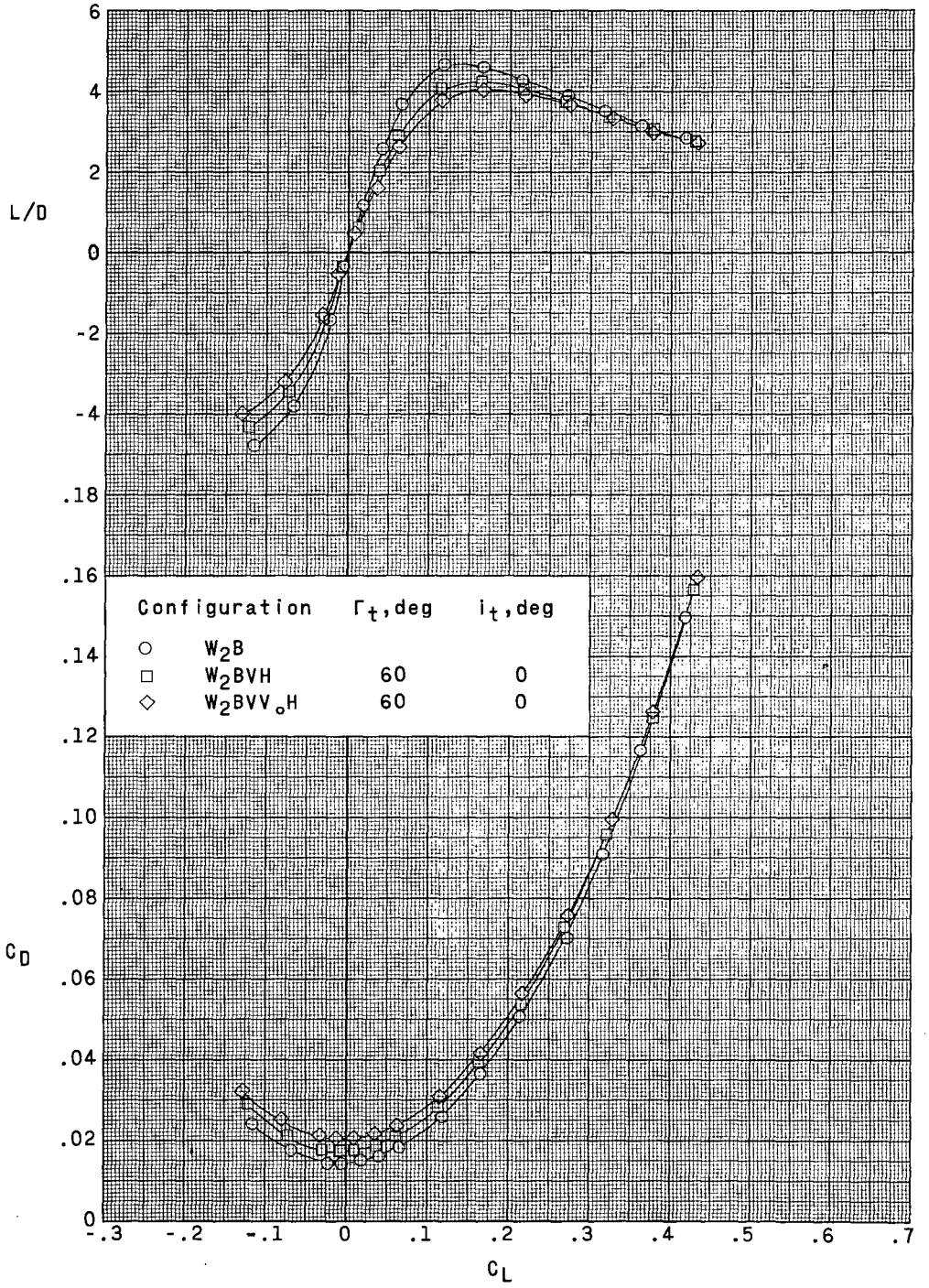

(d) Concluded.

Figure 8.- Continued.

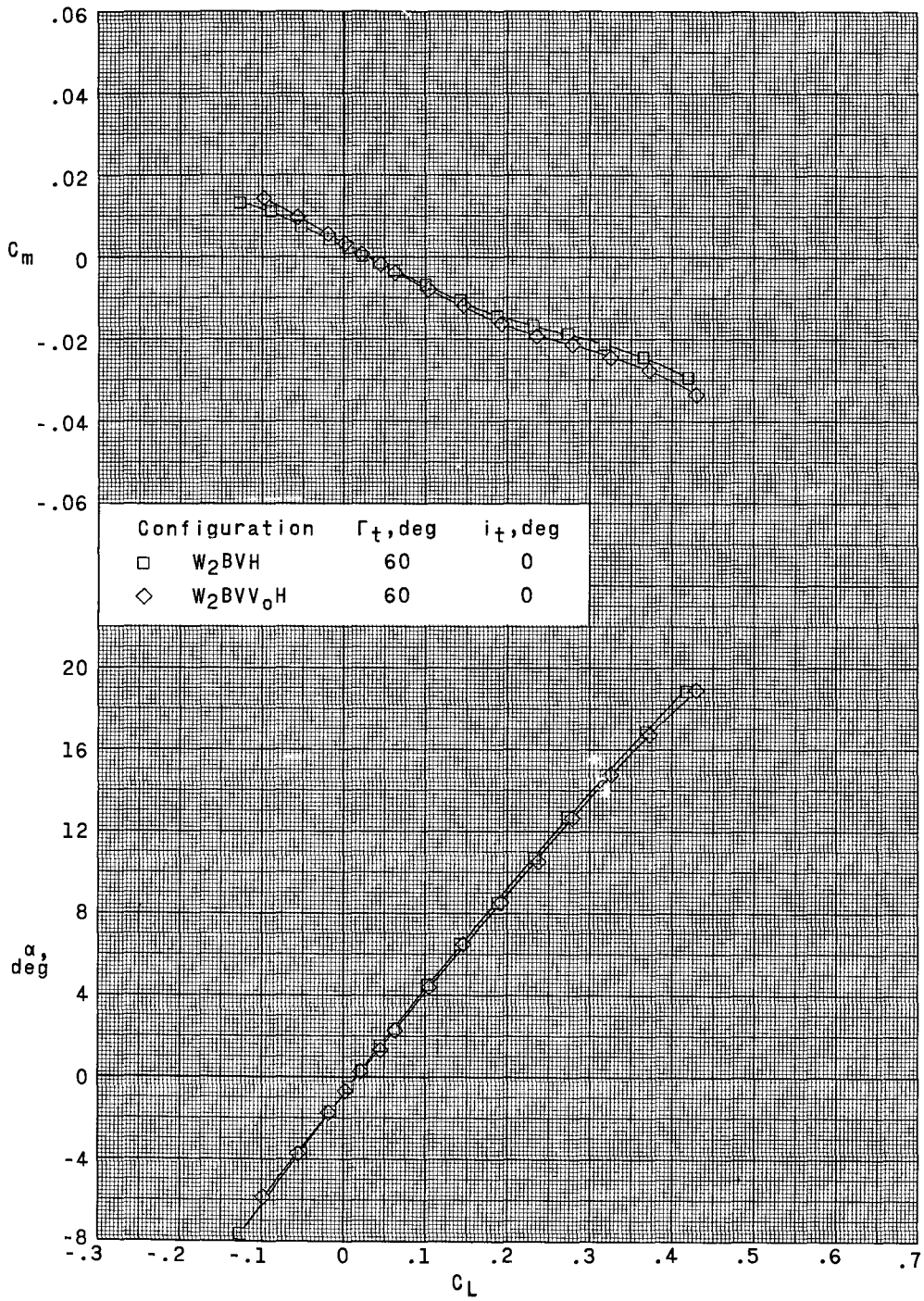

(e) M = 3.96.

Figure 8.- Continued.

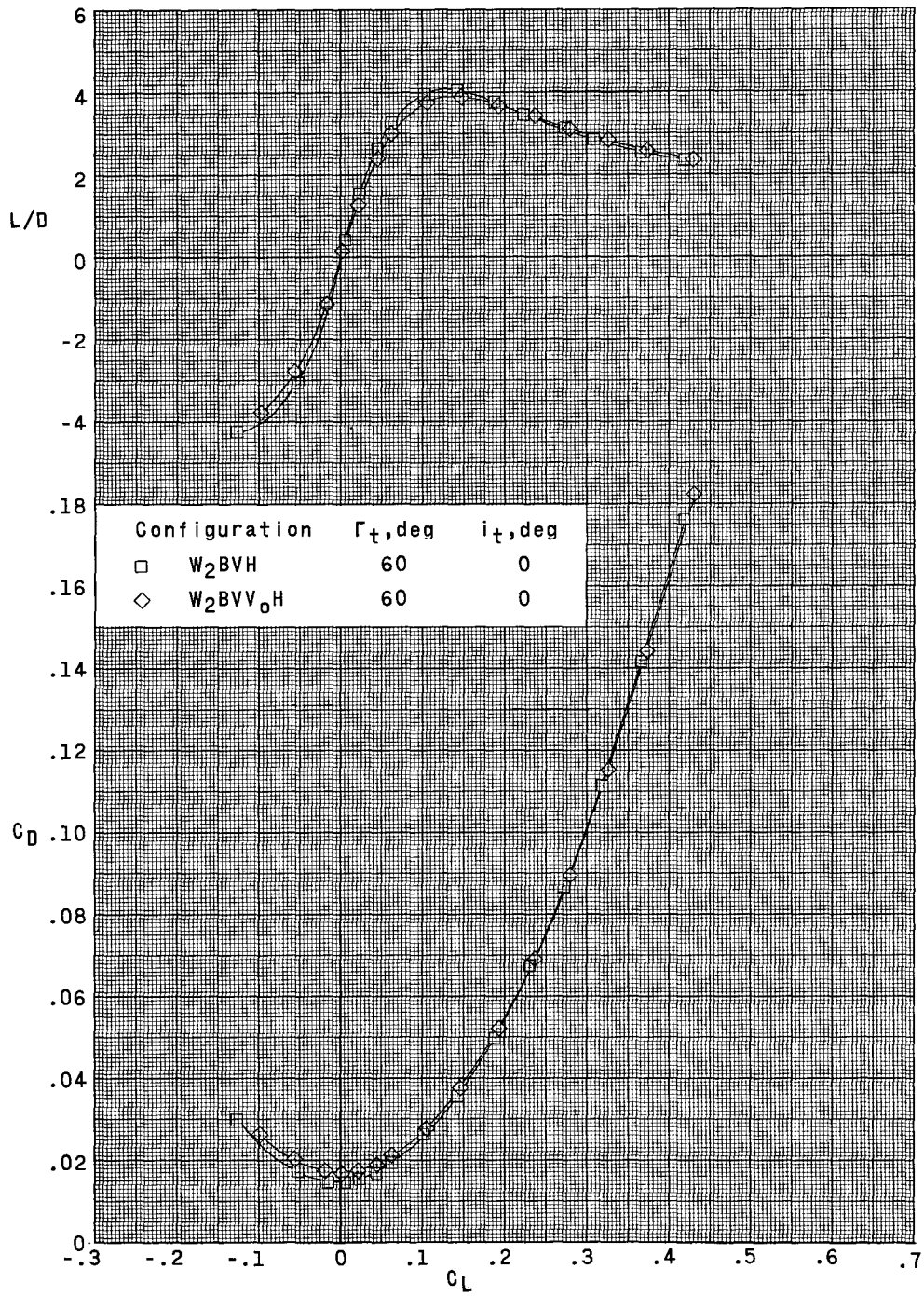

(e) Concluded.

Figure 8.- Continued.

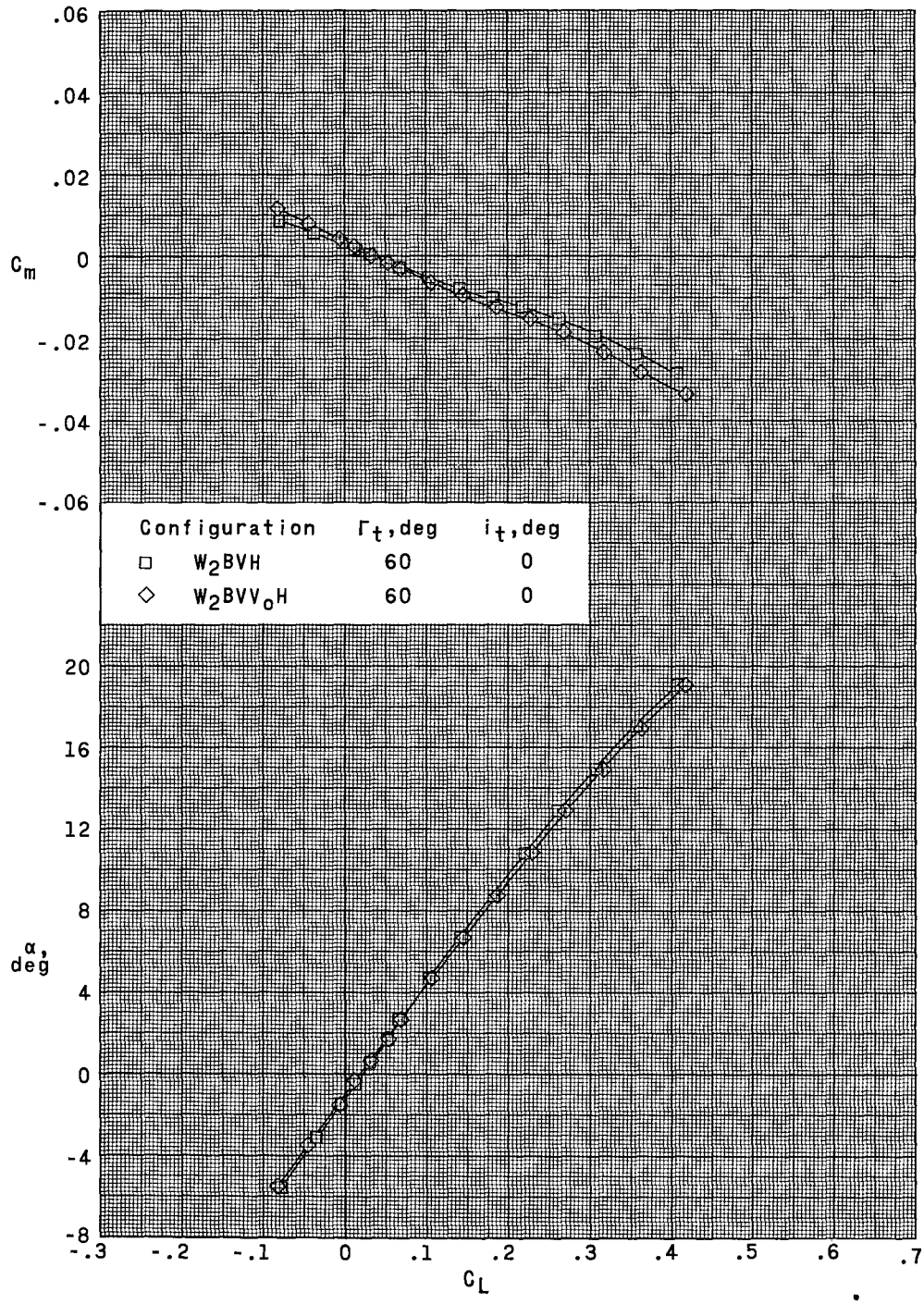

(f) M = 4.65.

Figure 8.- Continued.

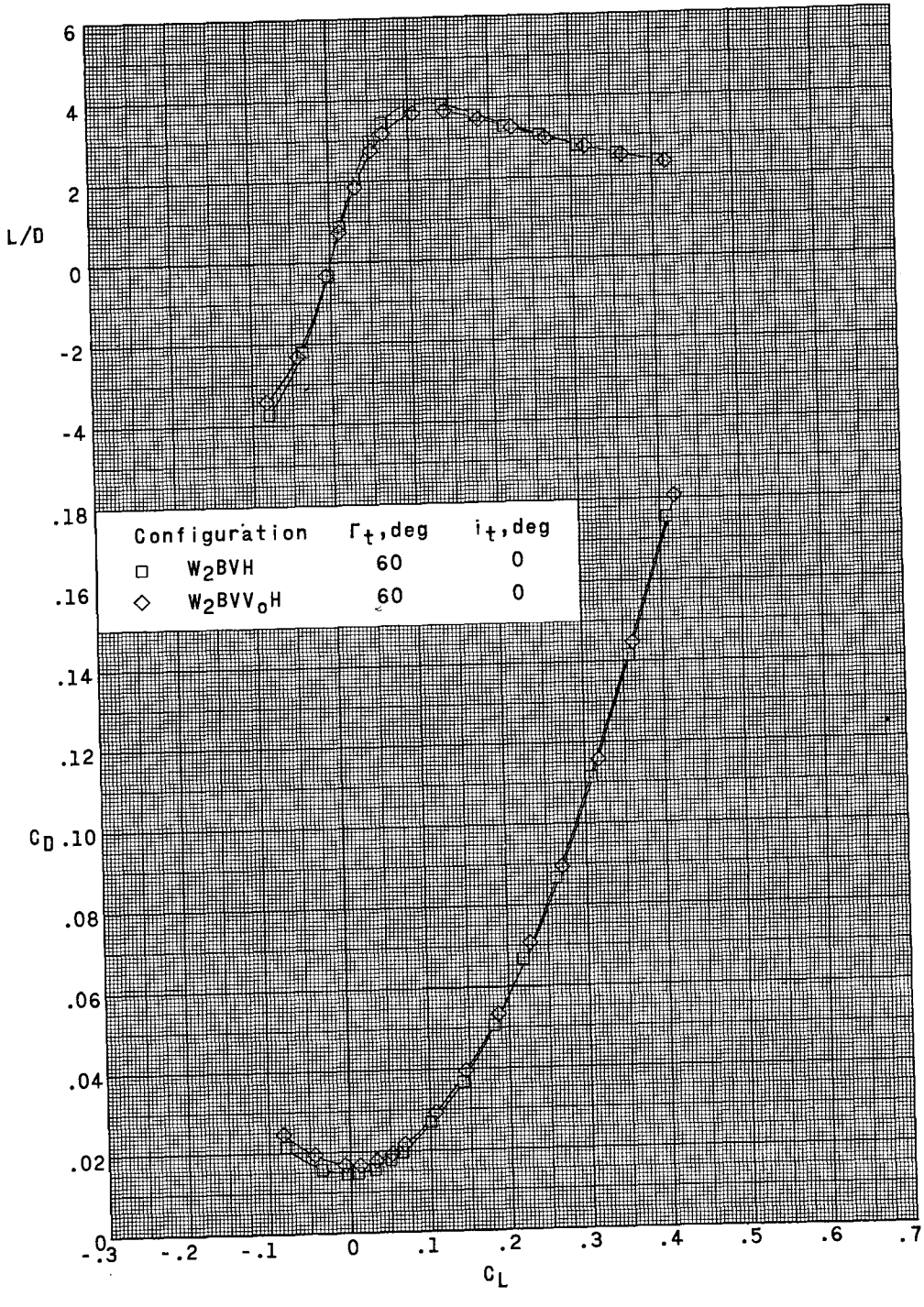

(f) Concluded.

Figure 8.- Concluded.

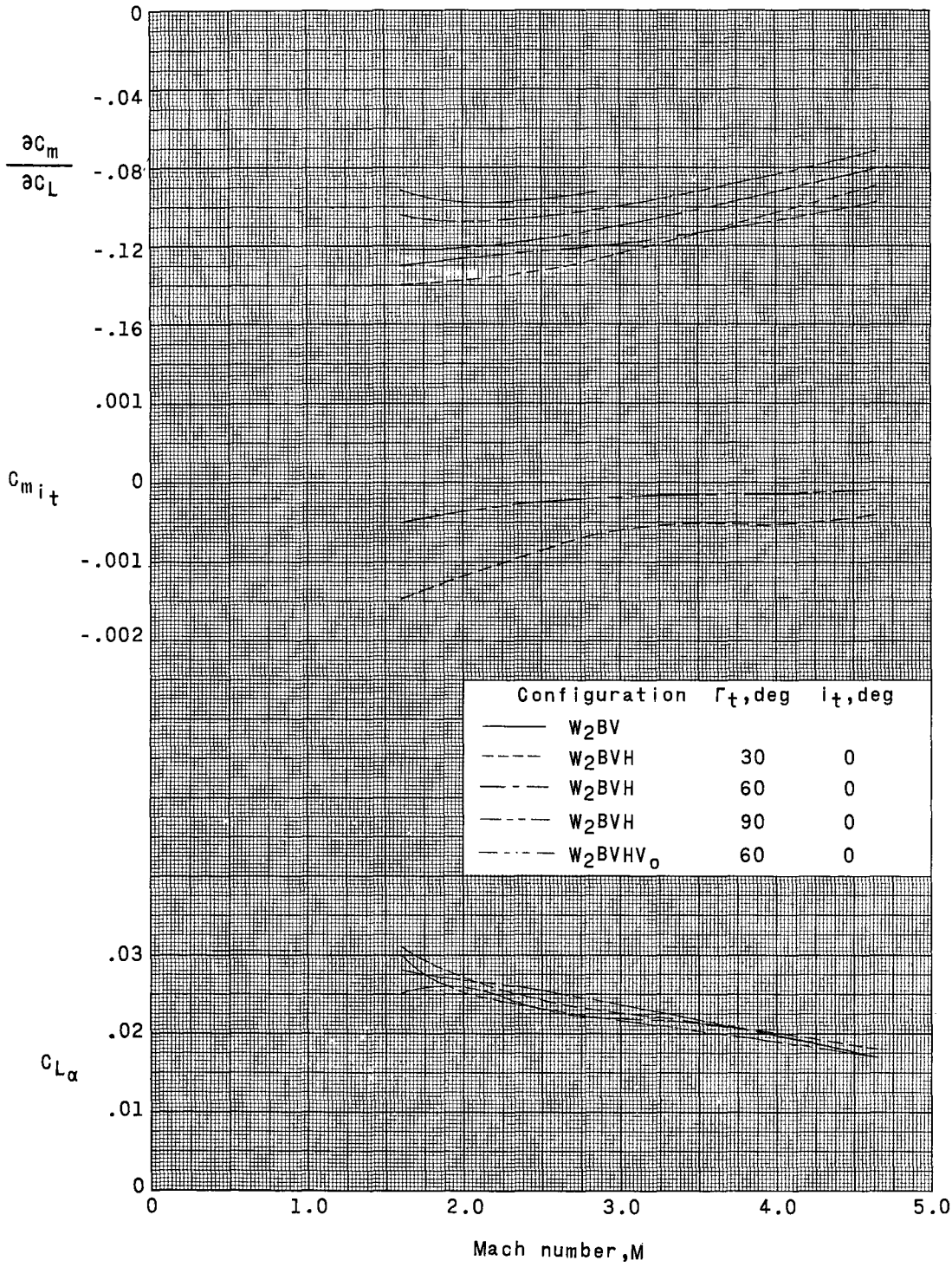

Figure 9.- The effects of horizontal-stabilizer anhedral at various Mach numbers on the longitudinal aerodynamic parameters $\partial C_m/\partial C_L$, $C_{m_{i_t}}$, and C_{L_α}.

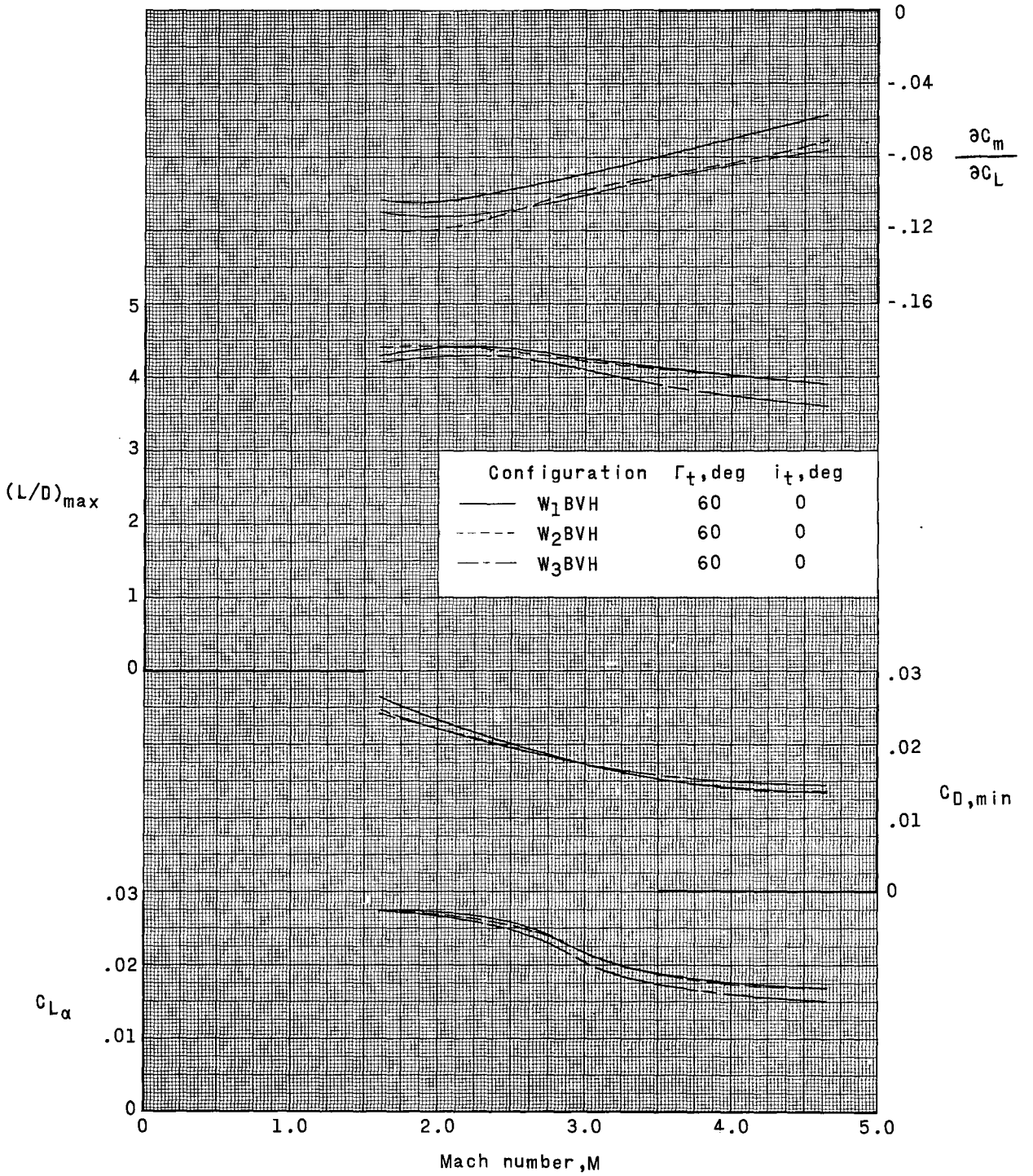

Figure 10.- Summary of the effects of Mach number on the longitudinal aerodynamic parameters, C_{L_α}, $C_{D,min}$, $(L/D)_{max}$, and $\partial C_m/\partial C_L$, for the three wing planforms tested.

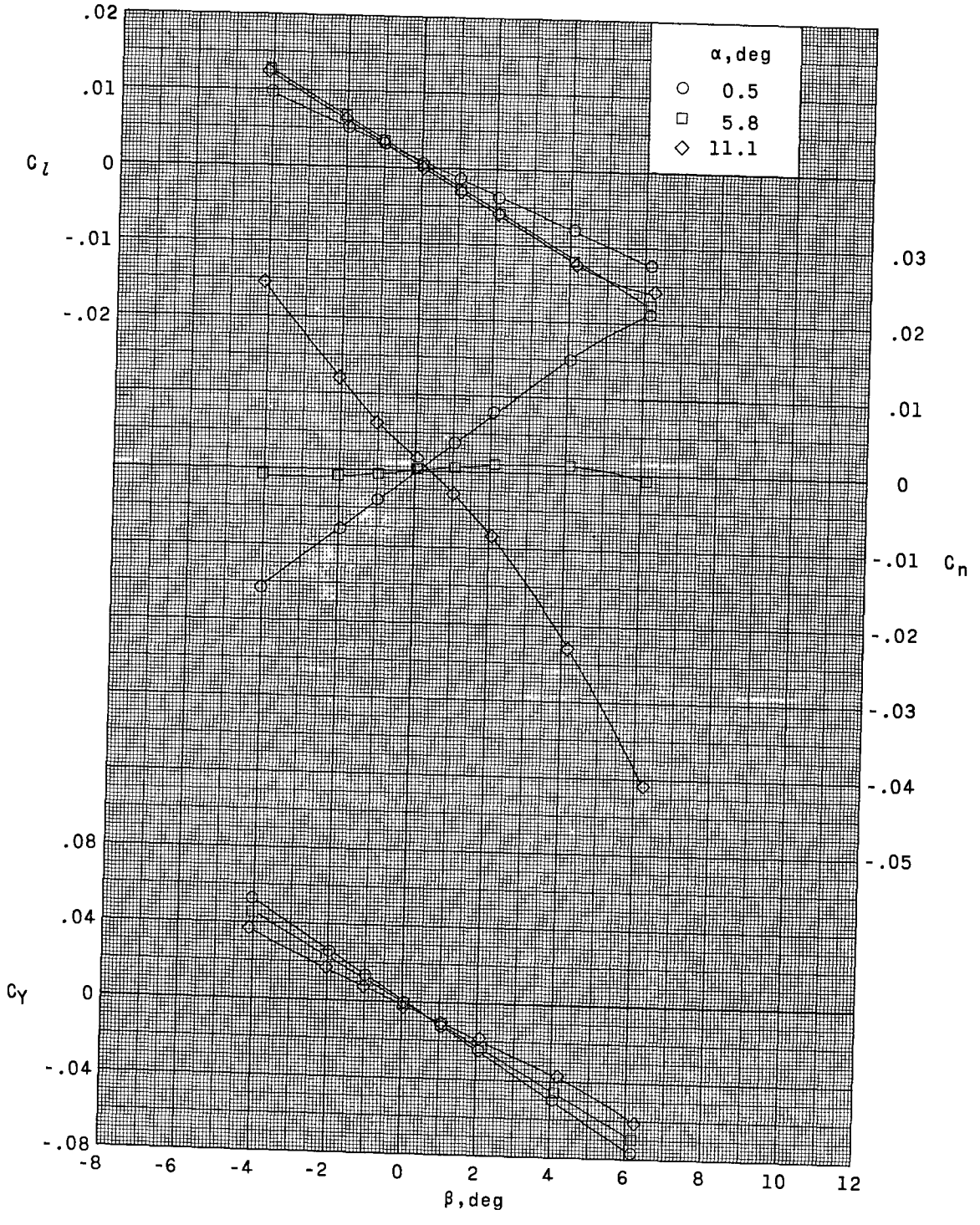

(a) M = 1.60.

Figure 11.- Aerodynamic characteristics in sideslip. W_2, $\Gamma_t = 30^\circ$, $i_t = 0^\circ$.

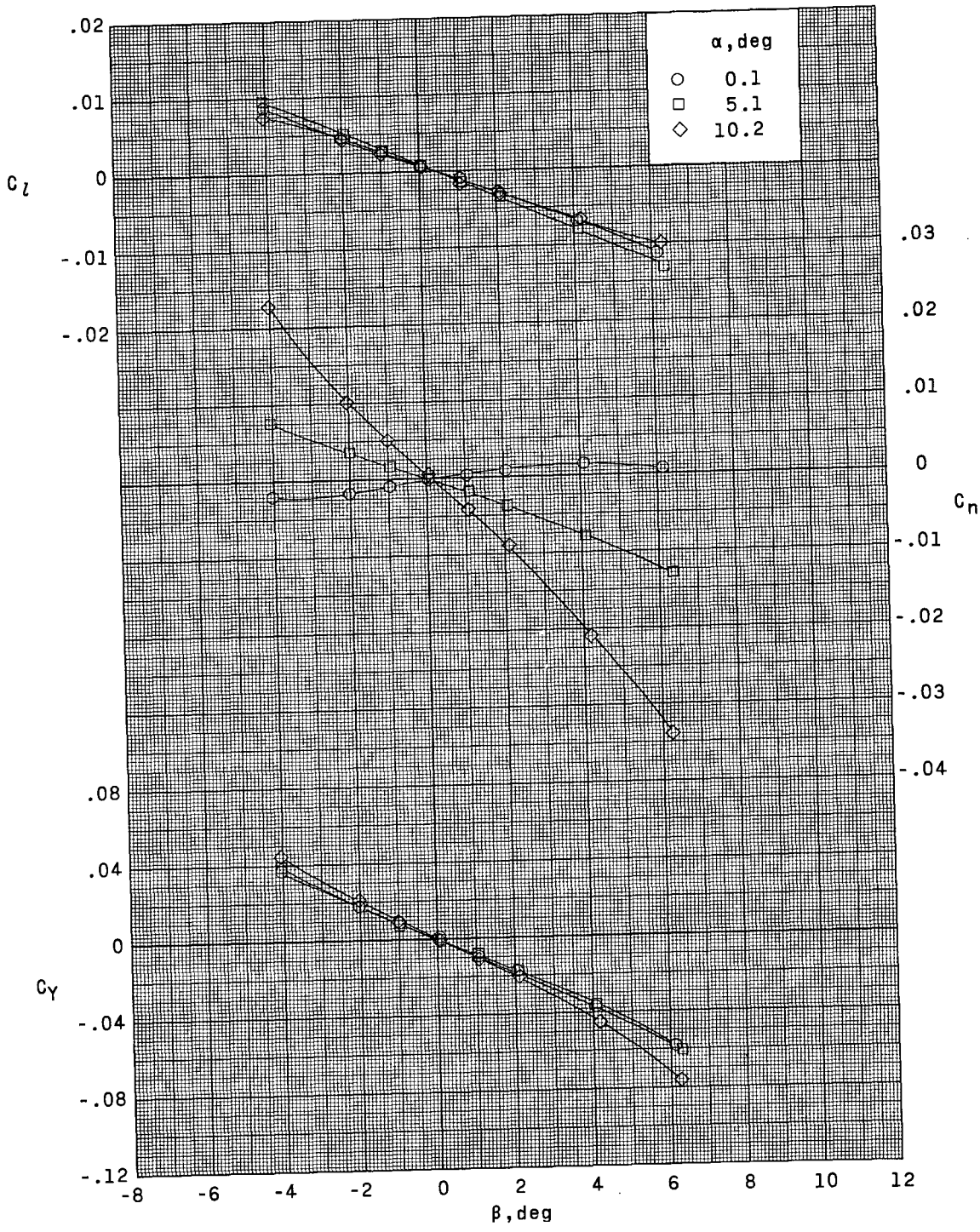

(b) M = 2.86.

Figure 11.- Concluded.

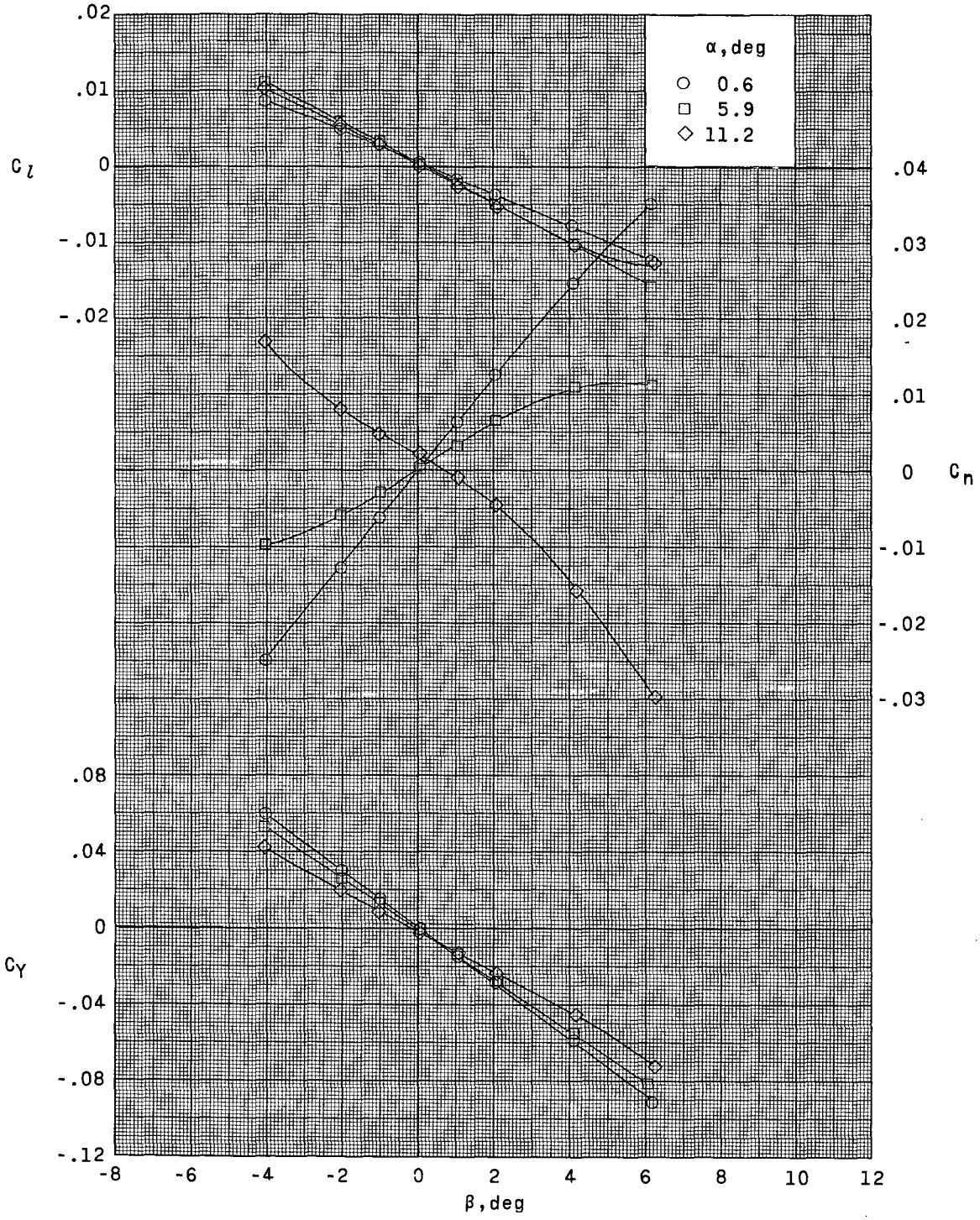

(a) M = 1.60.

Figure 12.- Aerodynamic characteristics in sideslip. W_2, $\Gamma_t = 60^\circ$, $i_t = 0^\circ$.

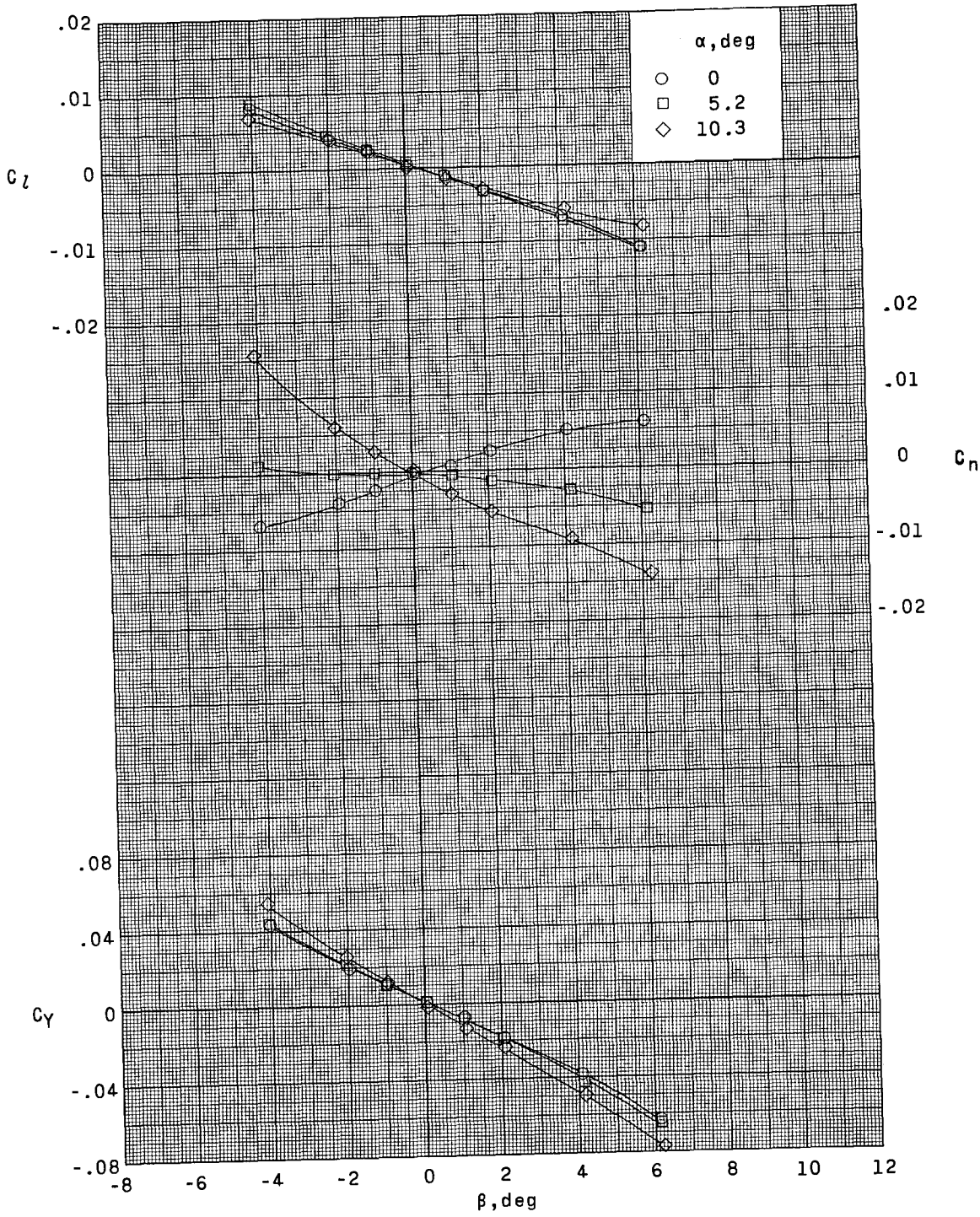

(b) M = 2.86.

Figure 12.- Continued.

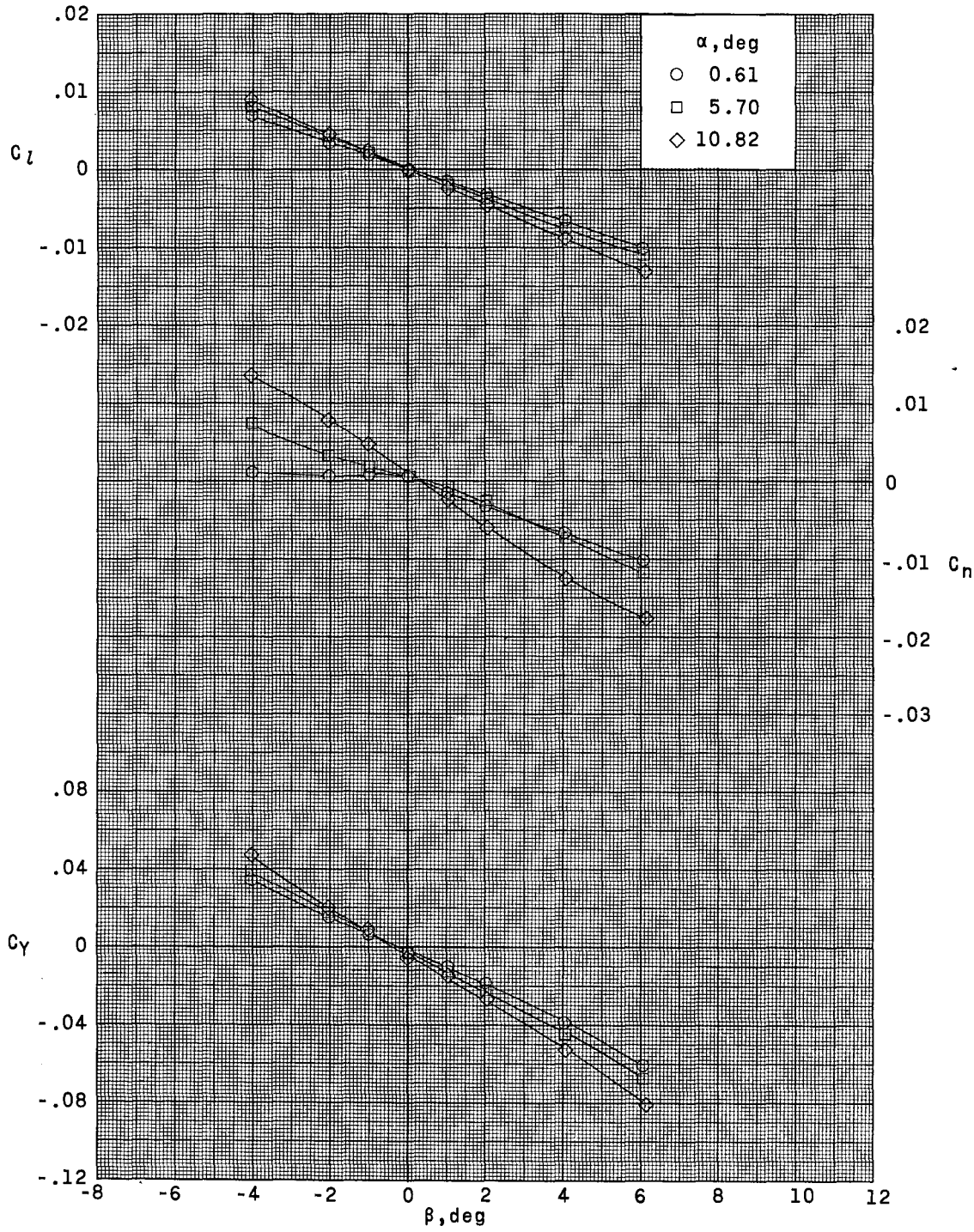

(c) M = 4.65.

Figure 12.- Concluded.

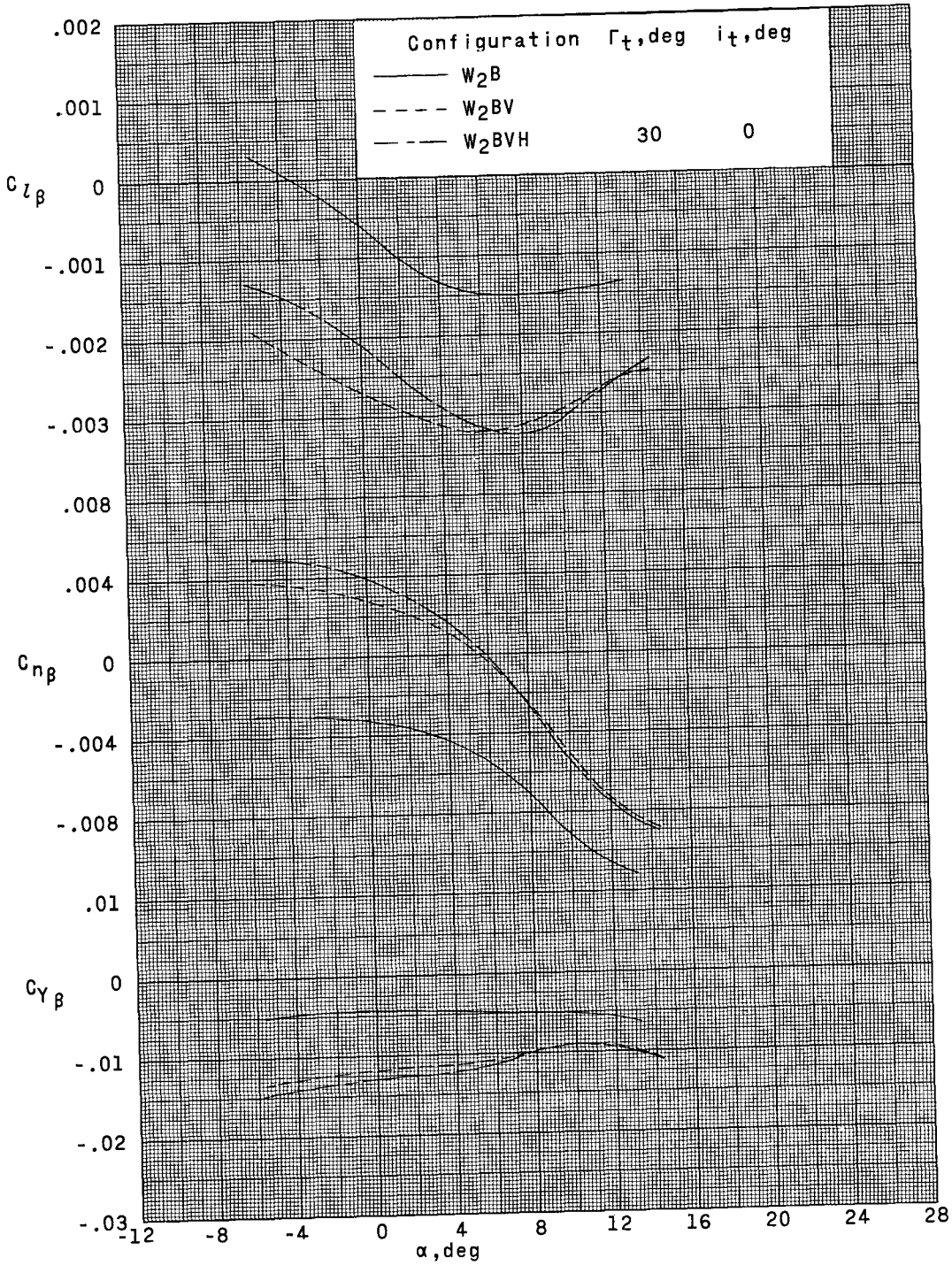

(a) M = 1.60.

Figure 13.- Effect of various components on the 75° modified arrow wing configuration.

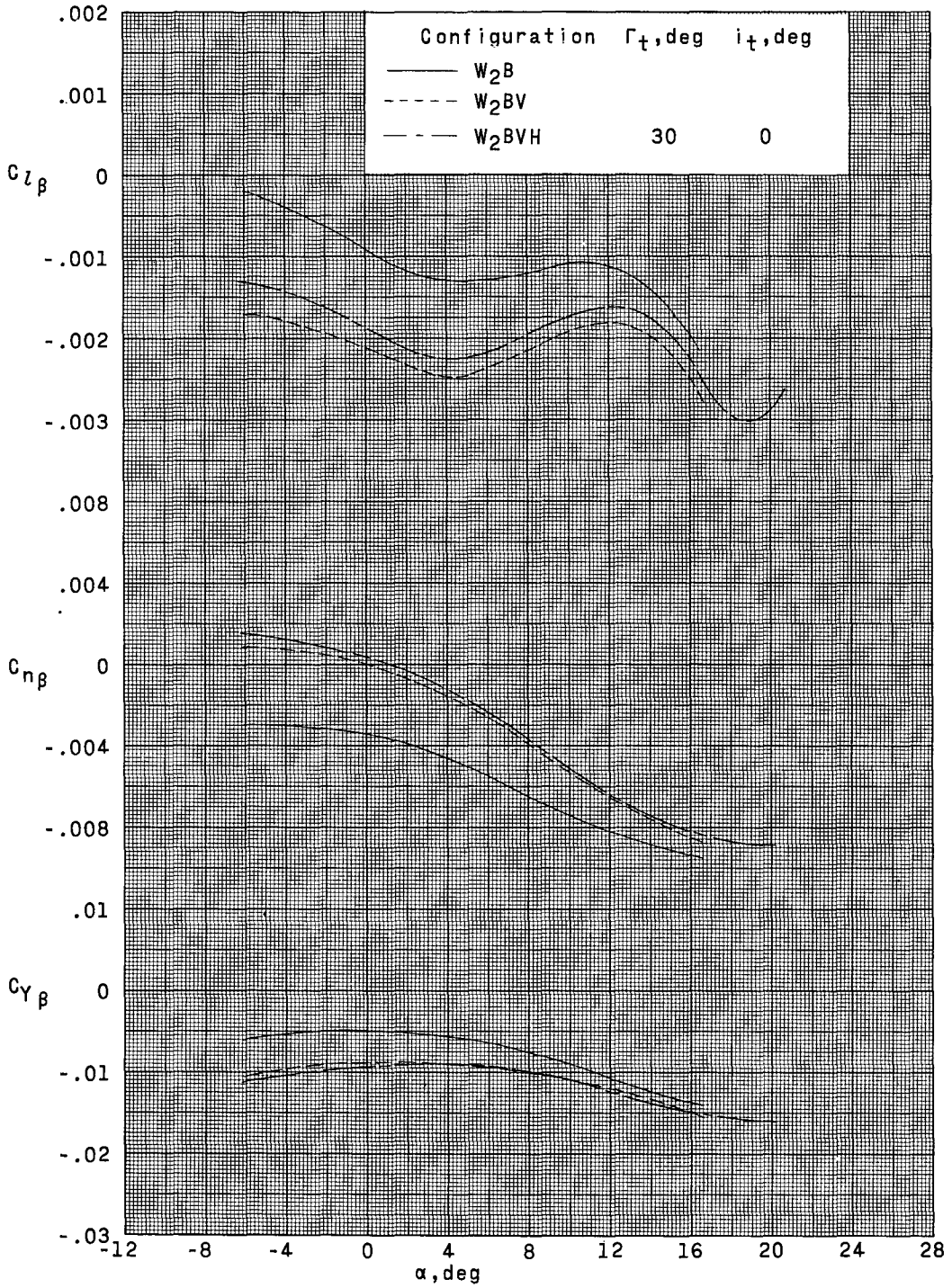

(b) M = 2.86.

Figure 13.- Concluded.

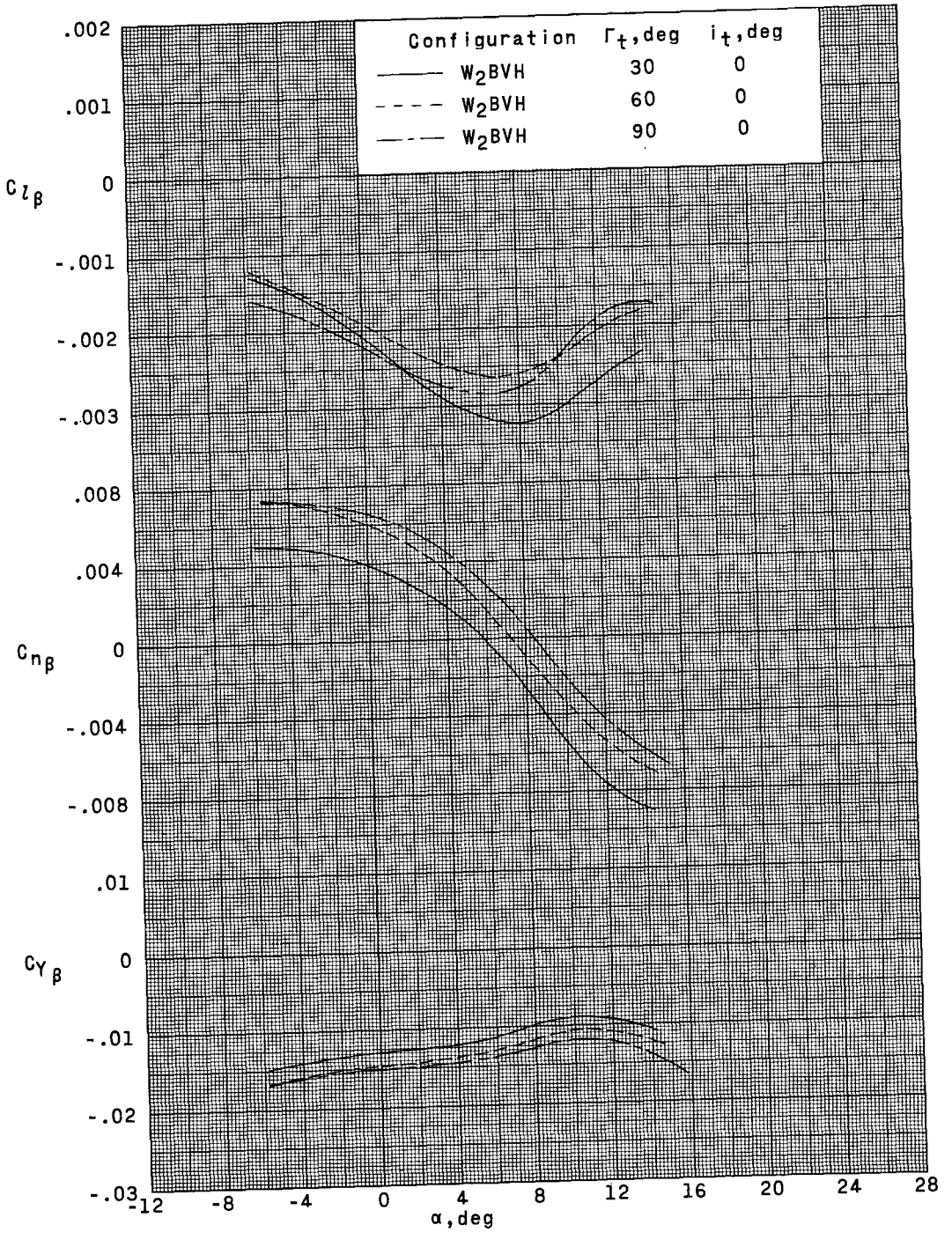

(a) M = 1.60.

Figure 14.- Effect of horizontal-stabilizer anhedral angle on the lateral characteristics of the 75° modified arrow wing configuration.

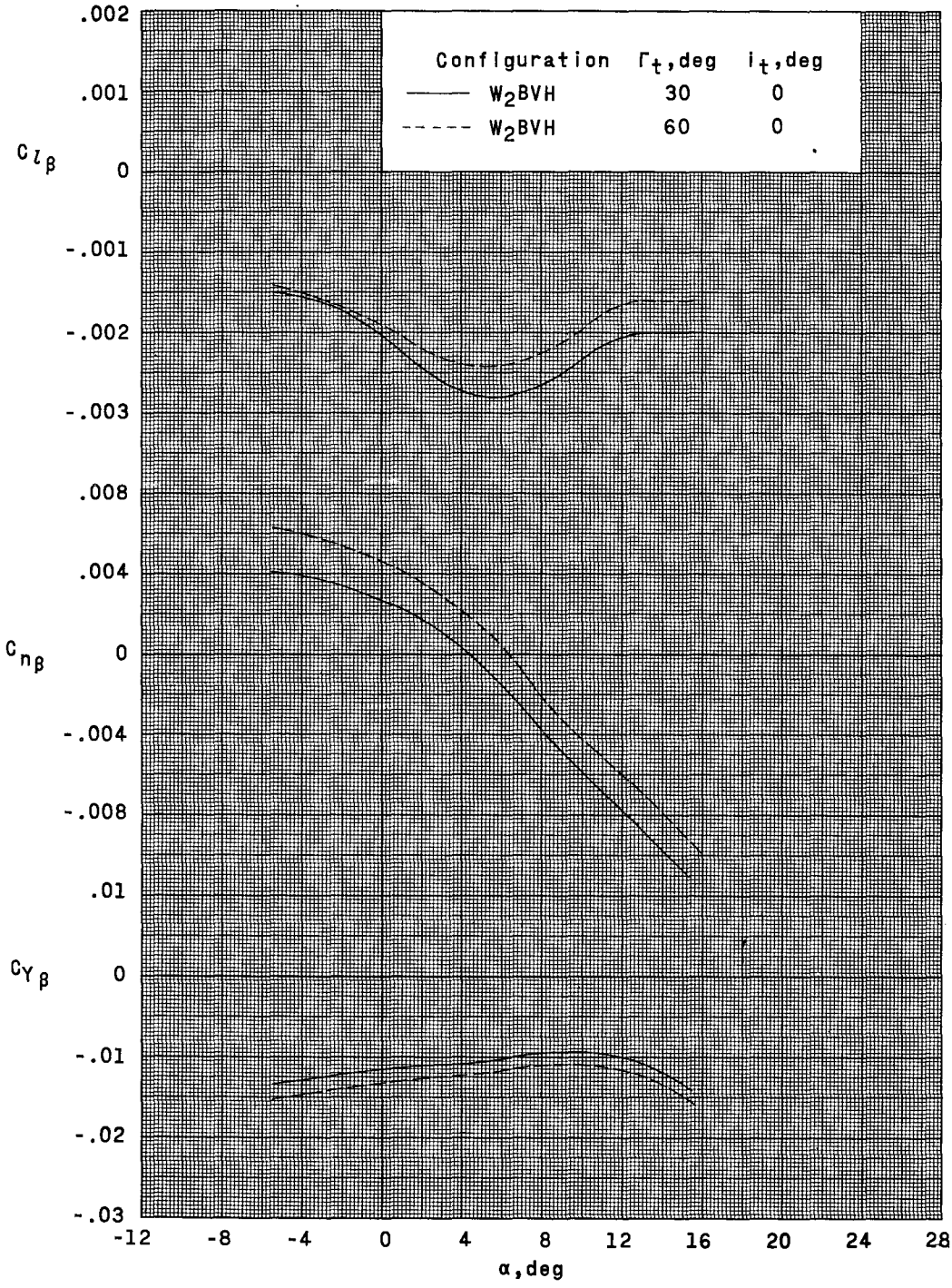

(b) M = 1.90.

Figure 14.- Continued.

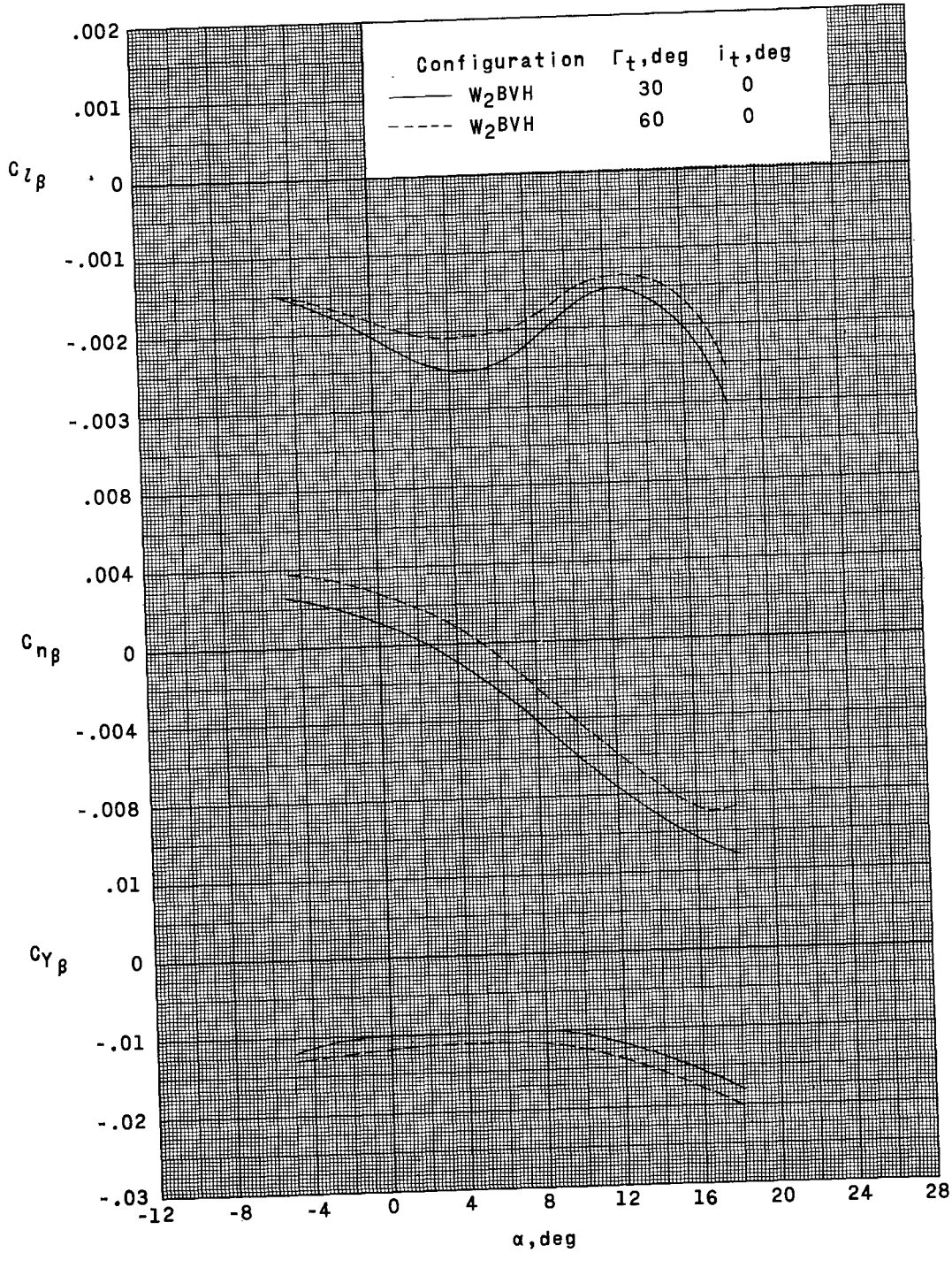

(c) M = 2.36.

Figure 14.- Continued.

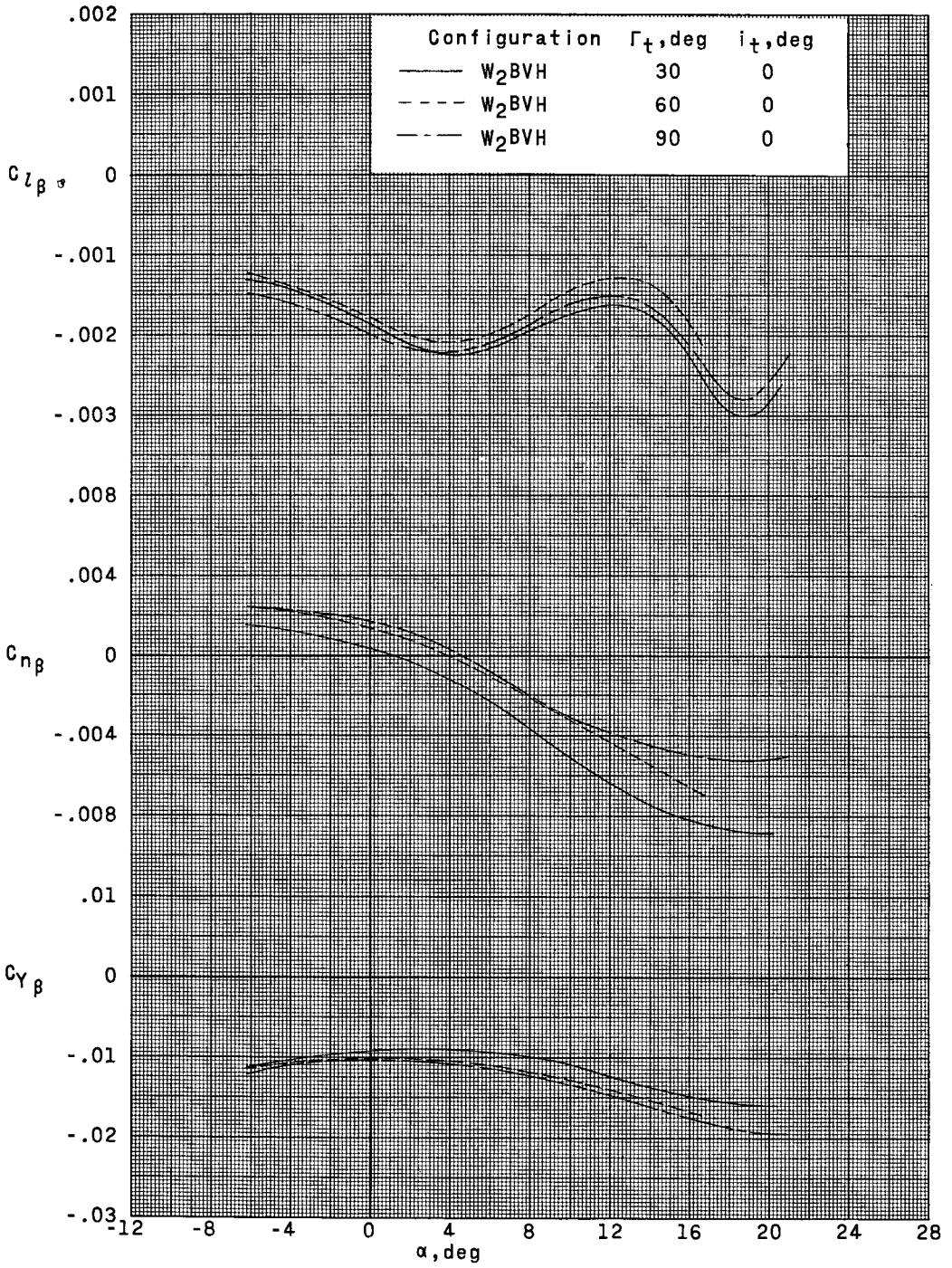

(d) M = 2.86.

Figure 14.- Continued.

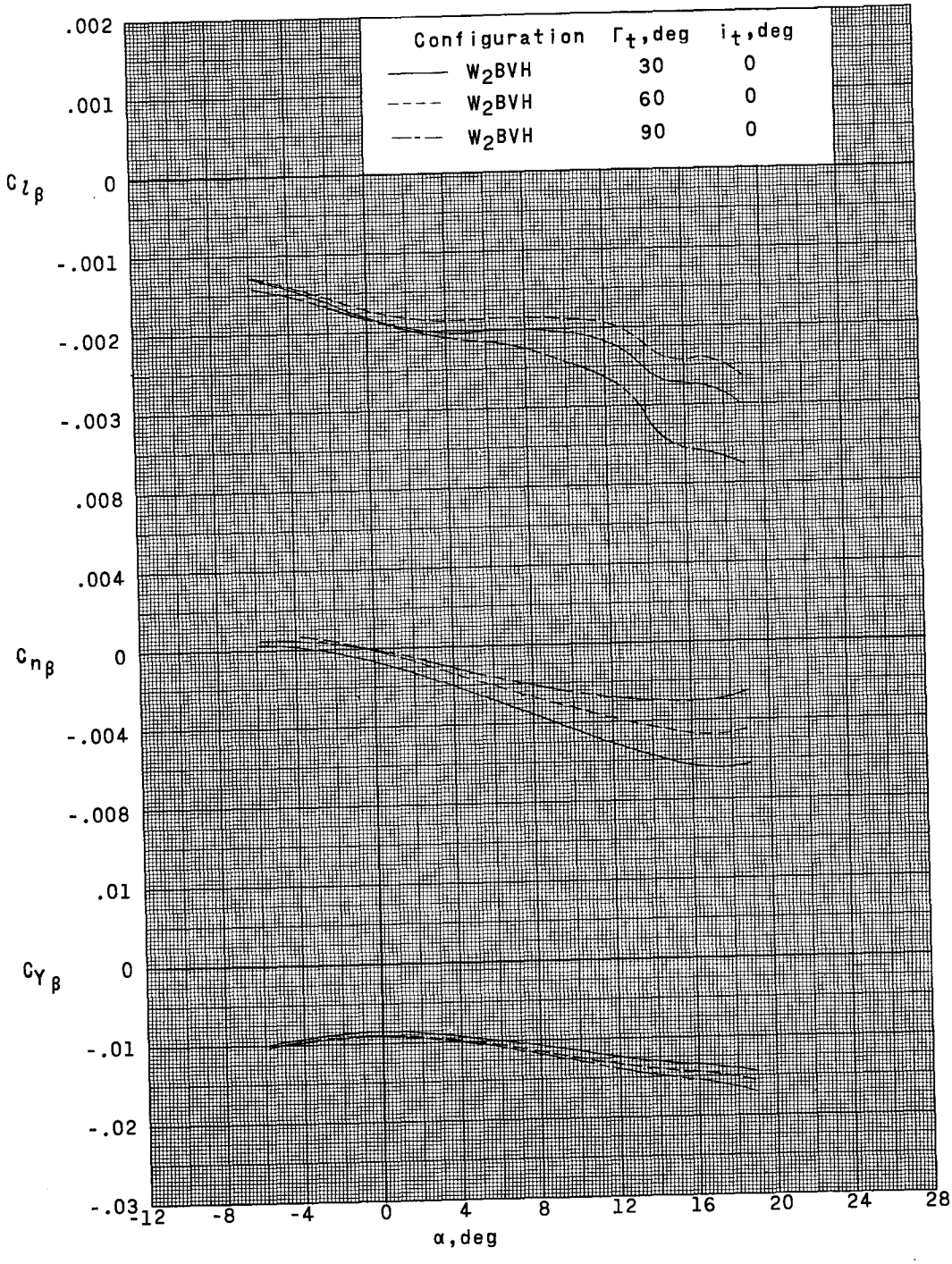

(e) M = 3.96.

Figure 14.- Continued.

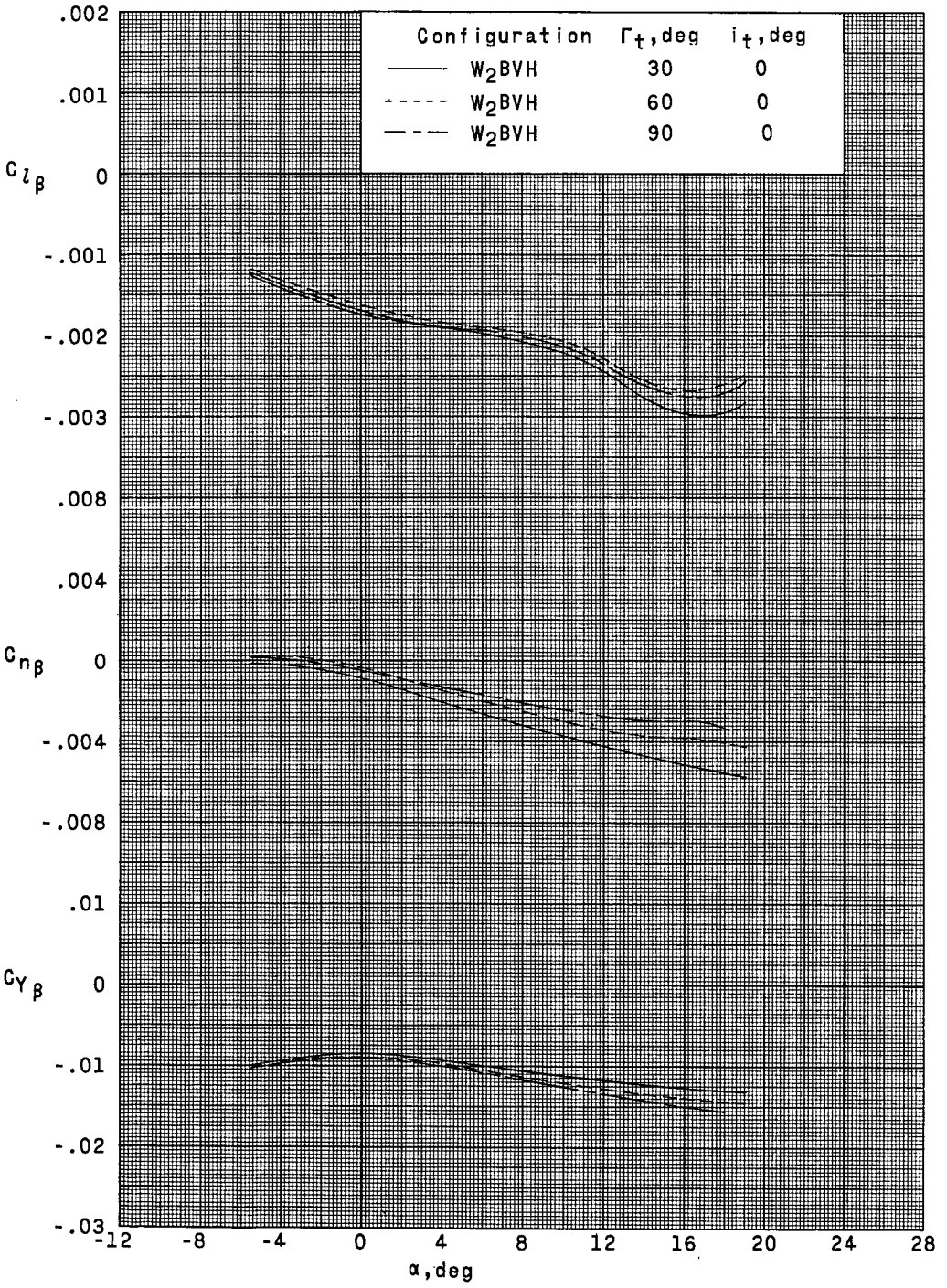

(f) M = 4.65.

Figure 14.- Concluded.

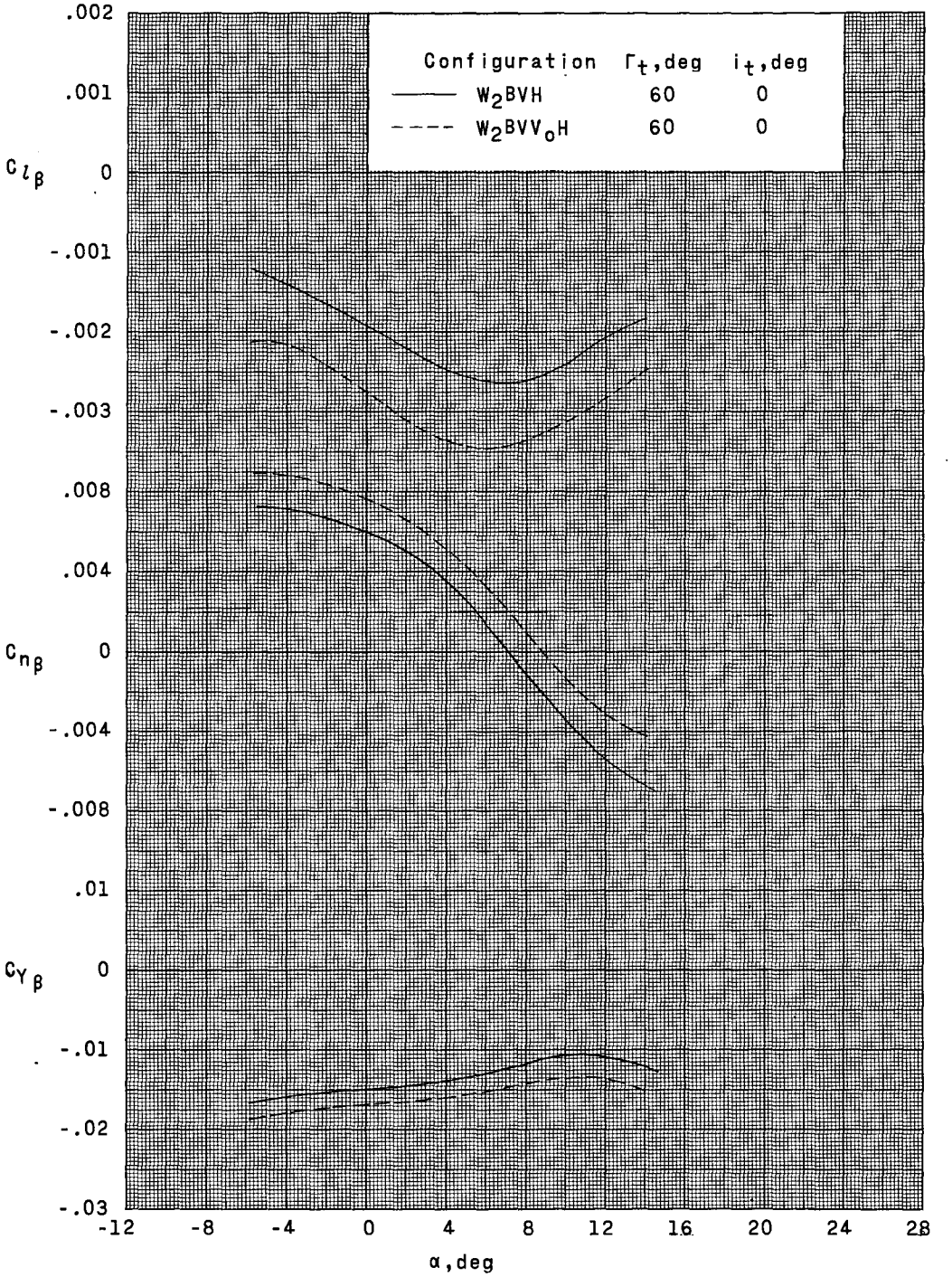

(a) M = 1.60.

Figure 15.- Effect of outboard vertical tails on the lateral characteristics of the 75° modified arrow wing configuration.

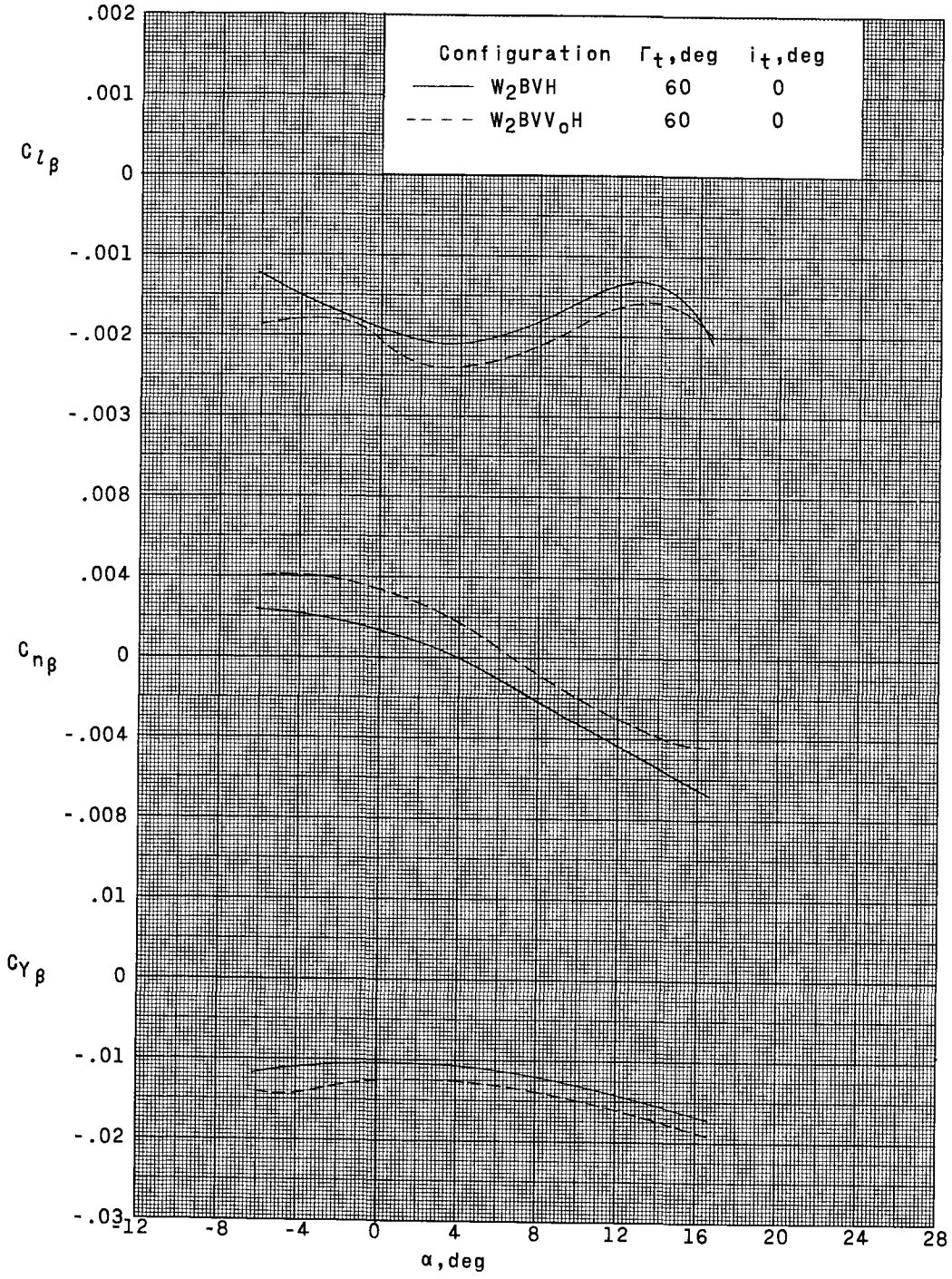

(b) M = 2.86.

Figure 15.- Continued.

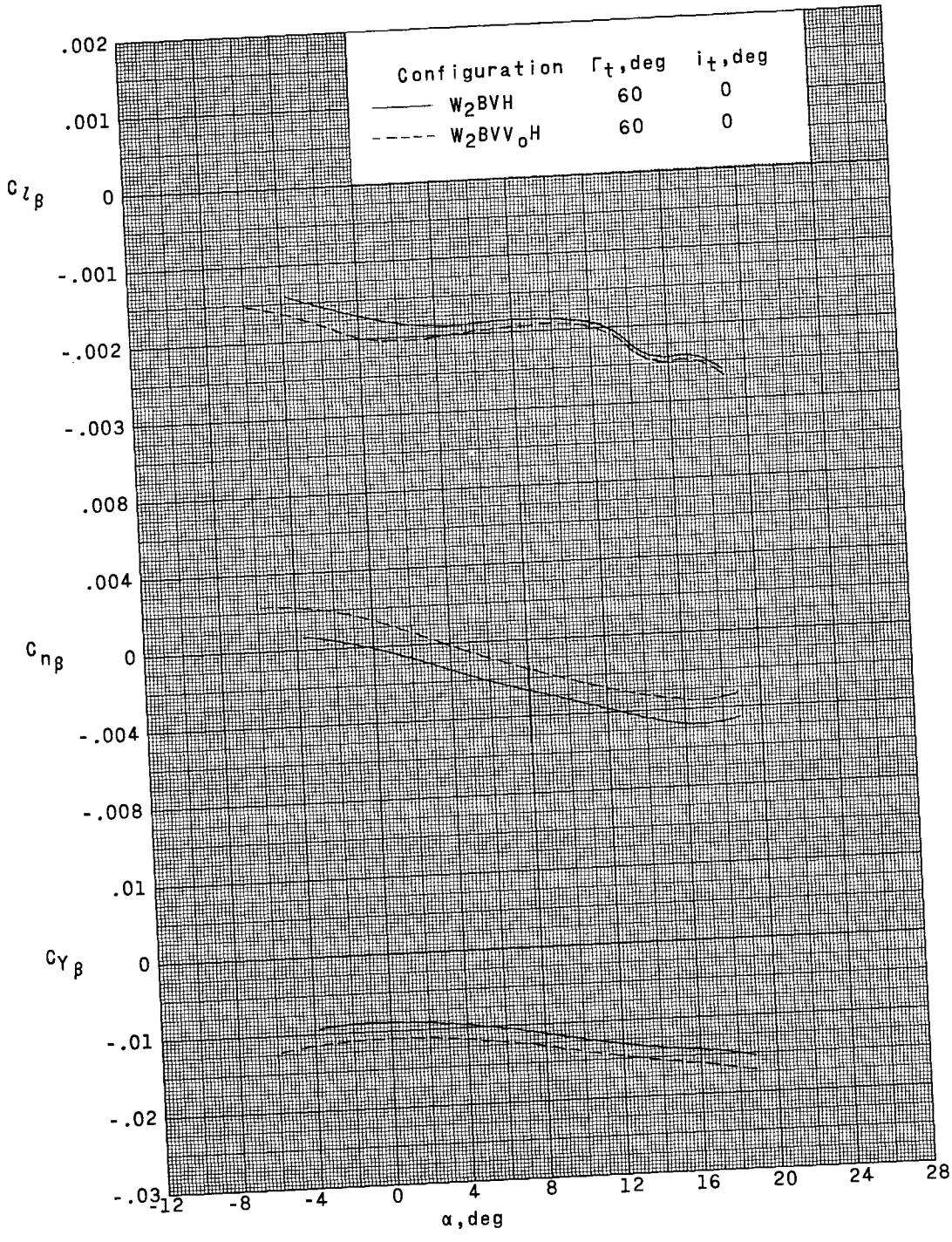

(c) M = 3.96.

Figure 15.- Continued.

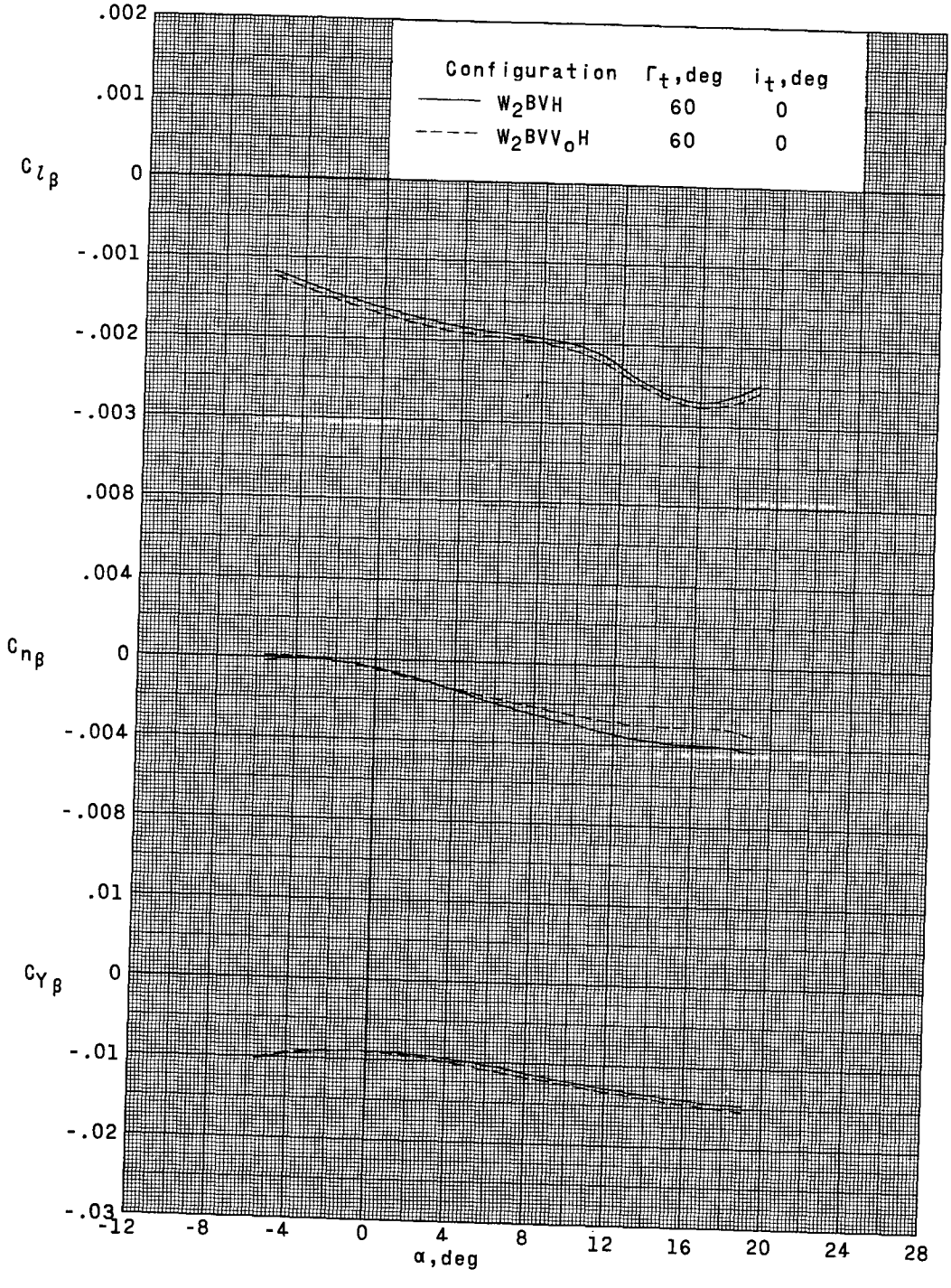

(d) M = 4.65.

Figure 15.- Concluded.

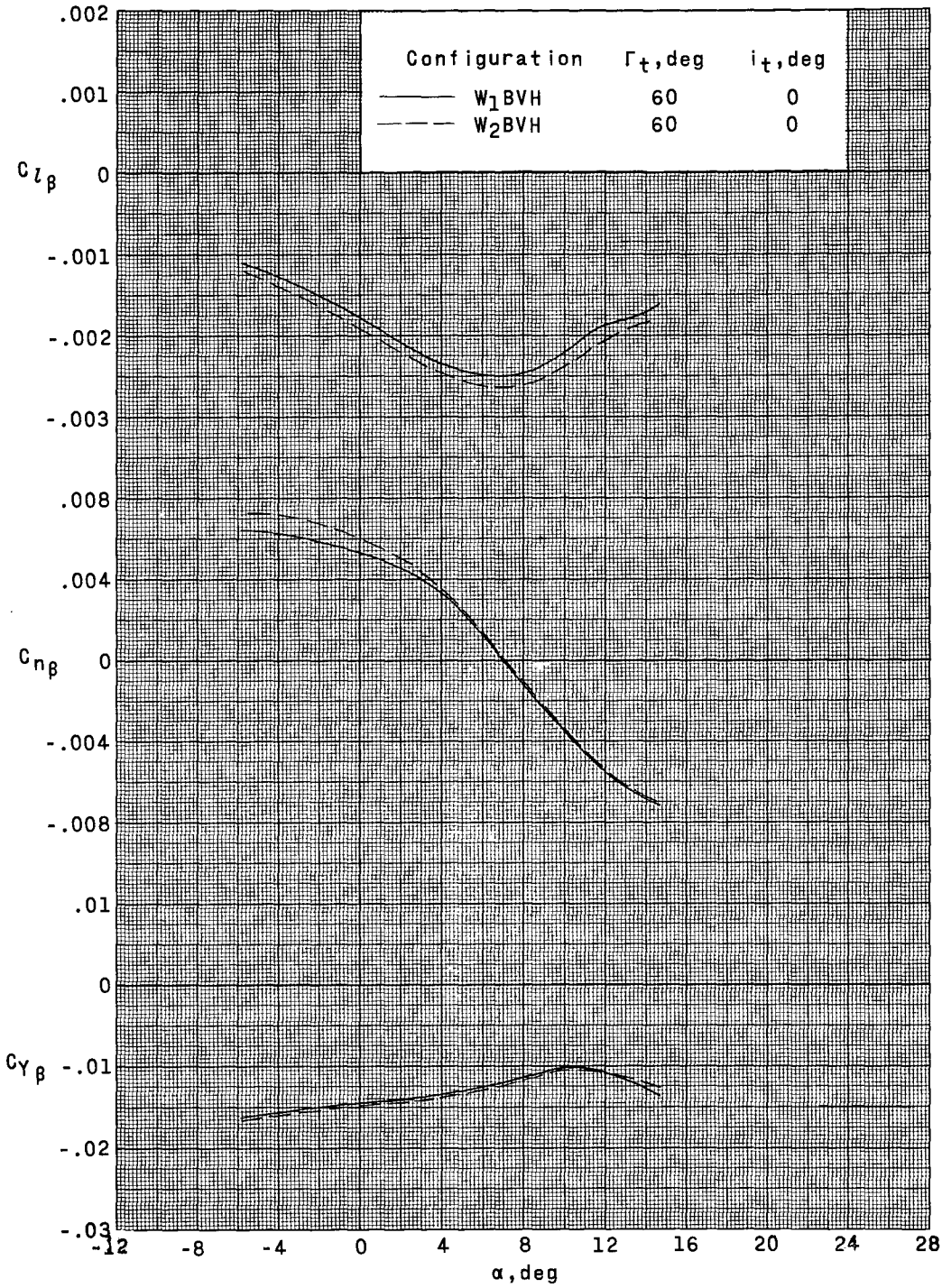

(a) M = 1.60.

Figure 16.- Lateral characteristics of two of the wing planforms.

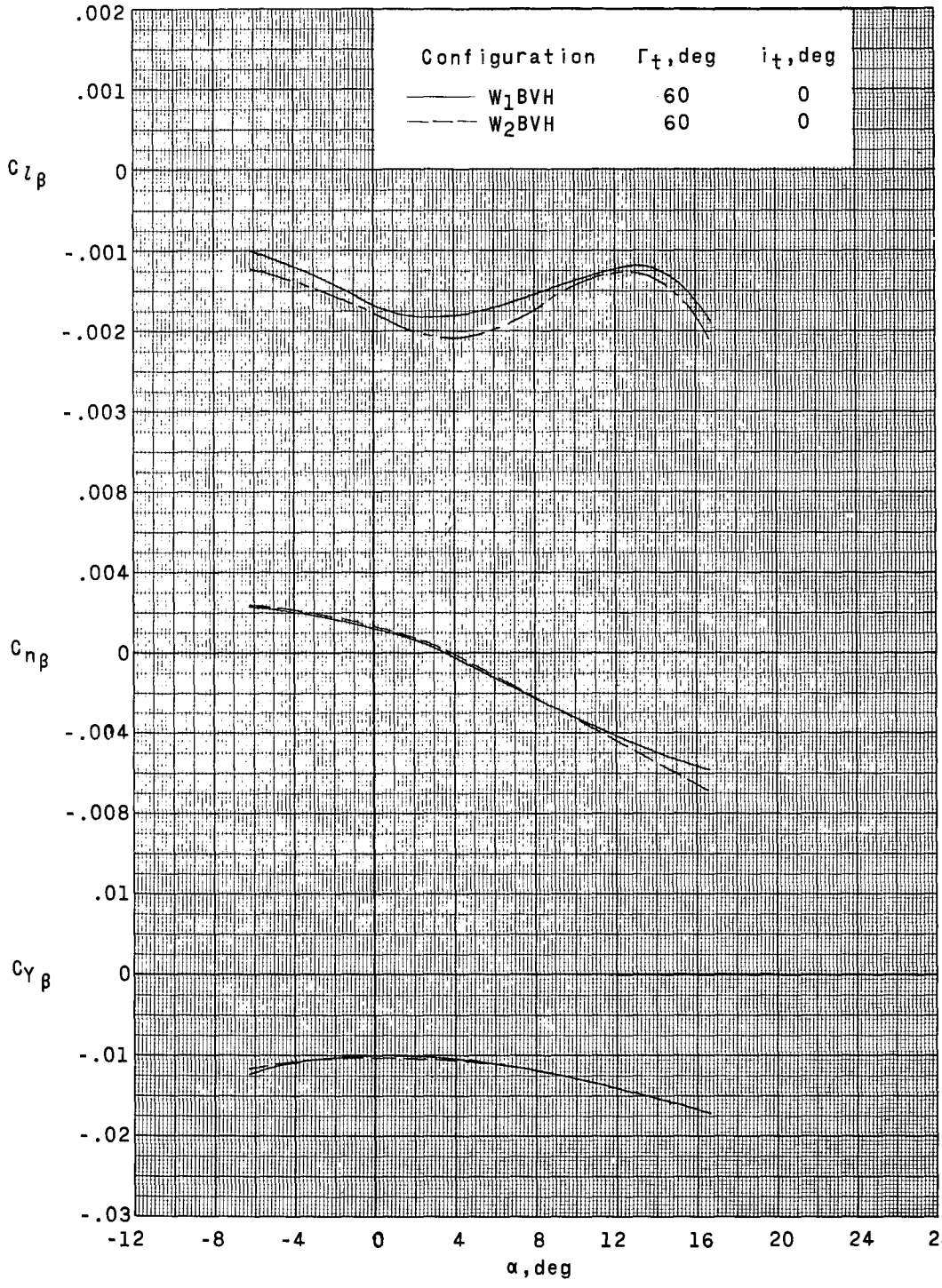

(b) M = 2.86.

Figure 16.- Concluded.

NASA-Langley, 1964 L-3818